

# **AG-WaMED** | Advancing non-conventional water management for innovative climate-resilient water governance in the Mediterranean Area

Grant Agreement Number: [Italy: 391 del 20/10/2022, Egypt: 45878, Tunisia: 0005874-004-18-2022-3, Greece: ΓΓΡ21-0474657, Spain: PCI2022-132929 ]

## Deliverable 3.1.2

## Complete watershed models for each LL

#### Partnership for Research and Innovation in the Mediterranean Area Programme (PRIMA)

The AG-WaMED project has received funding from the PRIMA Programme, an Art.185 initiative supported and funded under Horizon 2020, the European Union's Framework Programme for Research and Innovation. This project also received funding from the Italian Ministry of University and Research (MUR), Science and Technological Development Fund - STDF (Egypt), Ministry of Higher Education and Scientific Research - MESRS (Tunisia), Hellenic Republic, Ministry of Development and Investments (Greece), Agencia Estatal de Investigación (AEI) (Spain) and General Directorate for scientific research and technological development - DGRSDT (Algeria)























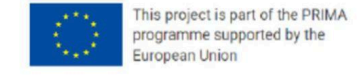














## **Deliverable Identification**

Deliverable No and Title	D3.1.2 - Complete wat	ershed models f	or each LL				
Grant Agreement No	Italy: 391 del 20/10/2 45878, Tunisia: 0005874-004-18-202 ГГР21-0474657, Spa PCI2022-132929	2-3, Greece:	Acronyn	า	AG-WaMED		
Project Full title	Advancing non-conv climate-resilient water						
Funding Instrument	Partnership for Rese Programme (PRIMA)		ation in th	e Med	literranean Area		
Call	PRIMA CALL SECTI	ON 2 2021 – N	//ULTI-TOF	PIC			
Work-Package No and Title	Work Package 3: DS socio-economic asse		sources sy	stem r	nodelling and		
WP- Main Beneficiary	Agricultural Economi Organization DIMITE		nstitute - H	ellenic	: Agricultural		
WP-Leader	Dr. Athanasios Ragk	os					
Task No and Title	Task 3.1.2 Complete	watershed mo	del for eac	h LL			
Task Leader	Politecnico di Milano						
Main Author	Davide Danilo Chiare	elli					
Contributors	All partners						
Status	Draft □ Final ⊠						
Dissemination Level	Internal □ Public □						
Reviewed by							
Abstract							
Key words	LL modeling, hydrolo	gical fluxes, SI	MPA, SWA	AT, WA	ATNEEDS		
DOCUMENT HISTORY	<b>1</b>						
Planned Release Date	30/04/2025 Rescheduled to 30/06/25	Actual Relea	ise Date	30/06	6/2025		
Version	V1	Released Ve No	rsion	1			



### **Abstract**

The water-energy-food-ecosystem (WEFE) nexus remains a central lens through which to address sustainability challenges in the Mediterranean, where water plays a pivotal role. In Deliverable D3.1.2, we finalize and adapt watershed-scale hydrological models for the four Ag-WaMED Living Labs (LLs) located in Italy, Spain, Egypt, and Algeria/Tunisia to assess the integration of alternative strategies. These include water transfers, small reservoirs, cisterns, and aquifer recharge, modeled using SWAT, SIMPA, and WATNEEDS, with local data where available. Building on D3.1.1, the updated models quantify current water balances and simulate stakeholder-driven scenarios. The models allow for the quantification of current water balances and simulation of alternative scenarios, developed through participatory processes with stakeholders. Specific analyses, such as the impact of revised ecological flow requirements on the Tagus-Segura transfer (Spain), highlight the trade-offs between environmental regulations and agricultural water supply. In Italy, the modeling of small agricultural reservoirs demonstrates the potential of decentralized storage to support climate-resilient irrigation. In Egypt and Algeria/Tunisia, models validate traditional cistern systems and explore aquifer recharge as viable NCW strategies. The results underscore the critical importance of localized, stakeholder-informed hydrological modeling for identifying feasible and context-sensitive solutions to water scarcity. These insights will directly inform the co-design of policy recommendations (WP4) and decision-support tools to advance sustainable water governance across the Mediterranean.



## 1. Introduction

This deliverable reports the complete watershed model for each LL, adjusted to respond to the needs of each LLs, a process initiated with Deliverable D3.1.1. Adjustments mainly focus on updates hydrological models developed to describe the potential of using non-conventional water within each Living Lab (LL) with the aim (I) to prove the effectiveness of alternative scenarios of water source and (ii) to define policies and guidelines to help their implementation within each LL (WP4). Indeed, hydrological modeling plays a key role in sustainable water management at both global and local levels. Advanced modeling techniques provide valuable insights into the dynamics of water systems and their current and future usage. These insights enable informed decision-making and help balance the competing demands of water, energy, and food. As such, hydrological models serve as a crucial tool to support co-design and participatory approaches, as exemplified by the AG-WAMED project.

In D3.1.1, we highlighted the complex interconnections and ongoing challenges posed by global dynamics and climate change. Within this context, the water-energy-food-ecosystem (WEFE) nexus has emerged as a critical focal point, underscoring the central role of water. These challenges stem from the ever-growing demand for goods and services driven by increasing population pressures and shifting climate patterns, which in turn place greater stress on natural resources. Understanding and addressing the WEFE nexus is essential for fostering long-term resilience. These same challenges are the one similarly observed across the various LLs involved in the Ag-Wamed project and discussed with the stakeholders during the LL meeting (WP2).

In this release, we present the updated hydrological models, originally calibrated and validated in D3.1.1. These models have been enhanced to incorporate non-conventional water sources as viable opportunities for each LL, aligning with the needs and expectations expressed by stakeholders.

## 2. Modelling approach

Different models were utilized based on the collective previous knowledge of each partner regarding their respective living lab (LL) as discussed in D3.1.1, gained from prior analyses, applications, and studies. The choice of model was made based on the size of the LL and the main water fluxes relevant for the analysis. We briefly recall here that the following hydrological models were considered: SWAT (Arnold et al., 2012) for assessing hydrological fluxes in the Italian LL, Egyptian LL, and Algerian/Tunisian LL; the SIMPA model (Álvarez et al., 2005) for evaluating water availability in the Spain LL; and a dedicated agro-hydrological model named WATNEEDS (Chiarelli et al., 2020), specifically used to assess crop water demand for irrigation in each of the 4 LL. Input data for these water models include gridded information on climate (e.g., precipitation), land use (e.g., agriculture, forests, urban areas), soil types, and Digital Elevation Model (DEM). When possible, local data were collected in each LL in Spain (Segura basin), Italy (Orcia basin), Egypt (Naghamish basin), Tunisia, and Algeria (Bayech basin) and then merged with regional or global data. The latter are usually easier to find available from freely accessible datasets. Each partner made significant efforts to collect local data, thus, when available, that information was preferred. Three main non-conventional water strategies were implemented in the hydrological models, including



water transfer system (Spain LL), small reservoirs (Italian LL) and cisterns (Egyptian and Tunisian/Algerian LLs).

We briefly recall the main model used before discussing the strategies adopted by each LL to respond to their specific challenges.

### 2.1 The SIMPA model, applied to The Spanish LL

The SIMPA model is a hydrological precipitation-runoff model developed by the Center for Studies and Experimentation of Public Works of Spain (Álvarez et al., 2005; Estrela et al., 1999; Estrela & Quintas, 1996). The model is quasi-distributed and continuous and simulates the process of precipitation transformation into runoff in a natural regime. The model works on a monthly time scale at a spatial resolution of 500 x 500 m2. The model is routinely run for the entire Spanish territory for the period 1940 to 2020 and model results can be downloaded from (MITECO, 2023).

The hydrological model depends on 4 parameters:  $H_{max}$  the maximum soil moisture capacity,  $\mathcal{C}$  the excess parameter,  $I_{max}$  the maximum Infiltration capacity and  $\alpha$  the coefficient of the discharge branch. In their distributed version, these equations represent the successive balances in each cell in which the territory is discretized. Variables and parameters are distributed to the aquifer tank model. The parameter  $\alpha$  simulates the set of hydrodynamic properties of an aquifer and its essence is aggregated. The drainage of each aquifer is assumed to be distributed, although constant in all the cells of each of them. Although the time scale of the SIMPA model does not allow identifying the hydrological flows that occur because of individual rainfall episodes, the model provides information on the average behavior of the basins through the basic hydrological variables, which allows carrying out water balances and diagnosing possible behavioral changes.

# 2.2 The SWAT model, applied to the Italian, Egypt and Algerian/Tunisian LLs

The Soil and Water Assessment Tool (SWAT) is a hydrological model adopted for assessing the main hydrological fluxes within river basins and watersheds (Arnold et al., 2012). The model has been developed by the United States Department of Agriculture (USDA), SWAT is a process-based model that integrates various land management practices and climatic factors to simulate the movement of water, sediment, and nutrients within a defined geographical area (Arnold et al., 2012). The model works using the Hydrologic Response Unit (HRU) as the smallest spatial unit. Each HRU sums up all the similar information from topography, soil types, and land use within a user-defined subbasin.

The model requires the Digital Elevation model (DEM), the stream network, soil, and land use maps, the climatic time series of precipitation, maximum and minimum temperatures, solar radiation, air relative humidity, and wind speed (usually at daily time step). Once validation and calibration are done, the current water availability is modeled.

The procedure for application of the SWAT model is case specific for each LL, depending on the peculiar hydrological situation of each LL. Thus, we present the data and the procedure followed in each LL. For example, in the case of Italian LL, we resort to NCW practices that



are already established in the study area. This is the case of small reservoirs that are then properly modeled in the SWAT model.

## 2.3 Modeling Non-Conventional Water Source

In this section, we present the main challenge rise in the LLs and the way they have been addressed via a hydrological model to check their effectiveness. For each LL we briefly reported the status of the art before describing the actions implemented.

#### 2.3.1 **SPAIN**

In response to stakeholder feedback from the Spain Living Lab, we incorporated an analysis of future water availability from the Tagus-Segura Water Transfer. As a critical source for the basin, the transfer's contribution significantly varies with the hydrologic conditions in the Tagus basin. Based on stakeholder input, we have treated the Tagus-Segura Water Transfer as a component of non-conventional water (NCW) supply rather than actual NCW and adjusted the modelling framework accordingly.

#### 2.3.1.1 State of the art

The Campo de Cartagena Irrigation District (CRCC) is in Southeast Spain. It covers an area of 42,435 ha, divided into three main zones: Eastern Area (18 sectors), Western Area (3 sectors) and Elevation 120 Area (12 sectors). These three zones and their corresponding sectors are represented in Figure 2.3.1.1.



Figure 2.3.1.1. General layout of the irrigation District (Source: CRCC)

The potential demand of Campo de Cartagena Irrigation District is 140 hm<sup>3</sup>/yr, but actual water availability is much less than that. Water resources for Campo de Cartagena Irrigation District come from three different sources:

- Local water resources
- Water resources regulated in the Segura Basin
- Water resources transferred from the Tagus basin

Local water resources do not depend on local hydrology; they come from recycled water: effluent from urban wastewater treatment plants and some irrigation drainage. The main wastewater treatment plants that provide water for CRCC are Fuente Álamo (0.654 hm³/yr), Torre-Pacheco (1.825 hm³/yr), San Javier (2.894 hm³/yr), Balsicas-Roldán (1.000 hm³/yr), Los Alcázares (2.611 hm³/yr), La Aljorra (0.270 hm³/yr) and San Pedro del Pinatar (2.430 hm³/yr), but the concession is shared with other irrigation districts. Water from irrigation drainage ditches has a high salinity and must be mixed with water of better quality before it can be applied to irrigation. The Campo de Cartagena Irrigation District also receives a small water allocation from the Segura Basin Regulation System, usually less than 4.2 hm³/yr.

Figure 2.3.1.2 shows the location of the Campo de Cartagena Irrigation District (CRCC) in the Segura River Basin District. The main watercourses in the Segura River Basin District are the Segura River and its tributary, Guadalentín River. The Segura Basin occupies most of the area covered by the Segura River Basin District. However, Campo de Cartagena Irrigation District is located outside the Segura River Basin. It covers part of the Rambla del Albujón River Basin and of two interbasins draining to the Mar Menor.



Figure 2.3.1.2. Segura River Basin District

Most of the resources come from the Tagus-Segura Water Transfer, but the amount fluctuates depending on the hydrologic conditions in the Tagus basin. A schematic representation of the Tagus-Segura Water Transfer (ATS) is shown in Figure 2.3.1.3. Water is taken from the headwaters of the Tagus basin, right after the major regulation reservoirs of Entrepeñas and Buendía. The water transfer canal was designed for a capacity of 1000 hm³/yr, but the amount currently allocated cannot exceed 600 hm³/yr. In fact, the average amount transferred since 1980 is 333 hm³/yr, of which 125 hm³/yr are allocated to urban supply and the remaining 208 hm³/yr to irrigation. Campo de Cartagena has an allocation of 122 hm³/yr but has received only 64 hm³/yr on average.

The deficit is partially compensated with the purchase of desalinated water from two desalination plants: Torrevieja (22.9 hm³/yr) and Escombreras (4.0 hm³/yr), but a very high cost and with significant water quality problems due to the presence of boron. Emergency measures are also adopted during extreme drought, like negotiating contracts for the



cession of water rights, usually with farmers in the Tagus basin, or pumping groundwater from drought emergency wells.

Recently, the Tagus River Basin Plan has established a substantial increase in ecological flows in the Tagus River reaches located immediately downstream of the abstraction point of the Tagus-Segura Transfer. The need to attend to these ecological flows from the reservoirs at the head of the Tagus, which also regulate water for the transfer, means that the availability of water may be significantly reduced.



Figure 2.3.1.3. Tagus-Segura water transfer

The managers of the Campo de Cartagena Irrigation District have requested the AGWAMED project to calculate the impact that the new environmental flows of the Tagus River will have on the future water availability for the Transfer. Although this analysis was not initially foreseen in the project, it is considered very relevant, as it will determine how much water will have to be replaced by non-conventional resources (mainly desalination) in order to maintain agricultural activity in the district. The analysis carried out is presented in this report.

#### 2.3.1.2 Study area

The Tagus River is the longest watercourse on the Iberian Peninsula and encompasses the region's third-largest drainage basin, covering 83,678 square kilometers. Its course begins in Spain, flowing through its upper and middle sections, and continues into Portugal through its lower reaches. The Tagus Basin is the most densely inhabited in the peninsula and includes major urban centers such as Madrid and Lisbon. This study specifically examines the Upper Tagus Basin, situated entirely within Spanish territory, where approximately 70% of the basin's population resides. Water resource management within the Spanish section is overseen by the Tagus River Basin Authority through the Tagus River Basin Management Plan. Resource allocation is organized by exploitation systems (Figure 2.3.1.4), which are



designated areas capable of meeting their water demands using primarily local sources and generally align with the catchment areas of the river's main tributaries.

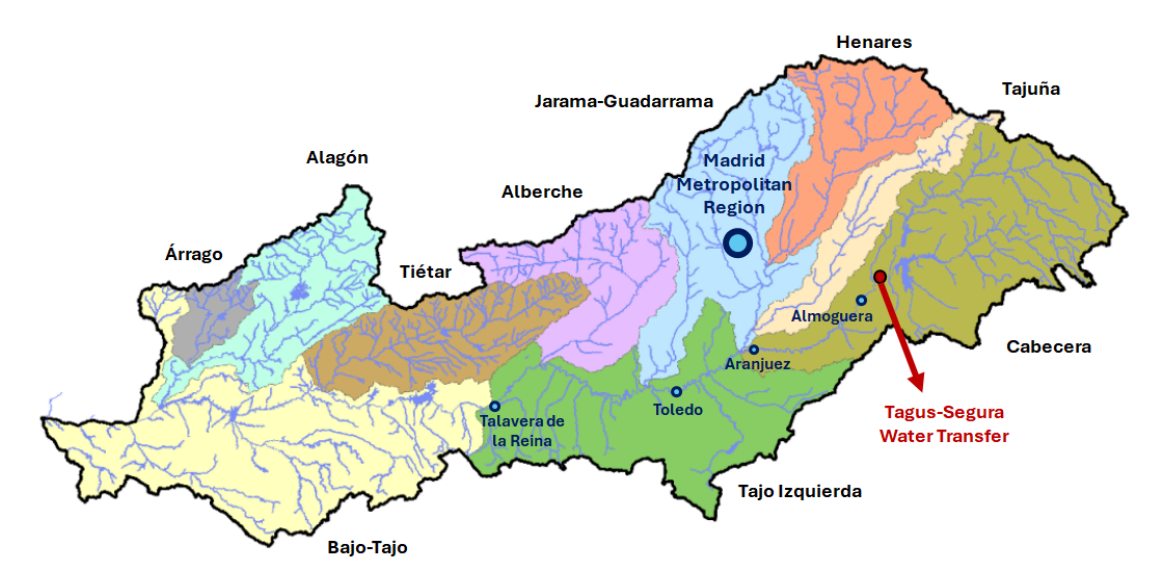


Figure 2.3.1.4. Tagus exploitation systems, taken from the River Basin Management Plan

The Upper Tagus Basin includes the following exploitation systems: Cabecera, Tajuña, Henares, Jarama-Guadarrama, Alberche and Tajo-Izquierda. It is a very relevant area for water resources. It supplies a significant portion of the basin's renewable water resources and satisfies most of the water demands, including the Tagus Segura Water Transfer and the water supply to the Madrid metropolitan region. The intake to the Tagus-Segura Water Transfer is located in the Bolarque reservoir, just downstream of the two major regulation reservoirs of the headwaters: the Entrepeñas reservoir in the Tagus River and the Buendía reservoir in the Guadiela River. The outlet of the Upper Tagus Basin is located at the tail of the Azután reservoir, close to the city of Talavera de la Reina. The four major points for control of environmental flows: Almoguera, Aranjuez, Toledo and Talavera de la Reina, are also highlighted in the figure.

#### 2.3.1.3 Objective of the study

Recently, the Tagus River Basin Plan has established a substantial increase in ecological flows in the Tagus River reaches located immediately downstream of the abstraction point of the Tagus-Segura Transfer. The need to attend to these ecological flows from the reservoirs at the head of the Tagus, which also regulate water for the transfer, means that the availability of water may be significantly reduced.

The objective of this study is to compare the water availability for the water transfer under the following situations:

- Situation prior to the approval of the Tagus River Basin Management Plan.
- Ecological flows imposed in the Tagus River Basin Management Plan.

The minimum flows prior to the approval of the Tagus River Basin Management Plan are presented in Table 2.3.1.1 and the ecological flows imposed in the Tagus River Basin Management Plan are presented in Table 2.3.1.2.

Table 2.3.1.1: Minimum flows prior to the approval of the Tagus River Basin Management Plan



Location		Discharç	ge (m³/s)		Annual Volume
Location	oct-dic	ene-mar	abr-jun	jul-sep	(hm³/a)
Almoguera	6	6	6	6	189.22
Aranjuez	6	6	6	6	189.22
Toledo	10	10	10	10	315.36
Talavera	10	10	10	10	315.36

Table 2.3.1.2: Ecological flows imposed in the Tagus River Basin Management Plan

Location		Discharç	ge (m³/s)		Annual Volume	
Location	oct-dic		ene-mar abr-jun		(hm³/a)	
Almoguera	7.8	10.3	9.1	7.2	270.87	
Aranjuez	7.9	10.4	9.1	7.2	272.44	
Toledo	15	23	18	13	535.16	
Talavera	16	24	19	13	567.04	

Water is taken from the headwaters of the Tagus basin, right after the major regulation reservoirs of Entrepeñas and Buendía. The water transfer canal was designed for a capacity of 1000 hm<sup>3</sup>/yr, but the amount currently allocated cannot exceed 600 hm<sup>3</sup>/yr. In fact, the average amount transferred since 1980 is 333 hm<sup>3</sup>/yr, of which 125 hm<sup>3</sup>/yr are allocated to urban supply and the remaining 208 hm<sup>3</sup>/yr to irrigation. Campo de Cartagena has an allocation of 122 hm<sup>3</sup>/yr but has received only 64 hm<sup>3</sup>/yr on average.

The deficit is partially compensated with the purchase of desalinated water from two desalination plants: Torrevieja (22.9 hm³/yr) and Escombreras (4.0 hm³/yr), but a very high cost and with significant water quality problems due to the presence of boron. Emergency measures are also adopted during extreme drought, like negotiating contracts for the cession of water rights, usually with farmers in the Tagus basin, or pumping groundwater from drought emergency wells.

#### 2.3.1.4 Approach of the analysis

The central question is whether an increase in minimum ecological flows leads to a corresponding and consistent increase in reservoir releases throughout the year. In theory, this should be the case. To ensure maximum efficiency in water use, only the volumes strictly necessary to meet ecological requirements and water demands within the Tagus basin should be released from the reservoirs. Downstream of Aranjuez, the Tagus River converges with the Jarama River, which typically contributes to a higher natural flow than the Tagus at that point. Additionally, the Jarama carries regulated return flows from the Madrid metropolitan water supply system. These combined flows generally ensure that downstream demands are met without requiring additional releases from the headwaters. Under normal operating conditions, therefore, releases from the headwater reservoirs should only be needed to satisfy ecological flows and water demands in the river section between Bolarque and Aranjuez. Since water intended for consumption is extracted at designated intake points along this stretch, the full volume of ecological flow required at Aranjuez must be supplied from the reservoirs.

Assuming an operational regime aimed at maximizing efficiency, any increase in the ecological flow requirement at Aranjuez should correspond directly to an equal increase in



reservoir releases. As a result, the volume available for the Tagus-Segura Water Transfer would decrease by the same amount. Therefore, a first-order estimate of the impact of increased minimum flows on transferable water is simply the volume of that increase.

However, actual operating conditions often diverge significantly from this ideal due to several practical limitations. The river stretches between Bolarque and Aranjuez is extensive, making it difficult to regulate reservoir releases with precision based on real-time demand. Additionally, many of the irrigated areas that extract water along this section have not undergone modernization. As a result, they lack the infrastructure to draw only the water they need, generating substantial return flows, some of which re-enter the Tagus River. Furthermore, to ensure compliance with ecological flow requirements, operators tend to include a buffer or "operational slack" in releases, guarding against unforeseen incidents that could cause flow levels to fall below mandated minimums. Due to these factors, actual flows at Aranjuez have historically exceeded the official minimums, particularly during the irrigation season.

In this context, even if ecological flow requirements are raised, it may not be necessary to increase reservoir releases proportionally throughout the year, as flows under the existing regime already surpassed the newly established minimums in many months. A second, more refined estimate of the impact can thus be made by comparing historical flow data under the previous regime with the revised minimum flow requirements.

Nevertheless, it would be unrealistic to assume that, moving forward, flows will align precisely with the new minimum thresholds. It is reasonable to expect that the same operational slack applied in the past will continue to be applied to the updated flow targets. Accounting for this margin provides a third, and more realistic, estimate of the impact on transferable volumes.

Finally, evaporation losses in the headwater reservoirs must also be considered. The introduction of new ecological flow requirements is likely to alter the reservoir operating regime and result in lower storage levels, which could increase evaporation rates. These additional losses further reduce the water available for transfer and must be included in any comprehensive impact assessment.

#### 2.3.1.5 Water resources simulation model

To take all these factors into consideration, a water resources simulation model of the Upper Tagus Basin has been developed. The model incorporates all the data of the new planning cycle and the current operating rules of the Tagus-Segura Transfer and was used to estimate water availability from the Tagus-Segura Water Transfer.

The work methodology is based on the estimation of the water needs of the headwaters of the Tagus, including the entire basin up to Talavera de la Reina. The sum of the water needs constitutes the so-called "reference demand", which is the release of water that must be made from the Entrepeñas and Buendía reservoirs to meet these needs. The data on these needs, together with those on infrastructures and modulations and coefficients of return of demands, were taken from the Tagus River Basin Management Plan. The streamflow series were also taken from the Tagus River Basin Management Plan. The operating rules incorporate the criteria established in the "Tajo-Segura Memorandum" of 2013.

The Aquatool software is used to simulate the operation of the system during a period of analysis and allows to obtain the operating balances that are required for decision-making in

hydrological planning. Aquatool is a specialized software suite designed for integrated water resources management. Developed by the Universidad Politécnica de Valencia (Spain), it's widely used in Spain and Latin America for planning and simulating the operation of water resource systems, especially river basins. Aquatool models the behavior of complex water systems to support decision-making in: Water allocation, reservoir operation, drought management, environmental flow implementation and planning under climate or demand scenarios. The SIMGES simulation module was used in this analysis. It simulates the management of water resource systems (rivers, reservoirs, aquifers, users, etc.) under different hydrological and management conditions. It helps assess how water is distributed across a basin and how demands and the environmental flows are met. This software is adequate because it incorporates rules for reservoir operations, priorities among users, and constraints.

The model developed for the Upper Tagus basin is shown in Figure 2.3.1.5. As can be seen in the figure, the model has an appreciable degree of complexity. Components of different types are configured and related: surface water bodies, groundwater bodies, series of natural inputs, aquifer recharge, infrastructures (reservoirs, canals), demands, returns, discharges, evaporation in reservoirs, losses according to efficiencies, operating rules, ecological flows, reserves for flood control, reliability criteria and environmental objectives.

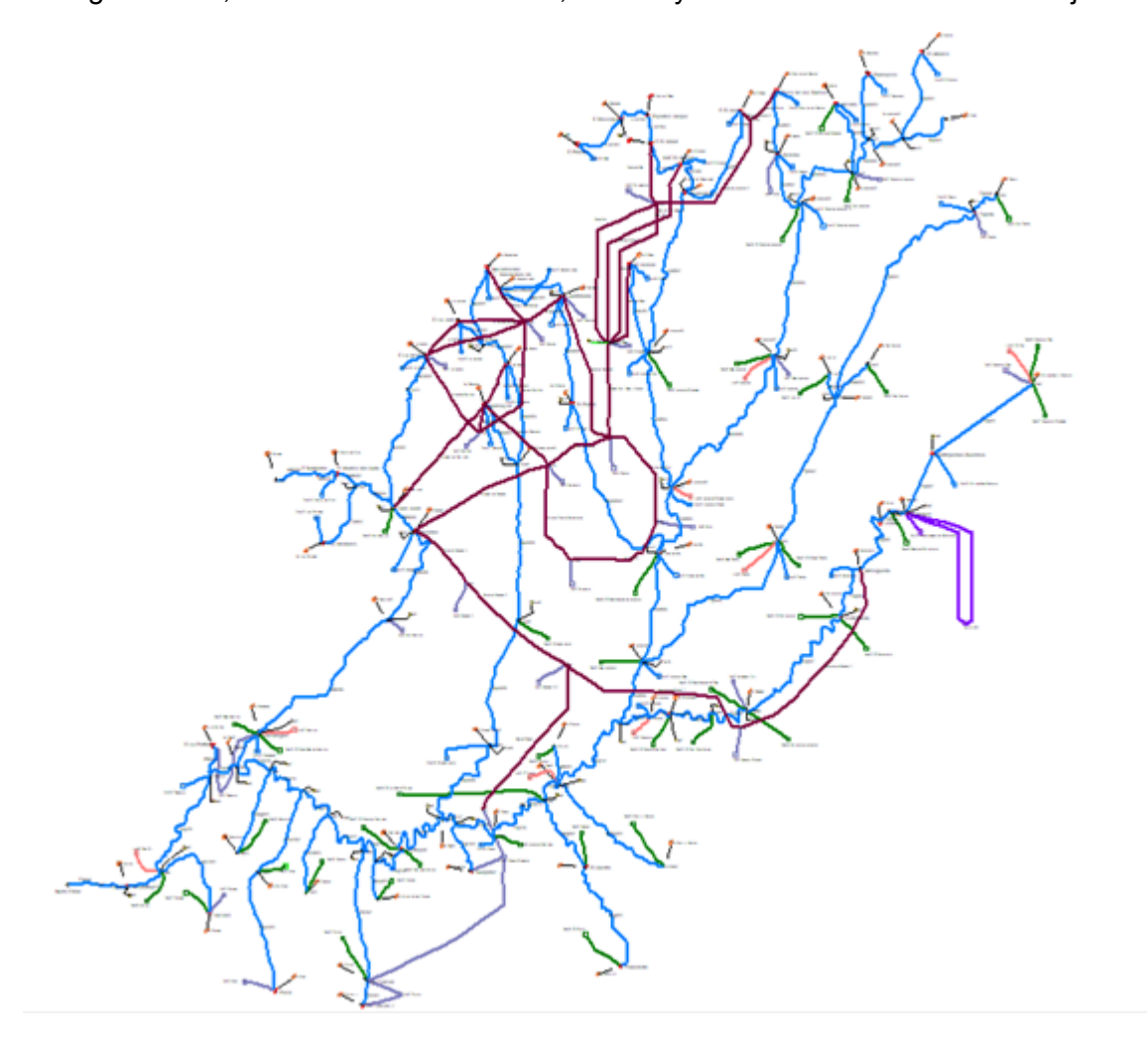


Figure 2.3.1.5. Aquatool model of the Upper Tagus Basin used in this study



The model built has 73 inflow nodes, 42 reservoirs, 110 demands, 94 river reaches, 33 pipelines and canales and 43 return points. The inflow data are shown in Table 2.3.1.3, the reservoir data are shown in Table 2.3.1.4 and the demand data are shown in Table 2.3.1.5.

Table 2.3.1.3. Inflows in the Aquatool model of the Upper Tagus Basin

Location	Flow hm³/yr	Location	Flow hm³/yr	Location	Flow hm³/yr	Location	Flow hm³/yr	Location	Flow hm³/yr	Location	Flow hm <sup>3</sup> /yr
EntBue	780.24	Atance	15.45	Riosequillo	39.90	Navalmedio	5.21	Cazalegas	61.53	Cedena	23.48
Bolarque	10.93	Palmaces	25.81	PuentesVieja	66.89	LaJarosa	7,47	Guaten	15.78	Pusa	19.44
Zorita	1.46	Alcorto	67.76	ElVillar	5.79	LasNieves	47.62	MartinRoma	21.99	RioPusa	21.35
Almoguera	11.08	PozoRamos	113.78	ElAtazar	41.04	Valmayor	23.68	Taj01	3.04	Sangrera	9.79
Estremera	4.31	Belena	11.77	Valdentales	36.22	Gua01	9.23	Finisterre	15.41	Taj03	19.56
Valdajos	18.47	Dulce	27.88	ElVellon	40.46	Gua02	19.17	Castro	4.56	LaPortina	1.40
Embocador	3.06	Hen01	19.81	Jar01	37.36	Burguitto	311.53	Toledo	9.59	Gevalo	29.24
Aranjuez	0.98	Hen02	7.59	Jar02	57.87	CharcoCura	3.01	Guajaraz	8.90	Azutan	76.67
Tajera	35.90	Hen03	4.67	Navacerrada	8.73	Acena	15.77	Taj02	10.15		li conserva
Ungria	13.72	Hen04	17,35	Santillana	82.89	Morales	2.55	Castrejon	4.73		
SanAndres	2.21	Hen05	25.82	ElPardo	37.88	SanJuan	123.12	Acuevas	2.33		
Tjn01	13.16	ElVado	138.08	ElRey	38.10	Picadas	6.91	Torcon2	4.30		
Tjn02	19.13	Pinilla	121.27	Jar03	19.57	Alb01	48.05	Torcon	15.16		

Table 2.3.1.4. Reservoirs in the Aquatool model of the Upper Tagus Basin



Identification	Vol (	hm³)	Sup					Evapo	ration ra	te mm/	month				
identification	Max	Min	(ha)	oct	nov	dec	jan	feb	mar	арг	may	jun	jul	aug	sep
E El Atance	34.8	2	209	65	<b>4</b> 0	25	20	35	55	80	90	115	165	160	80
E Pál maces	31	2	209	65	40	25	20	35	55	80	90	115	165	160	80
E <b>A</b> lcorlo	180	1	424	65	40	25	20	35	55	80	90	115	165	160	80
E Tajera	68	0.2	409	35	21	16	15	22	42	72	92	98	135	93	59
E Entrepeñas-Buendía	2358	118	10164	61	30	19	24	39	74	102	134	167	187	160	105
E Bolarque	30.7	21.9	514	71	37	30	27	38	59	74	88	109	164	160	105
E Zorita	2.6	1.1	57	71	37	30	27	38	59	74	88	109	164	160	105
E.Almoguera	6.5	0.2	186	71	37	30	27	38	59	74	88	109	164	160	105
E Estremera	0.45	0.1	28	71	37	30	27	38	59	74	88	109	164	160	105
E Pozo de los Ramos	1.1	0	350	65	<b>4</b> 0	25	20	35	55	80	90	115	165	160	80
E Bel eña	50	33	227	65	40	25	20	35	55	80	90	115	165	160	80
EEI Vado	43	5	223	65	40	25	20	35	55	80	90	115	165	160	80
EPinilla	38	25	376	75	50	<b>3</b> 0	30	30	40	55	80	105	135	135	110
E Riosequillo	49	35	265	75	50	30	30	30	40	55	80	105	135	135	110
E Puentes Viejas	49	25	250	75	50	30	30	30	40	55	80	105	135	135	110
E El Villar	22	10	119	75	50	<b>3</b> 0	30	30	40	55	80	105	135	135	110
E El Atazar	425	150	977	75	45	25	20	30	40	55	80	105	135	135	110
E El <b>V</b> ellón	41	10	380	75	45	25	20	30	40	55	80	105	135	135	110
E Santillana	91	5	985	90	55	35	30	45	60	75	95	130	155	150	125
E El Pardo	44	0.2	51	90	55	35	30	45	60	75	95	130	155	150	125
ENavacerrada	11	5	85	90	55	35	30	45	60	75	95	1 <b>3</b> 0	155	150	125
E La Jarosa	7.18	5	60	90	55	35	30	45	60	75	95	130	155	150	125
E Val mayor	124	10	562	90	55	35	30	45	60	75	95	130	155	150	125
ENavalmedio	0.71	0.2	7	90	55	35	30	45	60	75	95	130	155	150	125
E Finisterre	133	10	1050	71	37	30	27	38	59	74	88	109	164	160	105
E El Castro	7.6	3	120	71	37	30	27	38	59	74	88	109	164	160	105
E Guajaraz	25	2.5	115	99	51	50	40	56	74	108	146	216	233	245	183
E Castrejón	41	1	550	99	51	50	40	56	74	108	146	216	233	245	183
E El Torcón	6.8	2.5	58	99	51	50	40	56	74	108	146	216	233	245	183
E El Torcón II	6.8	2.5	58	99	51	50	40	56	74	108	146	216	233	245	183
E Pu <b>s</b> a	0.64	0.15	28	99	51	50	40	56	74	108	146	216	233	245	183
E Gévalo	22	5	319	99	51	50	40	56	74	108	146	216	233	245	183
E <b>A</b> zután	113	2	1013	99	51	50	40	56	74	108	146	216	233	245	183
E La Aceña	23	19	108	90	55	35	30	45	60	75	95	130	155	150	125
EBurquillo	98	20	803	72	33	22	22	32	101	126	159	234	242	210	120
E Charco del Cura	3.4	1.6	35	72	33	22	22	32	101	126	159	234	242	210	120
E San Juan	74	0.5	627	72	33	22	22	32	101	126	159	234	242	210	120
E Picadas	16	4	92	72	33	22	22	32	101	126	159	234	242	210	120
E Los Moral es	2.34	1	33	72	33	22	22	32	101	126	159	234	242	210	120
E Cazalegas	11	1	150	99	51	50	40	56	74	108	146	216	233	245	183
E La Portiña	5	0.1	90	99	51	50	40	56	74	108	146	216	233	245	183
E Val dental es	5	0.1	150	75	45	25	20	30	40	55	80	105	135	135	110

The simulations were performed for the period from the hydrologic year 1980-81 to the hydrologic year 2017-18, because these are the streamflow data available in the Tagus River Basin Management Plan. The objective of the simulations is to obtain the sequence of water transfer volumes that result from the operation of the system, ensuring that all local demands of the Tagus basin are fully satisfied before any transfer is allowed. The results are compared to historical data available relative to the actual volumes transferred to the Segura basin and the evolution of storage in the Entrepeñas and Buendía reservoirs. In order to obtain a meaningful comparison with the historical record, the initial condition of the system was set at the actual values for October 1980, when the joint storage in Entrepeñas and Buendía reservoirs was 1518.1 hm³ and the storage in Bolarque reservoir was 21.9 hm³.

Table 2.3.1.5. Demands in the Aquatool model of the Upper Tagus Basin



Urban and industria	ıl	Irrigation		Environmental flow	rs
Identification	Value hm³/yr	Identification	Value hm³/yr	Identification	Value hm³/yr
Ab22 Toledo-Guajaraz	12.26	Reg01 ZR Estremera	18.86	Qec01 Entrepeñas-Buendía	152.16
Ab12 Pino Alto	13.58	Reg02 ZR Real Acequia del Tajo	18.85	Qec02 Almoguera	189.21
Ab16 Este	71.76	Reg03 ZR Caz Chico-Azuda	13.59	Qec03 Aranjuez	189.21
Ab01 Cabecera Tajo	1.99	Reg04 ZR Canal de las Aves	37.06	Qec04 Tajera	9.75
Ab02 Algodor-Girasol	23.65	Reg05 ZR Almoguera	22.07	Qec05 Tajuña	27.19
Ab03 Ampliación CYII	7.37	Reg07 Cabecera Guadiela	17.48	Qec06 El Atance	3.97
Ab04 Tajuña	3.60	Reg06 Cabecera Tajo	11.98	Qec07 Pálmaces	2.60
Ab05 Cabecera Henares	0.75	Reg08 Bolarque-Estremera	4.12	Qec08 Alcorlo	6.30
Ab06 MAS	40.95	Reg09 Estremera-Jarama	41.26	Qec09 Pozo de los Ramos	14.80
Ab07 Bajo Henares	3.02	Reg10 ZR Medio Tajuña	12.65	Qec10 Beleña	15.98
Ab08 Torrelaguna	15.35	Reg11 Alto Tajuña	1.11	Qec11 Canal del Henares	54.33
Ab09 Guadatix	1.18	Reg12 Ungria	1.02	Qec12 Henares	67.69
Ab10 Colmenar	10.22	Reg13 San Andrés	2.81	Qec13 El Vado	14.25
Ab11 Reunión	28.33	Reg14 Bajo Tajuña	34.95	Qec14 Pinilla	27.72
Ab13 Noroeste	31.54	Reg15 ZR Bornova-Cogolludo	21.26	Qec15 El Atazar	39.50
Ab15 Suroeste	114.99	Reg16 ZR Canal del Henares	45.37	Qec16 Santillana	17.95
Ab14 Madrid	253.77	Reg17 Alto Henares	11.48	Qec17 El Pardo	25.27
Ab17 La Aceña	1.09	Reg18 Bajo Henares	24.47	Qec18 El Vellón	5.73
Ab18 Alto Alberche	6.86	Reg19 ZR Real Acequia del Jarama	99.68	Qec19 Jarama Alto	49.03
Ab19 Picadas 1	17.60	Reg20 Jarama-Guadalix	32.52	Qec20 Jarama Medio	63.57
Ab20 Picadas 2-3	5.41	Reg21 Guadarrama	15.93	Qec21 Presa del Rey	135.27
Ab21 Talavera	6.88	Reg22 Bajo Jarama	25.42	Qec22 Jarama Bajo	191.26
Ab23 Torcón	1.39	Reg23 ZR Canal Bajo del Alberche	68.19	Qec23 Navacerrada	1.70
Ab24 Pusa	1.32	Reg25 Bajo Alberche	22.60	Qec24 Navalmedio	1.15
Ab25 Gévalo	1.36	Reg24 Alto Alberche	15.68	Qec25 La Jarosa	0.98
Total urban	676.23	Reg26 ZR La Sagra-Torrijos	30.38	Qec26 Las Nieves	9.07
DOWN THE PARTY OF		Reg27 ZR Canal de Castrejón	51.59	Qec27 Valmayor	4.32
Ind01 CN Trillo	37.80	Reg28 ZR Mora	5.00	Qec28 Guadarrama	24.85
Ind02 CT Ateca	31.54	Reg29 Guatén	1.59	Qec29 La Aceña	2.96
Ind03 Cabecera	8.70	Reg30 Martin Roman	8.53	Qec30 Los Morales	0.24
Ind04 Tajuña	0.20	Reg31 Algodor	1.80	Qec31 Charco del Cura	20.85
Ind05 Henares	2.00	Reg32 Cuevas	1.52	Oec32 Picadas	30.69
Ind06 Jarama-Guadarrama	26.92	Reg33 Torcon	1.35	QEc33 Cazalegas	37.93
Ind07 Alberche	0.35	Reg34 Cedena	0.81	QEc34 Toledo	315.36
Ind08 Tajo MI	5.05	Reg35 Pusa	3.10	QEc35 Talavera	315.36
Total industrial	112.56	Reg36 Sangrera	1.11	Total environmental	2068.23
		Reg37 Gévalo	1.48		
		Reg38 Azután	4.80		
		Reg39 Jarama-Castrejón	65.70		
		Reg40 Castrejón-Azután	53.56		
		Total irrigation	852.72		

#### 2.3.1.6 Operating rules

In order to analyze the impact of the increase in minimum flows on the availability of water for the Tagus-Segura Transfer, it is necessary to take into consideration the exploitation of the section of the Tagus River between Bolarque and Aranjuez, which is carried out based on the guidelines established in Royal Decree 773/2014, of 12 September, which approves various regulations governing the transfer through the Tagus-Segura aqueduct. The operation is based on the setting of monthly levels based on the joint storage in the Entrepeñas and Buendía reservoirs and the inflows recorded in the last twelve months. For each of the four established levels, the rules that determine the volumes that are transferred monthly are defined.

The four operating levels are defined as follows:

**Level 1**: Is declared when storage in Entrepeñas and Buendía is larger than 1300 hm<sup>3</sup> or when inflow to the reservoirs in the last 12 months is larger than 1400 hm<sup>3</sup>/year. A water transfer of 60 hm<sup>3</sup>/month is authorized in this condition.



**Level 2**: Is declared when storage in Entrepeñas and Buendía is smaller than 1300 hm<sup>3</sup> and larger than monthly values presented in Table 2.3.1.6. A water transfer of 27 hm<sup>3</sup>/month is authorized in this condition.

Table 2.3.1.6: Minimum storage in Entrepeñas and Buendía to declare operating level 2.

Variable	oct	nov	dec	jan	feb	mar	apr	may	jun	jul	aug	sep
Storage (hm³)	613	609	605	602	597	591	586	645	673	688	661	631

**Level 3**: Is declared when storage in Entrepeñas and Buendía is smaller than monthly values presented in Table x and larger than 400 hm<sup>3</sup>. A water transfer of 20 hm<sup>3</sup>/month is authorized in this condition.

**Level 4**: Is declared when storage in Entrepeñas and Buendía is less than 400 hm<sup>3</sup>. No water transfer is authorized in this condition.

A table of "reference releases" is also established, which may not be exceeded by more than 25% during normal operation. The reference releases are presented in Table 2.3.1.7.

Table 2.3.1.7: Reference releases authorized from Entrepeñas and Buendía reservoirs.

Variable	oct	nov	dec	jan	feb	mar	apr	may	jun	jul	aug	sep
Flow (hm <sup>3</sup> /m)	25	18	19	19	18	23	23	31	42	60	51	36
Flow (m <sup>3</sup> /s)	9.3	6.9	7.1	7.1	7.4	8.6	8.9	11.6	16.2	22.4	19	13.9

Figure 2.3.1.6 shows a detail of the representation of the Tajo Segura transfer in the Aquatool model. The operating rules are represented through two intake elements. One element implements the restriction based on the cumulative inflows in the last 12 months and the other one implements the restriction based on the storage in the Entrepeñas and Buendía reservoirs.

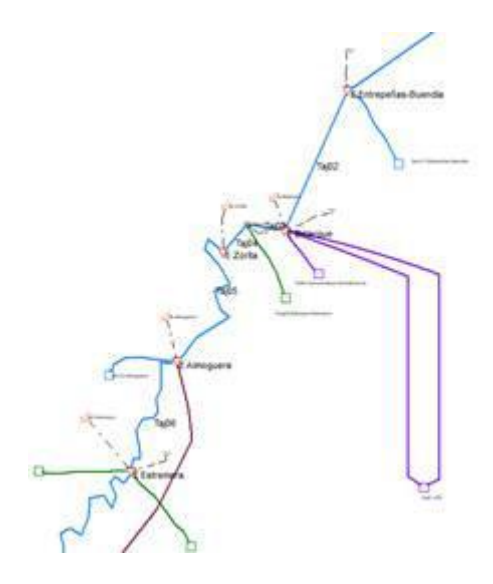


Figure 2.3.1.6. Detail of the Aquatool model showing the elements for the implementation of the operating rules of the Tagus-Segura water transfer

#### 2.3.1.7 Model results

Model results are presented in this section. First, the results of each of the two hypotheses analyzed are presented and then a comparison is presented.



#### 2.3.1.7.1 Simulation with minimum flows

The results for the simulation with the minimum flows prior to the approval of the Tagus River Basin Management Plan are presented in this section. All demands supplied from the Tagus River are fully satisfied, as shown in Table 2.3.1.8 for irrigation demands and Table 2.3.1.9 for non-irrigation demands. They not only comply with reliability criteria established in Spanish legislation; they do not show any deficit during the simulation.

Table 2.3.1.8. Results for irrigation demands in the simulation with minimum flows.

Irrigation demands	Annual Demand	Total Supplied	Average Deficit	Max Def 1 Year	Max Def 2 Years	Max Def 10 Years
inigation demands	hm <sup>3</sup>	hm <sup>3</sup>	hm <sup>3</sup>	%	%	%
Reg01 ZR Estremera	18.86	18.86	0.00	0.00	0.00	0.00
Reg02 ZR Real Acequia del Tajo	18.85	18.85	0.00	0.00	0.00	0.00
Reg03 ZR Caz Chico-Azuda	13.59	13.59	0.00	0.00	0.00	0.00
Reg04 ZR Canal de las Aves	37.06	37.06	0.00	0.00	0.00	0.00
Reg05 ZR Almoguera	22.07	22.07	0.00	0.00	0.00	0.00
Reg07 Cabecera Guadiela	17.48	17.48	0.00	0.00	0.00	0.00
Reg06 Cabecera Tajo	11.98	11.98	0.00	0.00	0.00	0.00
Reg08 Bolarque-Estremera	4.12	4.12	0.00	0.00	0.00	0.00
Reg09 Estremera-Jarama	41.26	41.26	0.00	0.00	0.00	0.00
Reg26 ZR La Sagra-Torrijos	30.38	30.38	0.00	0.00	0.00	0.00
Reg27 ZR Canal de Castrejón	51.59	51.59	0.00	0.00	0.00	0.00
Reg38 Azután	4.80	4.80	0.00	0.00	0.00	0.00
Reg39 Jarama-Castrejón	65.70	65.70	0.00	0.00	0.00	0.00

Table 2.3.1.9. Results for non-irrigation demands in the simulation with minimum flows.

Non-irrigation demands	Annual Demand hm³	Total Supplied hm <sup>3</sup>	Average Deficit hm³	Max Def 1 Month %	Max Def 10 Years %
Qec01 Entrepeñas-Buendía	152.16	152.16	0.00	0.00	0.00
Qec02 Al moguera	189.21	189.21	0.00	0.00	0.00
Qec03 Aranjuez	189.21	189.21	0.00	0.00	0.00
QEc34 Toledo	315.36	315.36	0.00	0.00	0.00
QEc35 Talavera	315.36	315.36	0.00	0.00	0.00
Ab01 Cabecera Tajo	1.99	1.99	0.00	0.00	0.00
Ab02 Algodor-Girasol	23.65	23.65	0.00	0.00	0.00
Ab03 Ampliación CYII	7.37	7.37	0.00	0.00	0.00
Ab22 Toledo-Guajaraz	12.26	12.26	0.00	0.00	0.00
Ab21 Talavera	6.88	6.88	0.00	0.00	0.00
Ind03 Cabecera	8.70	8.70	0.00	0.00	0.00
Ind 02 CT Ateca	31.54	31.54	0.00	0.00	0.00
Ind08 Tajo M	5.05	5.05	0.00	0.00	0.00

Figure 2.3.1.7 shows the annual releases to the Tagus River obtained in the simulation with minimum flows. The average required releases under this hypothesis are 333. 95 hm<sup>3</sup>/yr, with a minimum of 306.98 hm<sup>3</sup>/yr and a maximum 347.25 hm<sup>3</sup>/yr. All values are below the reference releases of 365 hm<sup>3</sup>/yr established in the current operating rules.

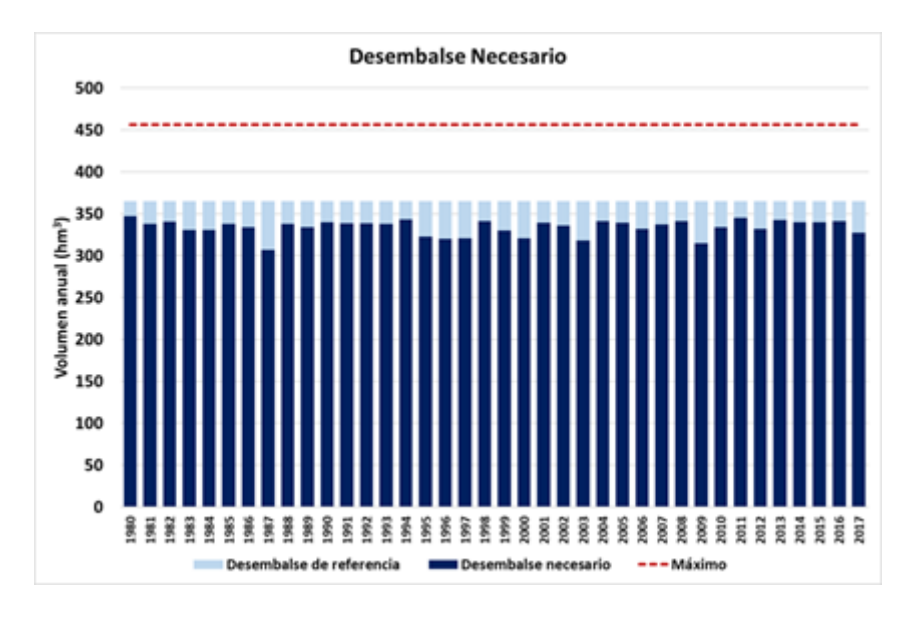


Figure 2.3.1.7. Required releases to the Tagus River for the simulation with minimum flows

Figure 2.3.1.8 shows the sequence of transfer volumes compared to the historical transfers. Under the simulated conditions, the water transfer is less than that recorded over the historical period. The average volume transferred in the simulation is 319.4 hm<sup>3</sup>/yr compared to an average of 333.54 hm<sup>3</sup>/yr recorded over the same period.

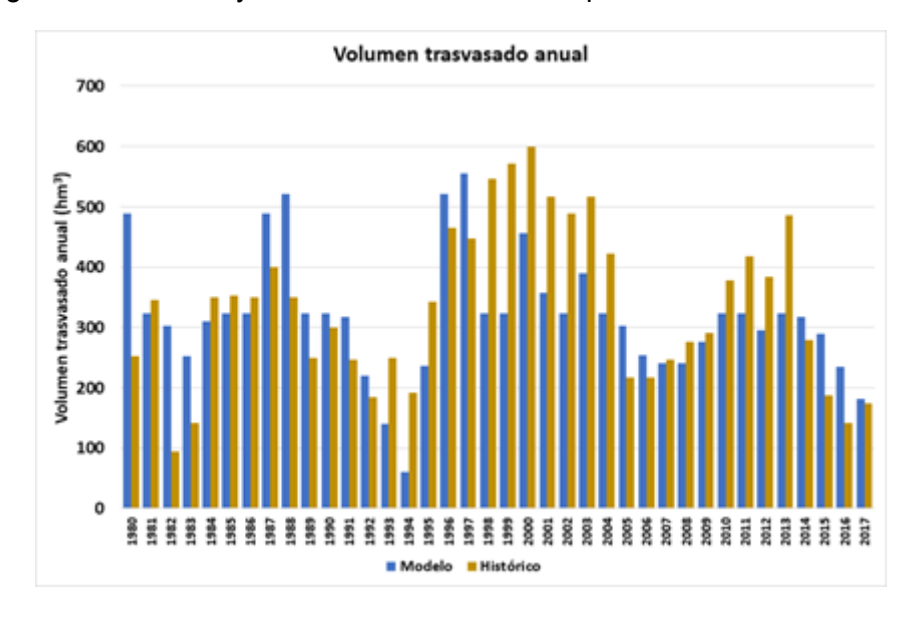


Figure 2.3.1.8. Transfer volumes for the simulation with minimum flows

Figure 2.3.1.9 shows the sequence of volumes stored in Entrepeñas and Buendía reservoirs compared to the historical record. Under the simulated conditions, reservoir storage is very similar, but slightly higher than that recorded over the historical period. The average storage volume in the simulation is 862.64 hm³ compared to an average of 826.9 hm³ recorded over the same period.

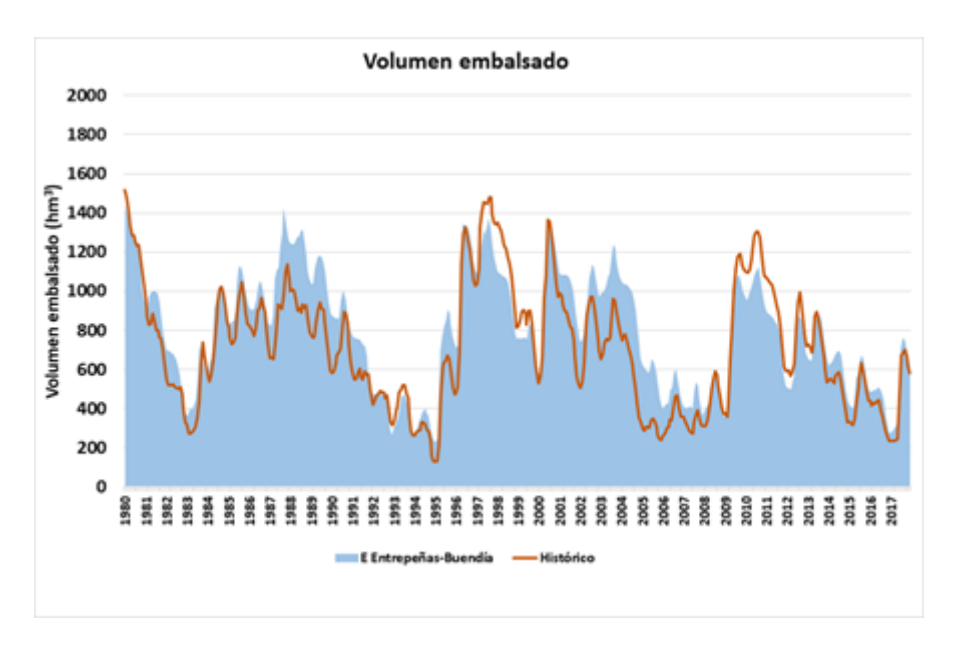


Figure 2.3.1.9. Stored volume for the simulation with minimum flows

Figure 2.3.1.10 shows the comparison between reservoir storage in Entrepeñas and Buendía reservoirs and monthly transfer volumes. It clearly shows how the transfer is restricted when reservoir volumes fall below those listed in Table 6.

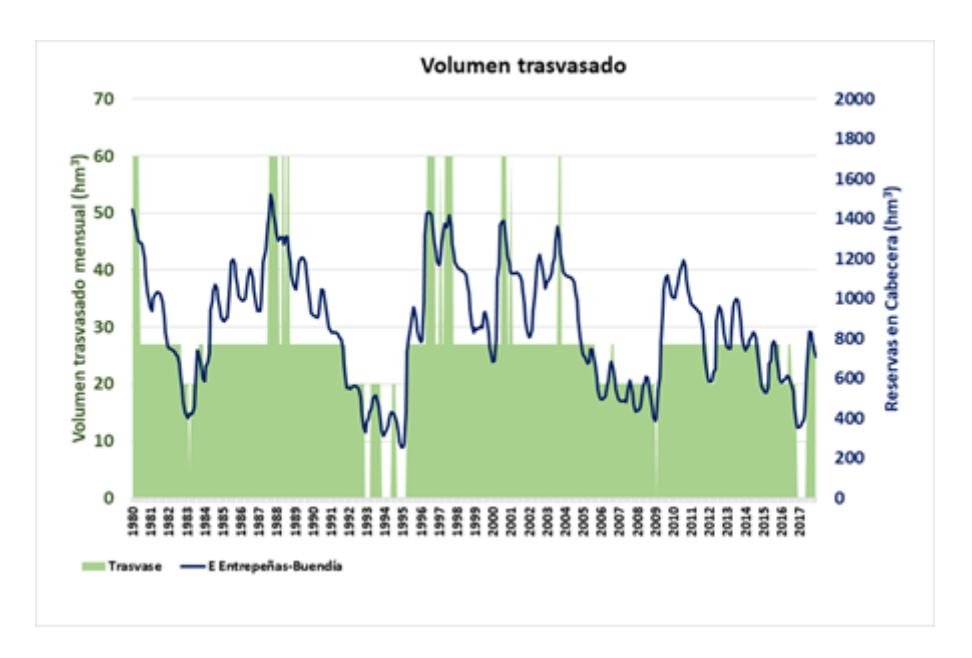


Figure 2.3.1.10. Comparison of stored volume and monthly water transfers for the simulation with minimum flows

Figure 2.3.1.11 illustrates the application of the operating rules. It shows the evolution of reservoir storage in Entrepeñas and Buendía reservoirs, using a color code to identify the operating levels, and the resulting restriction coefficient applied to the water transfer. The system is at level 1 during 7.89% of the time, allowing an average of 58.84 hm<sup>3</sup>/yr transferred under this condition. The duration of level 2 condition is 66.01% of the time, with an average transfer of 213.52 hm<sup>3</sup>/yr. The remaining 49.08 hm<sup>3</sup>/yr are transferred under level

3, which extends over 20.61% of the time. The system is at level 4 5.48% of the time, with no transfer allowed during those months.

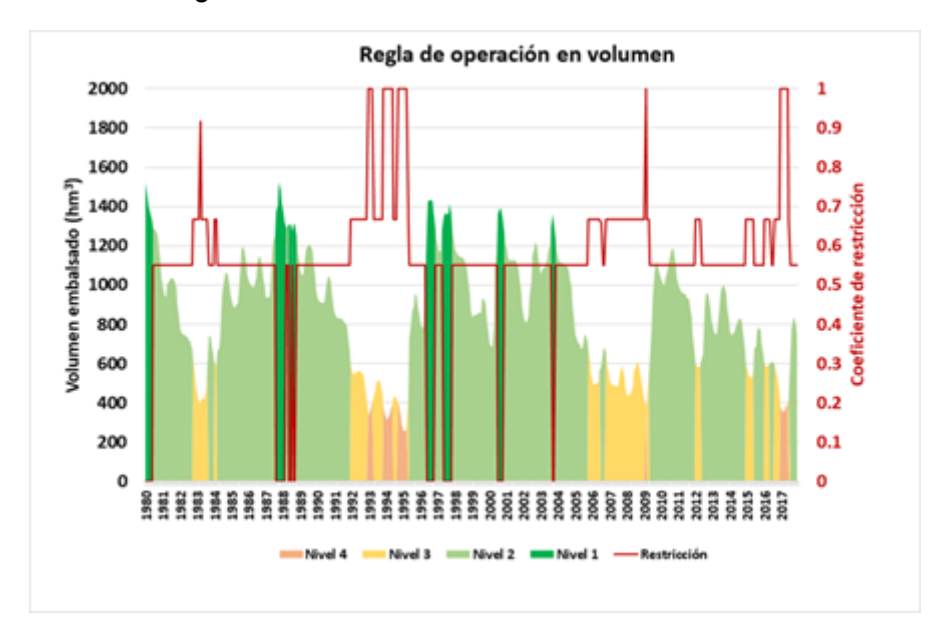


Figure 2.3.1.11. Result of the operating rule for the simulation with minimum flows

The summary of the water balance over the simulation with minimum flows is shown in Table 2.3.1.10. Bulk inflow to the headwaters system is 791.18 hm³/s. If the net water consumption upstream of the reservoirs is discounted, the net inflow to Entrepeñas and Buendía reservoirs is 747.97 hm³/yr. Outflows from the system are partitioned between releases to the Tagus River, 333.95 hm³/yr, water transfers, 319.44 hm³/yr, and evaporation losses, 115.80 hm³/yr. The difference in storage between the initial and the final month of the simulation represents a fictitious availability of 21.22 hm³/yr, which is really due to the emptying of the water initially stored in the reservoirs.

Table 2.3.1.10. Summary of water balance for the simulation with minimum flows.

Variable	Value (hm3)
Bulk inflow	791.18
Net consumption	43.20
Net inflow	747.97
Transferred volume	319.44
Evaporation	115.80
Reference releases	0.00
Additional releases	333.95
Initial storage	1540.00
Final storage	733.71
Change in storage	-21.22

#### 2.3.1.7.2 Simulation with ecological flows

The results for the simulation with the ecological flows imposed in the Tagus River Basin Management Plan are presented in this section. All demands supplied from the Tagus River are fully satisfied, as shown in Table 2.3.1.11 for irrigation demands and Table 2.3.1.12 for non-irrigation demands. They not only comply with reliability criteria established in Spanish legislation; they do not have any deficit during the simulation.



Table 2.3.1.11. Results for irrigation demands in the simulation with ecological flows.

Irrigation demands	Annual Demand	Total Supplied	Average Deficit	Max Def 1 Year	Max Def 2 Years	Max Def 10 Years
	hm <sup>3</sup>	hm³	hm <sup>3</sup>	%	%	%
Reg01 ZR Estremera	18.86	18.86	0.00	0.00	0.00	0.00
Reg02 ZR Real Acequia del Tajo	18.85	18.85	0.00	0.00	0.00	0.00
Reg03 ZR Caz Chico-Azuda	13.59	13.59	0.00	0.00	0.00	0.00
Reg04 ZR Canal de las Aves	37.06	37.06	0.00	0.00	0.00	0.00
Reg05 ZR Almoguera	22.07	22.07	0.00	0.00	0.00	0.00
Reg07 Cabecera Guadiela	17.48	17.48	0.00	0.00	0.00	0.00
Reg06 Cabecera Tajo	11.98	11.98	0.00	0.00	0.00	0.00
Reg08 Bolarque-Estremera	4.12	4.12	0.00	0.00	0.00	0.00
Reg09 Estremera-Jarama	41.26	41.26	0.00	0.00	0.00	0.00
Reg26 ZR La Sagra-Torrijos	30.38	30.38	0.00	0.00	0.00	0.00
Reg27 ZR Canal de Castrejón	51.59	51.59	0.00	0.00	0.00	0.00
Reg38 Azután	4.80	4.80	0.00	0.00	0.00	0.00
Reg39 Jarama-Castrejón	65.70	65.70	0.00	0.00	0.00	0.00

Table 2.3.1.12. Results for non-irrigation demands in the simulation with ecological flows.

Non-irrigation demands	Annual Demand	d Supplied Defic		Max Def 1 Month		
	hm <sup>3</sup>	hm <sup>3</sup>	hm <sup>3</sup>	%	%	
Qec01 Entrepeñas-Buendía	152.16	152.16	0.00	0.00	0.00	
Qec02 Almoguera	270.87	270.87	0.00	0.00	0.00	
Qec03 Aranjuez	272.44	272.44	0.00	0.00	0.00	
QEc34 Toledo	535.16	535.16	0.00	0.00	0.00	
QEc35 Talavera	567.04	567.04	0.00	0.00	0.00	
Ab01 Cabecera Tajo	1.99	1.99	0.00	0.00	0.00	
Ab02 Algodor-Girasol	23.65	23.65	0.00	0.00	0.00	
Ab03 Ampliación CYII	7.37	7.37	0.00	0.00	0.00	
Ab22 Toledo-Guajaraz	12.26	12.26	0.00	0.00	0.00	
Ab21 Talavera	6.88	6.88	0.00	0.00	0.00	
Ind03 Cabecera	8.70	8.70	0.00	0.00	0.00	
Ind02 CT Ateca	31.54	31.54	0.00	0.00	0.00	
Ind08 Tajo MI	5.05	5.05	0.00	0.00	0.00	

Figure 2.3.1.12 shows the annual releases to the Tagus River obtained in the simulation with ecological flows. The average required releases under this hypothesis are 416.28 hm³/yr, with a maximum 427.61 hm³/yr. All values are below the maximum allowed increment of 25% over the reference releases, 365 hm³/yr, established in the current operating rules, marked with a dashed red line in the figure.

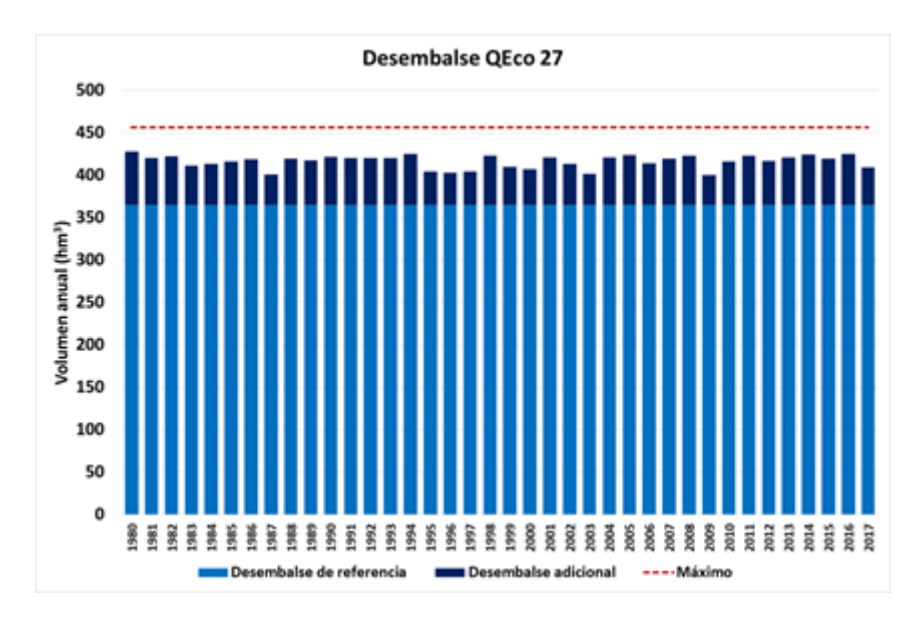


Figure 2.3.1.12. Required releases to the Tagus River for the simulation with ecological flows

Figure 2.3.1.13 shows the sequence of transfer volumes compared to the historical transfers. Under the simulated conditions, the transfer is less than that recorded over the historical period. The average volume transferred in the simulation is 248.68 hm<sup>3</sup>/yr compared to an average of 333.54 hm<sup>3</sup>/yr recorded over the same period.

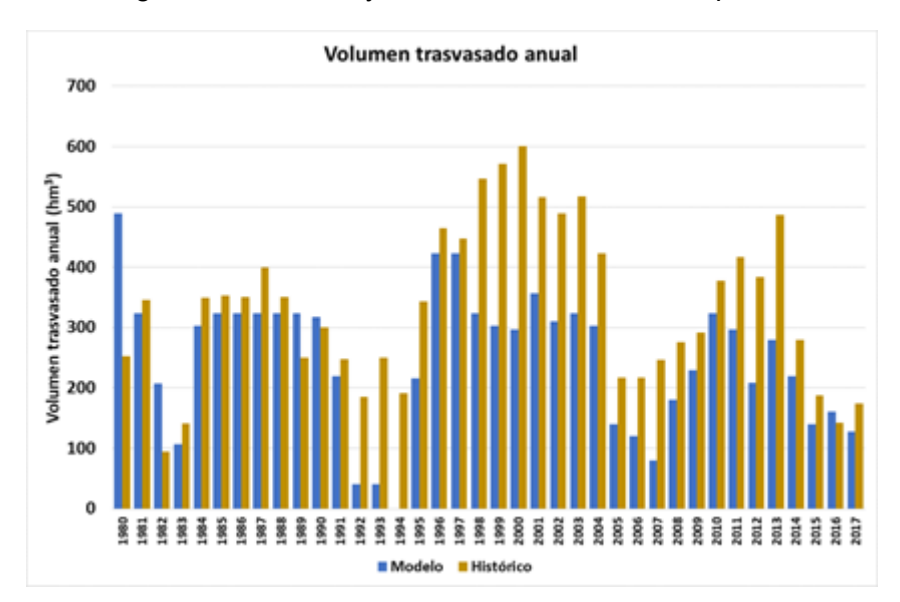


Figure 2.3.1.13. Transfer volumes for the simulation with ecological flows

Figure 2.3.1.14 shows the sequence of volumes stored in Entrepeñas and Buendía reservoirs compared to the historical record. Under the simulated conditions, reservoir storage is much lower than that recorded over the historical period. The average storage volume in the simulation is 692.51 hm³ compared to an average of 826.9 hm³ recorded over the same period.

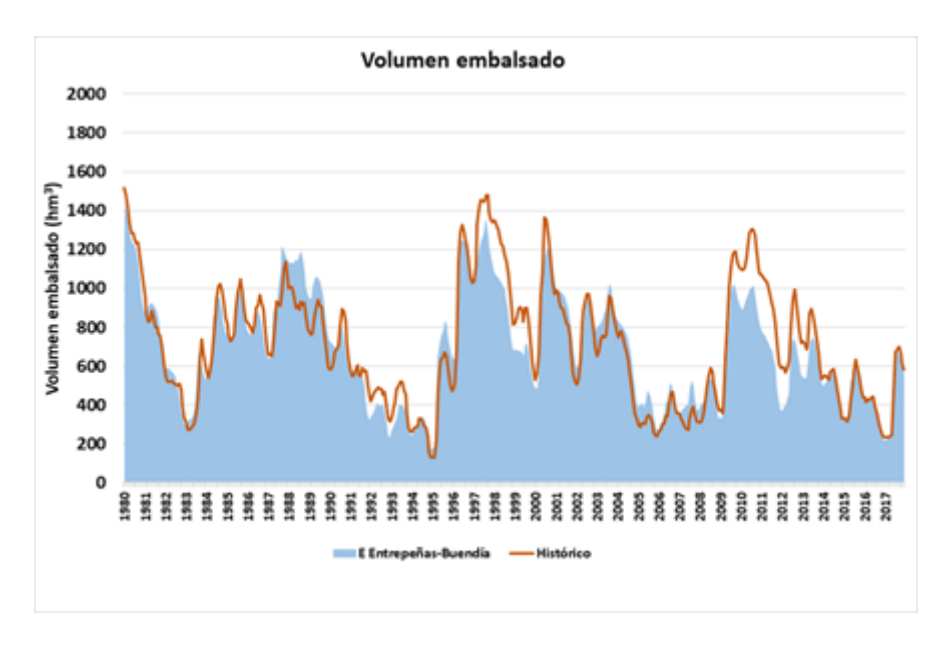


Figure 2.3.1.14. Stored volume for the simulation with ecological flows

Figure 2.3.1.15 shows the comparison between reservoir storage in Entrepeñas and Buendía reservoirs and monthly transfer volumes. It clearly shows that the transfer is restricted more often than in the simulation with minimum flows.

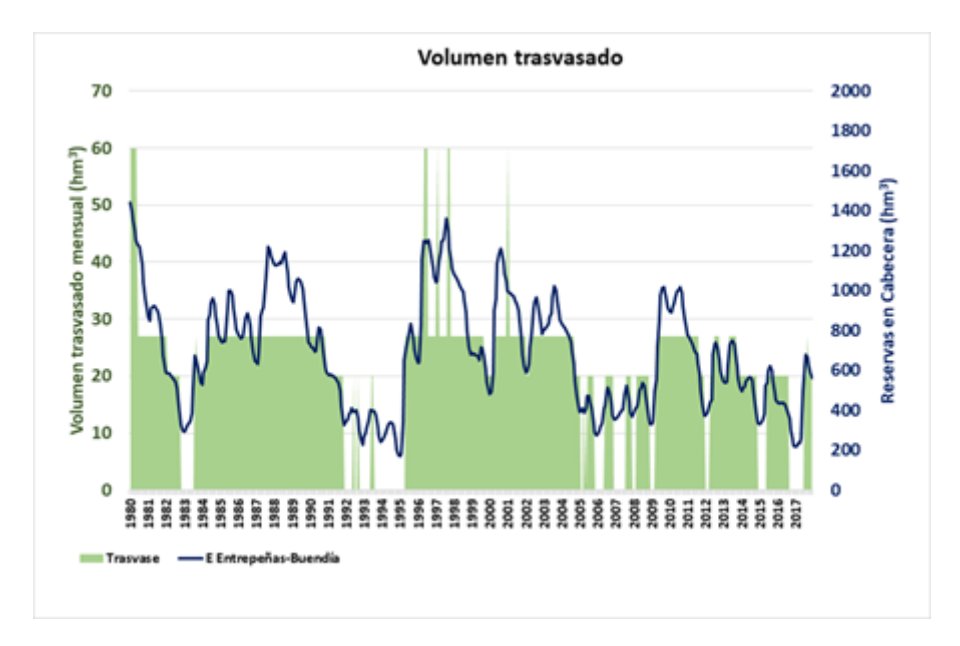


Figure 2.3.1.15. Comparison of stored volume and monthly water transfers for the simulation with ecological flows

Figure 2.3.1.16 illustrates the application of the operating rules. It shows the evolution of reservoir storage in Entrepeñas and Buendía reservoirs, using a color code to identify the operating levels, and the resulting restriction coefficient applied to the water transfer. The system is at level 1 during 2.63% of the time, allowing an average of 18.95 hm³/yr transferred under this condition. The duration of level 2 condition is 51.75% of the time, with an average transfer of 167.63 hm³/yr. The remaining 62.11 hm³/yr are transferred under level 3, which extends over 25.88% of the time. The system is at level 4 19.74% of the time, with no transfer allowed during those months.

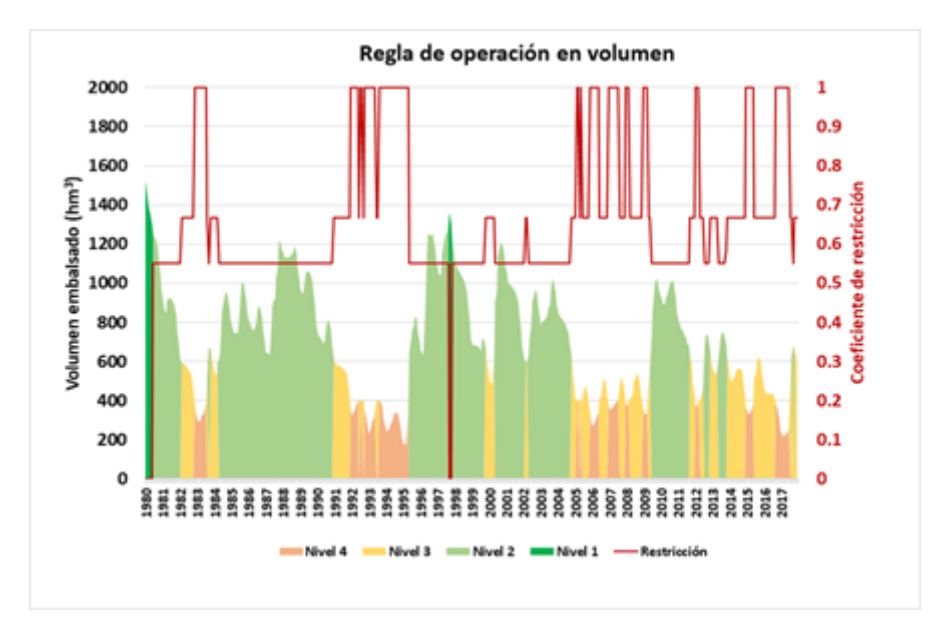


Figure 2.3.1.16. Result of the operating rule for the simulation with ecological flows

The summary of the water balance over the simulation with ecological flows is shown in Table 2.3.1.13. Bulk inflow to the headwaters system is 791.18 hm³/s. If the net water consumption upstream of the reservoirs is discounted, the net inflow to Entrepeñas and Buendía reservoirs is 747.97 hm³/yr. Outflows from the system are partitioned between releases to the Tagus river, 416.28 hm³/yr, water transfers, 248.68 hm³/yr, and evaporation losses, 108.20 hm³/yr. The difference in storage between the initial and the final month of the simulation represents a fictitious availability of 25.19 hm³/yr, which is really due to the emptying of the water initially stored in the reservoirs.

Table 2.3.1.13. Summary of water balance for the simulation with ecological flows.

Variable	Value (hm3)
Bulk inflow	791.18
Net consumption	43.20
Netinflow	747.97
Transferred volume	248.68
Evaporation	108.20
Reference releases	365.00
Additional releases	51.28
Initial storage	1540.00
Final storage	582.61
Change in storage	-25.19

#### 2.3.1.7.3 Comparison of the two hypotheses analyzed

The comparison of the two hypotheses analyzed is presented in this section. The hypothesis of minimum flows is identified as *QMin21DN* and the hypotheses of ecological flows is identified as *QEco21*. Figure 2.3.1.17 shows the comparison of volume stored in the reservoirs of Entrepeñas and Buendía during the simulation. Reservoir level is higher during the operation with minimum flows. The average reservoir level under the hypothesis of

minimum flows is 862.64 hm³ while the average reservoir level under the hypothesis of ecological flows is 692.51 hm³, a difference of 170.13 hm³.

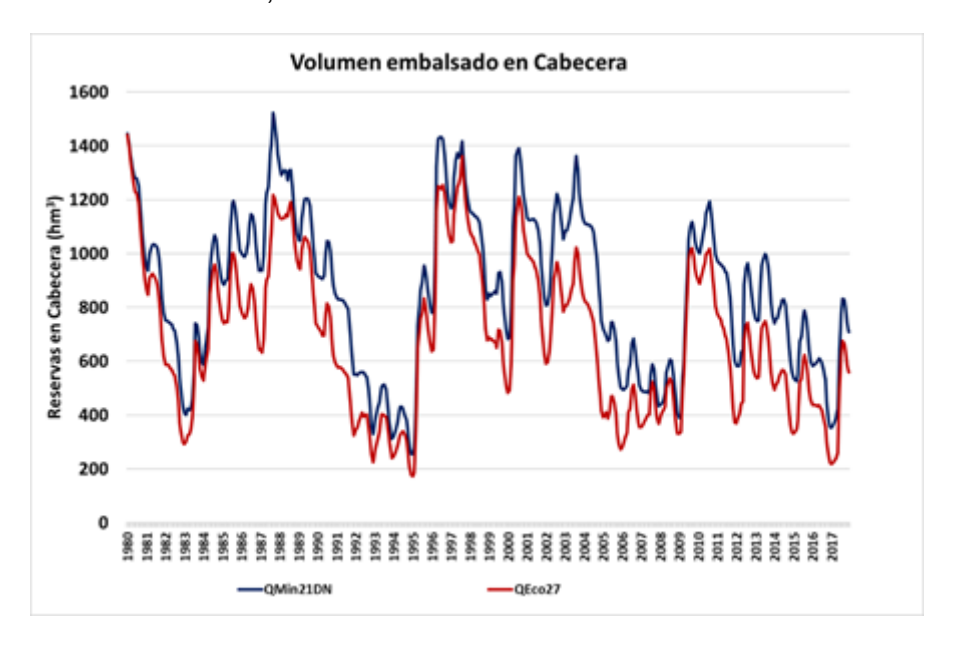


Figure 2.3.1.17. Comparison of stored volume

Figure 2.3.1.18 shows the comparison of monthly transferred volumes during the simulation. Reservoir level is higher during the operation with minimum flows. The higher reservoir levels imply that restrictions are applied less frequently and therefore the transferred volumes are higher under the hypothesis of minimum flows. There is a total of 176 months in which the transfer is larger for the hypothesis of minimum flows than for the hypothesis of environmental flows. In 24 months, the transfer is reduced by 33 hm³, in 3 months the transfer is reduced by 27 hm³, in 61 months the transfer is reduced by 20 hm³, in 84 months the transfer is reduced by 7 hm³ and in 4 months the transfer is reduced by less than 5 hm³. The total difference is 2688.85 hm³, which corresponds to an average transfer reduction of 70.76 hm³/yr over the 38 years of simulation.

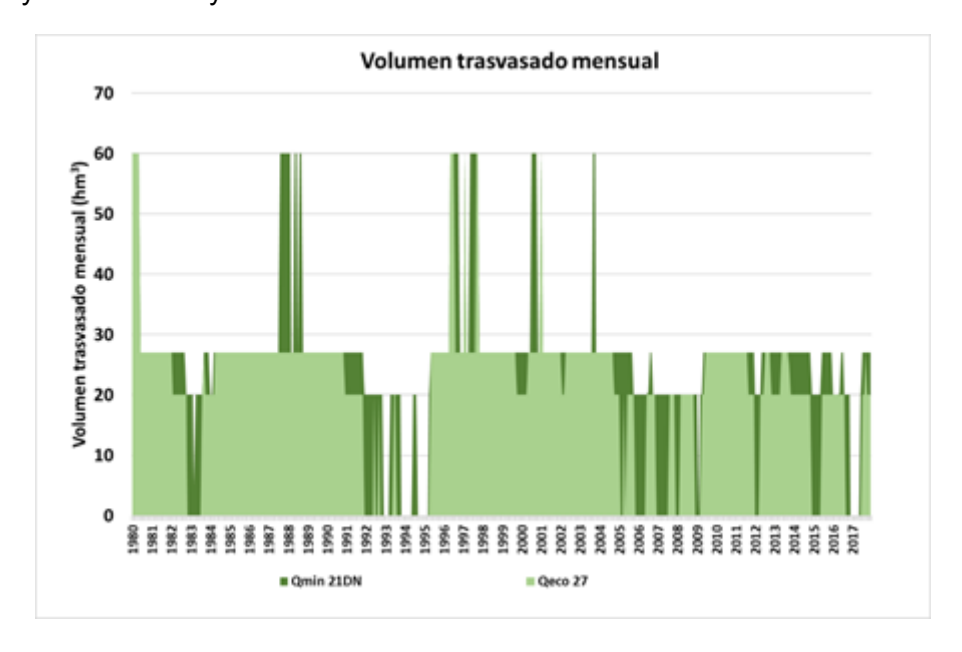


Figure 2.3.1.18. Comparison of monthly transferred volumes



Figure 2.3.1.19 shows the comparison of annual transferred volumes during the simulation. There are only 8 years in which the transferred volumes are equal under both hypotheses. In the remaining 30 years, the transferred volumes are larger for the minimum flow hypothesis than for the ecological flow hypothesis. The maximum difference of annual transferred volume is 198 hm³. There are 6 years in which the difference is larger than 150 hm³, 4 years in which the difference is between 100 hm³ and 150 hm³, 11 years in which the difference is between 50 hm³ and 100 hm³ and 9 years in which the difference is less than 50 hm³.

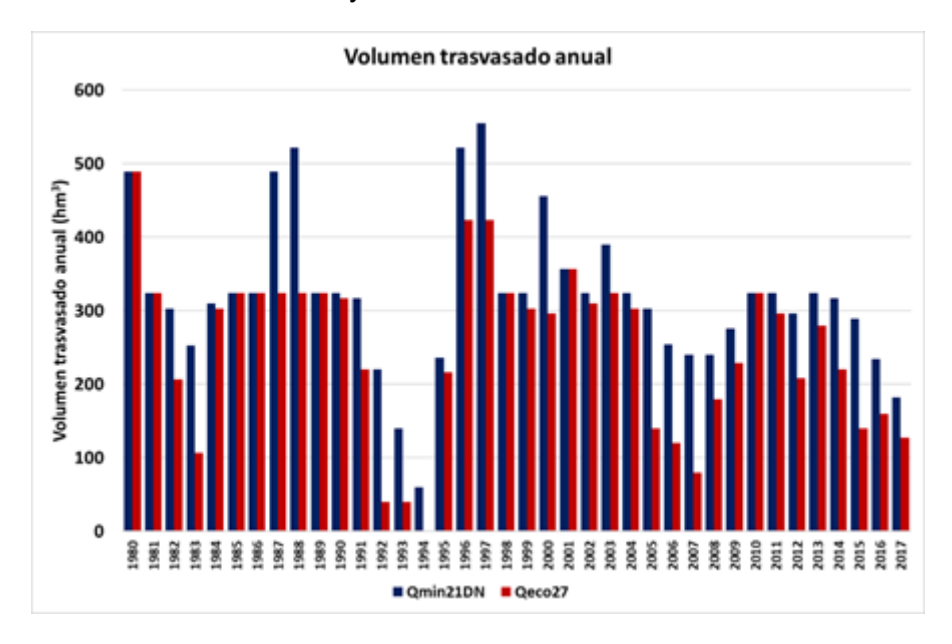


Figure 2.3.1.19. Comparison of annual transferred volumes

The summary of the comparison is presented in Table 2.3.1.14. The difference between minimum flow and ecological flow is 81.66 hm³/yr in Almoguera and 83.23 hm³/yr in Aranjuez. This increase translates into a reduction of water transfer of 70.76 hm³/yr. The difference is because of evaporation and final storage. The ecological flow hypothesis implies lower reservoir volumes, which translates into 7.60 hm³/yr less evaporation. At the end of the simulation, there is 151.10 hm³ less water stored in the reservoirs, which corresponds to an average of 3.98 hm³/yr due to net release from the reservoirs.

Table 2.3.1.14. Summary of the comparison of the two hypotheses analyzed.

Minimum flows	Value
IVIIIIIIIIIIIIIIIIIII	(hm³)
Bulkinflow	791.18
Net consumption	43.20
Netinflow	747.97
Transferred volume	319.44
Evaporation	115.80
Reference releases	0.00
Additional releases	333.95
Initial storage	1540.00
Final storage	733.71
Change in storage	-21.22

Ecological flours	Value
Ecological flows	(hm³)
Bulkinflow	791.18
Net consumption	43.20
Netinflow	747.97
Transferred volume	248.68
Evaporation	108.20
Reference releases	365.00
Additional releases	51.28
Initial storage	1540.00
Final storage	582.61
Change in storage	-25.19

n.iee	Value
Difference	(hm³)
Bulkinflow	0.00
Net consumption	0.00
Netinflow	0.00
Transferred volume	-70.76
Evaporation	-7.60
Reference releases	365.00
Additional releases	-282.67
Initial storage	0.00
Final storage	-151.10
Change in storage	-3.98

To avoid the effect of the net release from the reservoirs, simulations were performed in which the initial storage was set to the same value as the final storage, thus avoiding net release. The results of the comparison are presented in Table 2.3.1.15. The difference in transferred volume is 73.37 hm<sup>3</sup>/yr and the difference in evaporation is 8.92 hm<sup>3</sup>/yr. It should



be noted that, in order to obtain the same initial and final storage, the initial storage has to be set 149.70 hm<sup>3</sup> larger in the minimum flow hypothesis than in the ecological flow hypothesis.

Table 2.3.1.15. Summary of the comparison of the two hypotheses analyzed without net release from the reservoirs.

Minimum flows	Value
IVINIMUM HOWS	(hm³)
Bulkinflow	791.18
Netconsumption	43.20
Netinflow	747.97
Transferred volume	300.33
Evaporation	113.82
Reference releases	0.00
Additional releases	333.80
Initial storage	734.30
Final storage	735.22
Change in storage	0.02

Ecological flows	Value (hm³)
Bulk inflow	791.18
Net consumption	43.20
Netinflow	747.97
Transferred volume	226.96
Evaporation	104.91
Reference releases	365.00
Additional releases	51.13
Initial storage	584.60
Final storage	583.63
Change in storage	-0.03

Difference	Value (hm³)
Bulkinflow	0.00
Net consumption	0.00
Netinflow	0.00
Transferred volume	-73.37
Evaporation	-8.92
Reference releases	365.00
Additional releases	-282.67
Initial storage	-149.70
Final storage	-151.59
Change in storage	-0.05

#### 2.3.1.7.4 Conclusion

The reservoir release regime required to meet ecological flows and water demands within the Tagus River basin directly, though not immediately, affects the volumes available for the Tagus-Segura Water Transfer. This impact assessment assumes that the headwaters system functions as a closed system. Given that reservoir storage levels are typically low relative to their capacity, the likelihood of spills is minimal. Therefore, inflows to the reservoirs can only be allocated in three ways: to satisfy the Tagus basin's ecological flows and water demands, to be transferred, or to be lost through evaporation.

An increase in ecological flow requirements by 82 hm³/year results in a corresponding reduction of 73 hm³/year in transferable water. This discrepancy of 9 hm³/year is attributed to increased evaporation losses, which stem from operating the reservoirs at lower levels due to higher releases within the Tagus basin.

System operating rules define storage thresholds that determine the volume eligible for transfer each month. If these rules are adjusted to maintain reservoir levels similar to those seen in recent years, the reduction in transfer volumes would match the increase in ecological flow requirements. Although there may be a temporal lag between increased releases for the Tagus basin and the observed reduction in transfer volumes, the closed nature of the system ensures that this reduction will ultimately occur and in an amount equivalent to the additional releases.

#### 2.3.2 ITALY

In Italy, stakeholders expressed concern about increasing water availability during the peak crop growing season. They recommended exploring the potential of small reservoirs to meet high seasonal demand. In response, we updated the modelling for the Orcia Living Lab to incorporate small reservoirs (SMAR), following an initial review of the state-of-the-art and key input data used to calibrate and validate the SWAT model. Compared to the approach presented in Section 3.1.1, the updated version now explicitly integrates SMAR as detailed below.



#### 2.3.2.1 State of the art

The Val d'Orcia LL is located in the South of Tuscany and corresponds to the watershed of Orcia river, which downstream flows into the Ombrone river. The basin has a total area of 748 km2 and average annual precipitation of 715 mm. Its climate is classified as CSa, BSh, BSk according to Koppen and Geiger classification.

In this area, 4177 farms are present, many of them also have an important tourist vocation. Wide agricultural fields characterize this watershed, and the main crops are cereals, forages and tree crops (mainly olive groves and vineyards). Winter durum wheat is considered an important quality production and is the most common type of cultivation. Wine production is also an important asset of the territory with several excellence productions. Due to the extensive agricultural practices, the semi-natural vegetation is reduced to a few rare patches of woodland in the tributaries, to sparse herbaceous and shrub formations and to more extensive woodland coverings in the upland areas.

While previously agriculture in Val d'Orcia was mainly rainfed, now emergency irrigation is common in summer, when dry spells are becoming increasingly frequent due to climate change (Bartolini et al., 2022). This requires having additional water ready to be used in summer, and many farms are evaluating rainwater harvesting to irrigate their fields, as groundwater is hardly accessible and usable. Recently, the construction of a big water reservoir in San Piero in Campo was authorized to increase water availability in the area (La Nazione, 02/03/2023, President of reclamation consortium "Toscana Sud", personal communication). The main current challenges related to water in the Living Lab are: the distribution of water coming from public structures, the difficulties in restoring and building new water storages, and the need to shift from a farm-scale water management to a community-scale management.

#### 2.3.2.2 The SWAT model for Italy

#### 2.3.2.2.1 Model set up

We first reported the specific local data collected for the Italian LL in the following Table 2.3.2.1 (e.g., DEM, land use, soil properties, climate, and hydrological data).

Table 2.3.2.1 - Input data for the SWAT+ model for the Italian LL along with description and source

Input	Description	Source
DEM	Hydrological DEM of the Tuscany region (10 m resolution)	https://dati.toscana.it/dataset/dem10mt
Land use	2018 Corine Land Cover and Land Use map from the Copernicus Land Monitoring Service	https://land.copernicus.eu/en/products/corine-land -cover/clc2018



Soil map	Pedological Database of the Tuscany Region	https://dati.toscana.it/dataset/dbped
Climate	Regional Hydrological Service (SIR) of the Tuscany region	https://www.sir.toscana.it/consistenza-rete
Observation s	<ul> <li>Actual evapotranspiration from MOD16A2, aggregated at basin scale.</li> <li>Monthly streamflow at the Monte Amiata Scalo gauging station</li> </ul>	https://lpdaac.usgs.gov/products/mod16a2gfv006/
River network	Shapefile produced by the Tuscany region	https://www.regione.toscana.it/-/reticolo-idrografic o-e-di-gestione
Non-convent ional water	Shapefile with reservoirs produced by Lamma	https://www.lamma.toscana.it/
Additional land use information	ARTEA agency of the Tuscany region	https://dati.toscana.it/dataset/artea-piani-colturali- grafici-2022
Irrigation information	6th agricultural census (ISTAT, 2010)	http://dati-censimentoagricoltura.istat.it/Index.asp x
Planned large dam	Shapefile realized with information provided by Consorzio Bonifica 6	

We used SWAT+ version 60.5.4. The specific tools employed include: (1) QSWAT+ v2.4.0 for watershed delineation and creation of Hydrological Response Units (HRUs), (2) SWAT+Editor v2.3.3 for integrating climate data and modifying land use, crop types, management practices, and reservoir characteristics, and (3) the SWAT+Toolbox for calibration and validation. The simulation covers the period from 2010 to 2020, with a one-year warm-up period.

For watershed delineation, we used the DEM and river network provided by the Tuscany Region in QSWAT+. In the "complex" model setup, channel and stream thresholds were set to 5 and 200 ha, respectively, and subbasins smaller than 150 ha were merged, as well as short channels representing less than 10% of the subbasin. The Corine land use and soil maps, developed from Tuscany Region data (details in Villani et al., 2024), were used to create the HRUs. These HRUs were divided into three slope classes: 0-5%, 5-20%, and >20%. To enhance the accuracy of the representation of irrigated and rainfed croplands,



olive, grapevine, and general agricultural land were split based on catchment-scale data from ISTAT (2010) and ARTEA (2022).

We used QGIS to review the 1097 Small and Medium-sized Agricultural Reservoirs (SmARs) in the shapefile provided by the Lamma consortium. To ensure most SmARs were located on the channel network during watershed delineation in QSWAT+, we used the smallest threshold possible. A threshold of 5 ha was finally chosen, as using 1 ha caused errors during HRU creation. The stream threshold was less critical and was set at 200 ha.

Out of the original 1097 SmARs, we included 358 in the model. Of these, only 177 were directly positioned on the channel network. For those falling outside the network, we applied the following criteria to determine if they could be moved closer to the channel:

- The reservoir could be relocated to a "channel" as delineated by SWAT+ (but never to a SWAT+ "stream", which corresponds to the main rivers and largest tributaries).
- The reservoir had a reasonable upstream area. Practically, if it was distant from subbasin borders.
- It was clear which channel it could be moved to.
- The distance between the reservoir and the channel was no more than 150 m for reservoirs with an area larger than 400 m<sup>2</sup>.
- The distance between the reservoir and the channel was no more than 80 m for reservoirs with an area smaller than 400 m<sup>2</sup>.

While these criteria were largely followed, some subjective interpretation was necessary (see Fig. 2.3.2.2). Satellite imagery and the detailed channel network from the Tuscany region were used to inform decisions. Additionally, nearby reservoirs were grouped when applicable. In the end, we included 358 SmARs, of which 29 were merged with nearby larger reservoirs, and 152 were slightly relocated to the channel network. This resulted in a final total of 329 SmARs in the model.

Reservoir areas were derived from the shapefile, and reservoir volumes were calculated using the formula from Giambastiani et al. (2020) for small and medium reservoirs in Tuscany:

Reservoir volume  $(m^3) = 4.19 \times Reservoir surface <math>(m^2)$ 

A total of six alternative model setups were prepared to take into account the uncertainty in the SmARs representation, to simulate alternative water storage strategies (SmARs and planned large dam) and to calibrate and validate the model. Their characteristics are shown in Table 2.3.2.2. The simplified and complex models were used in the calibration and validation phase, while the others were used to compare different types of water storage in current and future climate scenarios.

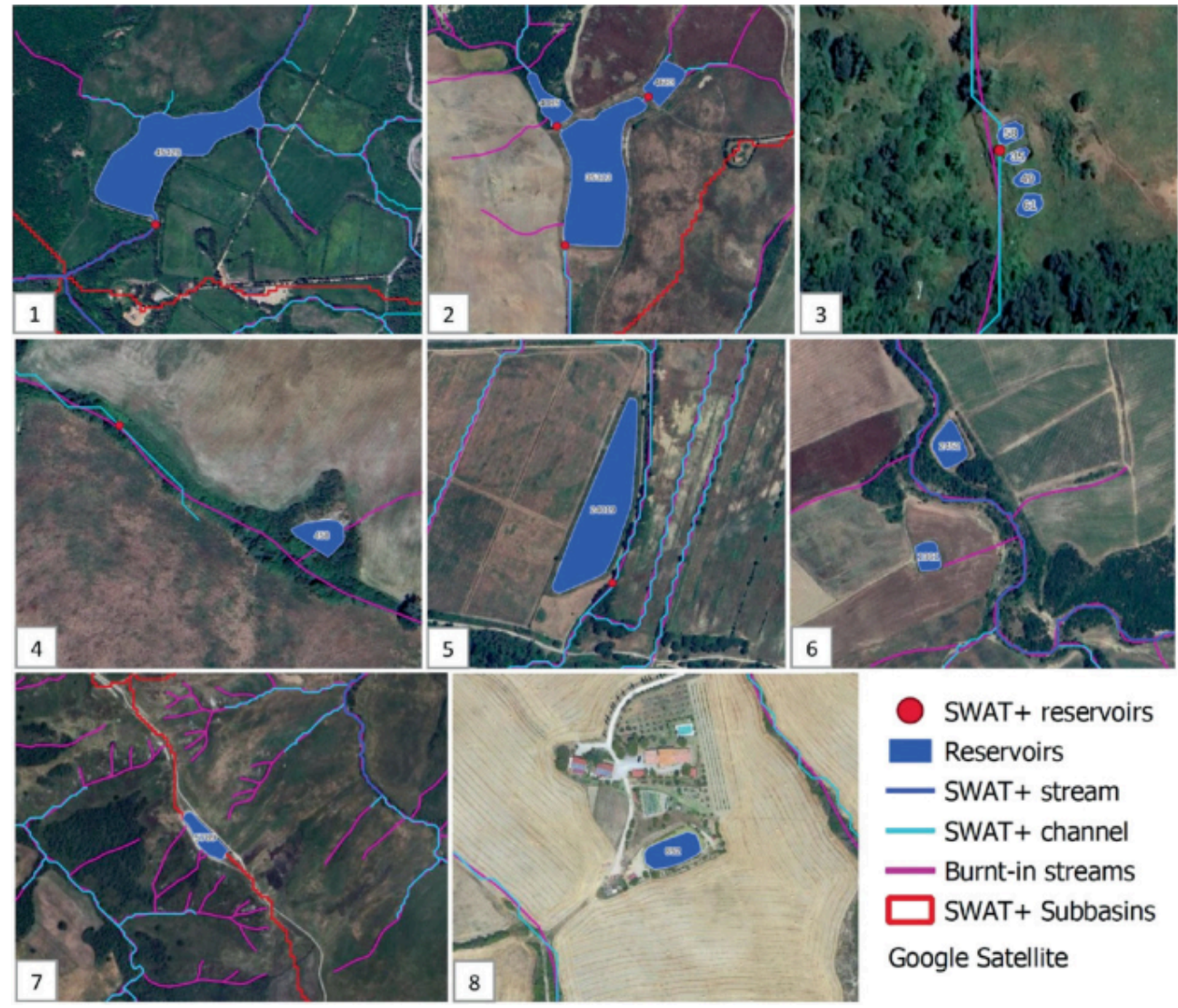


Figure 2.3.2.1: Screenshots from the procedure to place reservoirs in QSWAT+. In the middle of the SmAR, the area in m2 is reported. The SmAR in 1) is the biggest and it is included as it was placed on a stream. SmARs in 2) are included as they are placed on channels and not joined as they are relatively big, while those in 3) are also included but joined. The SmAR in 4) is moved to the channel network as it was on the channel network of the Tuscany region and distant <55 m. The SmAR in 5) is included as it is very close to the channel (<20 m). The SmARs in 6) are excluded because they could be moved to a stream, even if they are at a distance of 50–60 m. The SmARs in 7) and 8) are both excluded as it is not clear to which channel they should be placed, even if with a distance <150 m. Furthermore, the SmAR in 7) is on the subbasin border.

Table 2.3.2.2: Alternative model setups with description and characteristics.

N	Name	Description	HRUs	Subbasin s	Channel s	SmAR s	Large reservoi r
1	Simplified	Setup of the model used for calibration and validation	3773	20	220	0	0
2	Complex – All SmARs (complete)	Setup of the model used to check the performances of the model with the parameters calibrated in the "simplified" setup. During calibration, the model is	112401	194	786	329	0



		referred to as the "complex" setup, while later it is referred to as "All SmARs"					
3	No water storage	Setup of the model used as the reference when estimating the effects of the water storage solutions		194	529	0	0
4	Only SmARs on channels	Setup of the model prepared to account for the uncertainty in the representation of SmARs, in which we consider only the SmARs which are directly placed on the channel network and avoid moving them as done in the "All SmARs" setup.	103013	194	666	186	0
5	Only large reservoir	Setup of the model with only the large reservoir, without considering SmARs	91271	194	536	0	1
6	Two types of water storage	Setup of the model with both types of water storage combined. Used in the climate change analysis.		194	794	328	1

#### 2.3.2.2.2 Model calibration and validation

The variables used for calibration and validation are monthly streamflow at the Monte Amiata Scalo gauging station and basin monthly actual evapotranspiration retrieved from the MODIS satellite products. The calibration strategy adopted is to first calibrate and validate the simplified model and then transfer the validated parameters to the other complex models and evaluate the performances.

We considered the period from 2011 to 2016 as calibration period and the validation period was from 2017 to 2020. The final set of parameters is adapted from a previous study (Villani et al., 2024) in which a sensitivity analysis yielded cn2, esco, epco, bd and revap\_co as the most sensitive. Performances of the model are evaluated with the criteria of Moriasi et al. (2007, 2015), namely the Nash-Sutcliffe Efficiency (NSE), percent bias (PBIAS), Root Mean Square Error - observations standard deviation ratio (RSR), and coefficient of determination (R2), as reported in Table 2.3.2.3.

Table 2.3.2.3: Statistics used to evaluate SWAT+ performances with the respective rating criteria from Moriasi et al. (2007, 2015).

		Time		Performance rating			
Statistic	Variable	scale	Reference	Very good	Good	Satisfactory	Unsatisfactory
NSE	Flow, evapotranspiratio n	Monthl y	Moriasi et al., 2015	> 0.8	0.7 – 0.8	0.5 – 0.7	< 0.5
PBIAS	Flow, evapotranspiratio n	Monthl y	Moriasi et al., 2015	< 5%	5 – 10 %	10 – 15%	> 15%
RSR	Flow, evapotranspiratio n	Monthl y	Moriasi et al., 2007	< 0.5	0.5 – 0.6	0.6 – 0.7	> 0.7
R²	Flow, evapotranspiratio n	Monthl y	Moriasi et al., 2015	> 0.85	0.75 – 0.85	0.6 – 0.75	< 0.6

#### 2.3.2.3 Model Results

We achieved satisfactory performance, as defined by Moriasi et al. (2007, 2015), for NSE, PBIAS, RSR, and R² in both model setups and across both variables (Table 2.3.2.5, Figure 2.3.2.2). The representation of water storage strategies was deemed sufficiently accurate to



proceed with simulations for both current and future climate scenarios (Table 2.3.2.6). Using this approach, we successfully represented 358 SmARs out of 1097 (32.6%). While this is less than half of the total, the largest SmARs were included, and the total surface area and volume represented were 127 ha (out of 161 ha) and 5.3 million m³ (out of 6.7 million m³), respectively, accounting for nearly 80% of the total. Further details can be found in Forzini et al. (2025).

Table 2.3.2.4: The calibrated parameters and the respective changes after the automatic calibration using the SWAT+ Toolbox ("automatic changes" column) and after the manual adjustment ("final changes" column).

Parameter	Type of change	Min/max	Automatic changes	Final changes
cn2	Percent	+/- 20%	-10.22%	-20.00%
bd	Percent	+/- 20%	15.14%	15.14%
esco	Replace	0 - 1	0.068	0.118
ерсо	Replace	0 – 1	0.133	0.133
revap_co	Replace	0.02 - 0.2	0.123	0.123

Table 2.3.2.5: The statistics of the SWAT+ model for monthly streamflow and actual evapotranspiration during calibration and validation periods for the simplified and complex models.

Variable	Monthly s	treamflow	Monthly evapotranspiration				
Model	Simplified	Complex	Simplified	Complex			
Model	model model		model	model			
Calibration, 2011-2016							
NSE	0.78 <sup>2</sup>	0.78 <sup>2</sup>	0.84 <sup>2</sup>	0.85 <sup>1</sup>			
PBIAS	11.7% <sup>3</sup>	-0.9% <sup>1</sup>	6.9% <sup>2</sup>	1.9% <sup>1</sup>			
R <sup>2</sup>	0.85 <sup>2</sup>	0.83 <sup>2</sup>	0.86 <sup>1</sup>	0.86 <sup>1</sup>			
RSR	0.47 <sup>1</sup>	0.47 <sup>1</sup>	0.40 <sup>1</sup>	0.39 <sup>1</sup>			
Validation, 2017-2020							
NSE	0.87 <sup>1</sup>	0.87 <sup>1</sup>	0.74 <sup>2</sup>	0.73 <sup>2</sup>			
PBIAS	-5.7% <sup>2</sup>	1.3% <sup>3</sup>	1.6% <sup>1</sup>	-4.3% <sup>1</sup>			
R <sup>2</sup>	0.87 <sup>1</sup>	0.87 <sup>1</sup>	0.75 <sup>3</sup>	0.75 <sup>3</sup>			
RSR	0.37 <sup>1</sup>	0.37 <sup>1</sup>	0.51 <sup>2</sup>	0.52 <sup>2</sup>			

<sup>&</sup>lt;sup>1</sup> Very good, <sup>2</sup> Good, <sup>3</sup> Satisfactory, <sup>4</sup> Unsatisfactory

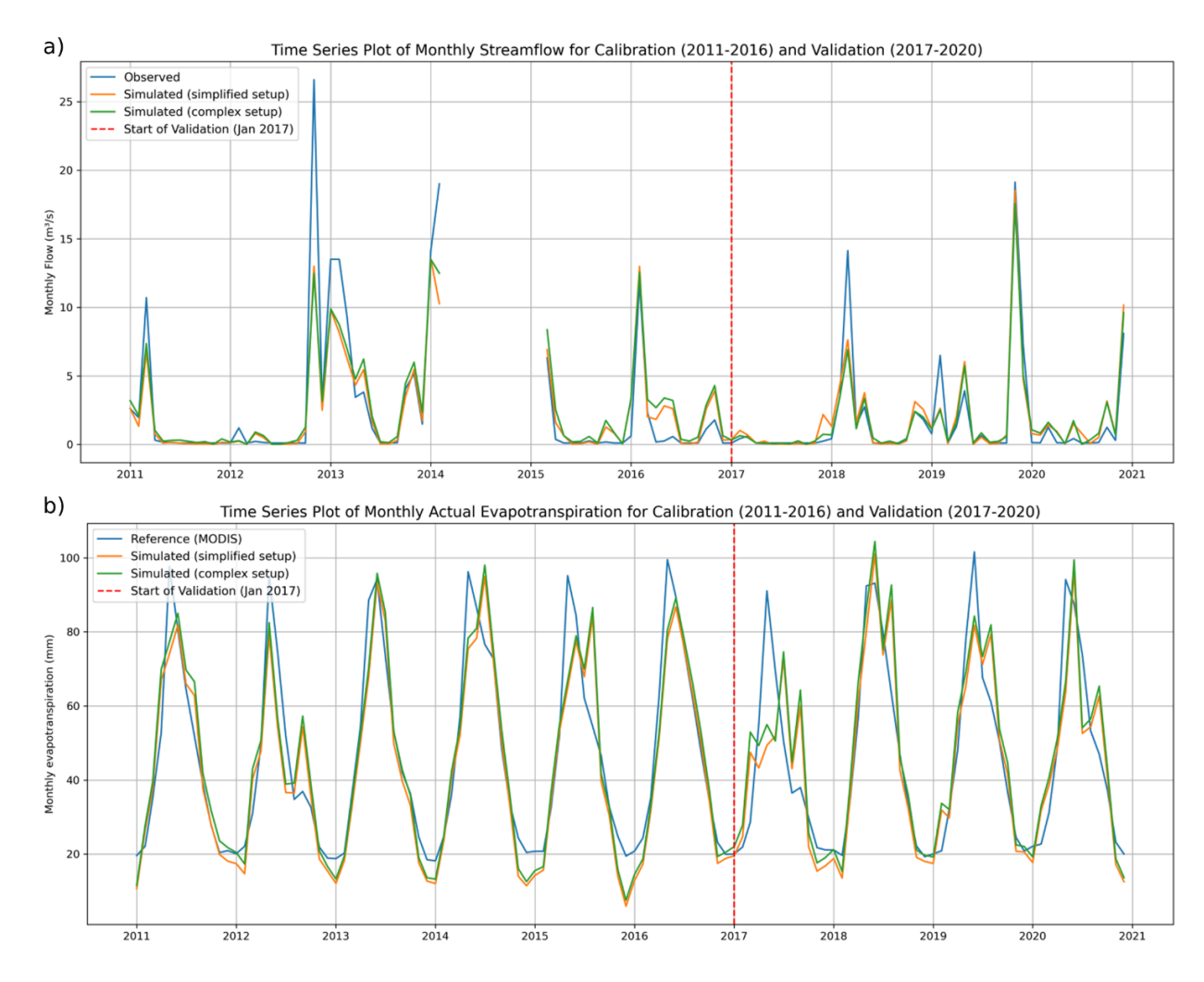


Figure 2.3.2.2: a) Observed and simulated monthly streamflow at Monte Amiata Scalo gauging station. Notice the lack of data from March 2014 to February 2015. b) Remote sensing and simulated monthly actual evapotranspiration for the whole Orcia catchment.

Table 2.3.2.6: Yearly average characteristics of the large dam, the largest SmAR, the aggregated SmARs and both types of water storage combined considering the outputs of the "Two types of water storage" SWAT+ setup. All columns report SWAT+ outputs except for "Area estimated (ha)" and "Volume estimated (ha)" which report the estimated values for comparison.

Reservoirs	Area SWAT+ (ha)	Area estimated (ha)	Volume SWAT+ (m³)	Volume estimated (m³)	Precipitatio n (m³)	Evaporatio n (m³)	Seepage (m³)	Flow out (m³)	Flow in (m³)
Large dam	107.81	171	18,290,000	17,000,000	842,920	555,600	1,889,900	17,635,400	15,755,400
Largest SmAR	4.01	4.54	202,300	190,347	42,628	20,462	70,305	387,240	336,889
Aggregate d SmAR	99.12	161*	4,187,587	6,700,000*	840,398	536,751	1,737,028	17,433,167	15,810,536
Both	206.93	332*	22,477,587	23,700,000	1,683,318	1,092,351	3,626,928	35,068,567	31,565,936
	* The estimates consider all SmARs existing in the Orcia catchment that we could not entirely represent in SWAT+								



#### 2.3.3 EGYPT

Following stakeholder requests during the recent meetings, we have now integrated the proposed systems into the Egyptian Living Lab. The section below presents the implementation of these systems within the updated modelling framework for the LL.

#### 2.3.3.1 State of the art in the use of resources

Egypt's LL Wadi Naghamish and Wadi El-Kheir are around 15 km East of Marsa Matrouh city. The total area of the two watersheds is 177 km2. The study area is characterized by an arid Mediterranean climate (BWh for Koppen classification, with hot, dry summer and warm, rainy winter), partially moderated by maritime influence in the northern part of the watershed. The maximum temperature is 29.7 °C and was recorded in August, while the minimum temperature is 8.4 Celsius Degrees and was recorded in January. The amount of rainfall is concentrated in October-March, where the maximum monthly rainfall is 33.2 mm in January. The average rainfall is around 150 mm/year. The maximum and the minimum relative humidity values were recorded from July to August and April, 73 % and 61 %, respectively. Prevailing winds come from the northwest in most of the year months. Surface wind velocity varies from 8.1 to 11.9 km/h.

According to the soil survey conducted by the EG-LL team, three soil mapping units are: 1) Moderately Deep Sand to Loamy Sand Non-Saline to Moderate Saline soils representing 6.3% of the study area, 2) Very Shallow Sand to Loamy Sand, Non-Saline to Slightly Saline soils with almost 7.6% and 3) Rock lands representing 79% of the total area. The rest of the area consists of limestone quarry and built-up areas. The main agriculture activities are olive and figs were located in the wadis course with total area 6.3% of the study area, and the rest of arable lands occupied with winter wheat and barley representing 7.6% of the total area.

Regarding the modeling procedure for Egypt, we use the same procedure reported for the Algerian/Tunisian case. EG-LL modeling process was done using QSWAT under QGIS 3.32.2. Moreover, input data used for SWAT modelling are shown in the following table.

Table 2.3.4.1 - Input data for the SWAT+ model in the Egyptian LL, with description and source.

Input	Resolution	Source	
Climate	(2000-2022)	NASA's Modern-Era Retrospective analysis for Research and Applications (MERRA-2)	
DEM	30 m	NASA Shuttle Radar Topographic Mission (SRTM)	
Land use	10 m	Sentinel-2	
Soil map	-	Data from local surveys	



#### 2.3.3.2 The SWAT+ model for Egypt

The Soil & Water Assessment Tool is a small watershed to river basin-scale model used to simulate the quality and quantity of surface and ground water and predict the environmental impact of land use, land management practices, and climate change. SWAT is widely used in assessing soil erosion prevention and control, non-point source pollution control and regional management in watersheds.

Over the past 20 years, the Soil and Water Assessment Tool (SWAT) has become widely used across the globe. The large numbers of applications across the globe have also revealed limitations and identified model development needs. Numerous additions and modifications of the model and its individual components have made the code increasingly difficult to manage and maintain. In order to face present and future challenges in water resources modeling SWAT code has undergone major modifications over the past few years, resulting in SWAT+, a completely revised version of the model.

Even though the basic algorithms used to calculate the processes in the model have not changed, the structure and organization of both the code (object based) and the input files (relational based) have undergone considerable modification. This is expected to facilitate model maintenance, future code modifications, and foster collaboration with other researchers to integrate new science into SWAT modules. SWAT+ provides a more flexible spatial representation of interactions and processes within a watershed.

SWAT model is developed by the USDA Agriculture Research Service (USDA-ARS), and it is a semi-distributed model of watershed scale and continuous time. The entire simulation process of the SWAT can be divided into two parts: the land surface (runoff and slope confluence) and the water surface (concentration of channel). The former controls the input of water, sediment, nutrients and chemical substances in the main channel of each sub-watershed. The latter determines the process of transferring the movement of water, sediment and other substances from the river network to the basin and the calculation of the load. The structure of SWAT model is mainly composed of sub-watershed, reservoir calculus and river calculus. Each module is composed of several sub-watersheds. In the process of applying SWAT model, due to different land use types and soil types, the sub-watersheds are divided into multiple hydrological response units (HRUs) to improve the simulation accuracy. The original data required include watershed Digital Elevation Model (DEM), land use map and index table, soil type and soil attribute table, meteorological data, observation runoff and management measures, reservoirs, wetlands, etc. The ungauged watersheds can use the SWAT weather generators to simulate daily wind, solar radiation and relative humidity.

#### Key process and algorithm used in swat are as follows:

- Climate: Weather generator WXGEN or user's input
- Hydrology: Canopy interception, runoff (SCS curve number, infiltration (Green-Ampt),
- Evapotranspiration (Penman-Monteith, Priestley-Taylor, or Hargreaves Samani)
- Land Cover/Plant growth: MRLC,NLCD or user define, water and nutrient uptake, crop and plant growth database
- Erosion: MUSLE using peak runoff rate
- Nutrient: Nitrogen and phosphorus cycle
- Agricultural management: planting, tillage, irrigation, fertilization, pesticide management, grazing, and harvesting.
- SWAT also handles auto fertilization and auto irrigation.



- Urban management: Build up and wash off approach
- Routing: Variable routing or Muskingum routing methods
- Sediment Transport: Based on stream flow and various equations are used to calculate sediment concentration and sediment transport

#### 2.3.3.2.1 SWAT COMPONENTS

#### 2.3.3.2.1.1 Weather Inputs

- Precipitation, solar radiation, temperature, relative humidity, and wind speed
- Can be measured or generated.

## 2.3.3.2.1.2 Hydrology

- Simulates canopy interception of precipitation, partitioning of precipitation, and snowmelt water.
- Simulates partitioning water between surface runoff and infiltration, redistribution of water within the soil profile, evapotranspiration, lateral subsurface flow from the soil profile, return flow from shallow aquifers, and deep aquifer recharge.

#### 2.3.3.2.1.3 Plant Growth

- Inputs: soil properties, management operations, and weather variables
- Estimates crop yields and biomass output for a wide range of crop rotations, grassland/pasture systems, and trees
- Simulates forest growth from seedling to mature stand
- Simulates planting, harvesting, tillage passes, nutrient applications, and pesticide applications for each cropping system with specific dates or with a heat unit scheduling approach

#### 2.3.3.2.1.4 Bacteria and Pathogens

 Simulates bacteria and pathogen loads through surface runoff in both the solution and eroded phases

#### 2.3.3.2.1.5 Nutrient and Pesticide Simulations

- Residue and biological mixing in response to each tillage operation
- Nitrogen and phosphorous applications in the form of inorganic fertilizer and/or manure inputs
- Biomass removal and manure deposition for grazing operations
- Continuous manure application for confined feeding operations
- Type, rate, timing, application efficiency, and percentage of application to foliage versus soil pesticide applications
- Accounts for pesticide fate and transport by degradation/losses by volatilization and leaching

Routes sediment, nutrient, pesticide, and bacteria loadings/concentrations through channels, ponds, wetlands, digressional areas, and/or reservoirs to the watershed outlet



#### 2.3.3.2.1.6 Land Management Simulations

- Conservation practices such as terraces, strip cropping, contouring, grassed waterways, filter strips, and conservation tillage
- Irrigation water on cropland from sources such as stream reach, reservoir, shallow aquifer, or a water body source external to the watershed

#### The SWAT modelling had been conducted for 41 years, from 1986 to 2000.

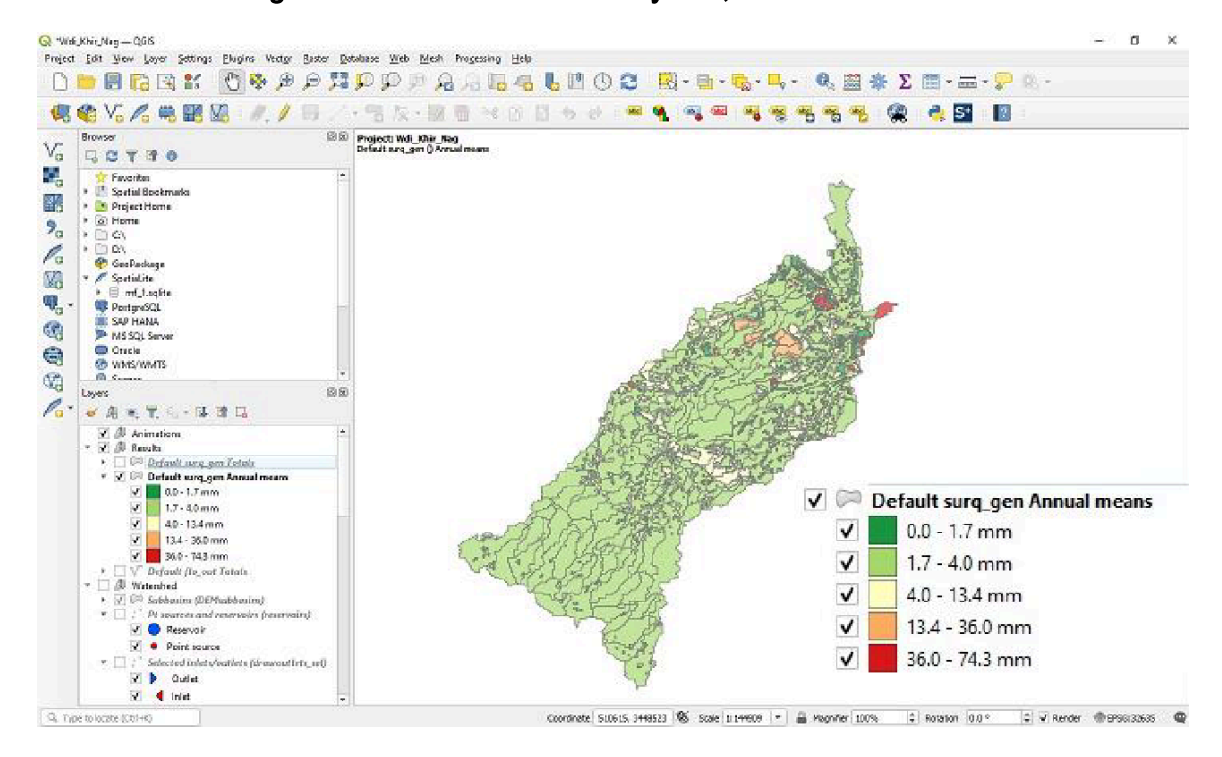


Figure 2.3.4.1: HRUs in Wadi Nagamish

The watershed was represented by 748 HRUs using the SWAT model (Figure 2.3.4.1). The streamline flow is shown in Figure (2.3.4.2) with a maximum flow of 0.643 m3/sec in the upper watershed and the minimum flow is 0.003 m3/sec in the downstream areas.

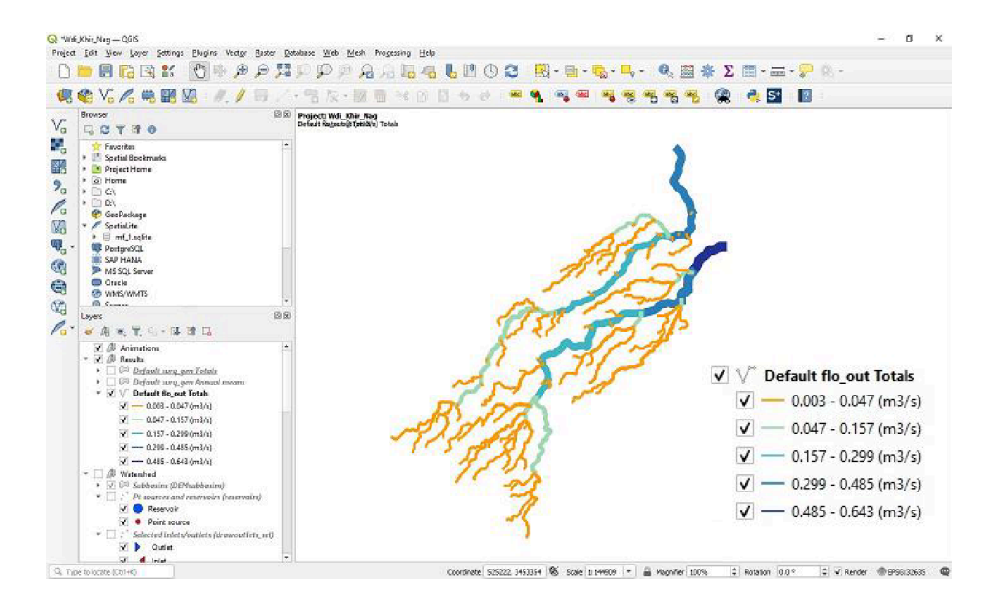




Figure 2.3.4.2: Visualization of the total flow out in the streams of Wadi Nagamish

#### 2.3.3.3 Catchment water balance

Water is an important resource needed in every aspect of life, e.g. human habitats, economic prosperity, food security, etc. There is a need to simulate and quantify the availability of water using hydrologic models with reliable data. In many arid and semi-arid regions, there is a limited available water resource which affects its potential demand.

The long-term water balance equation for a catchment is P = Q + AET + GW + DS, with all terms expressed in mm/year, where P is Precipitation, Q is Runoff, AET is actual evapotranspiration, GW is exchange with groundwater aquifer and DS is change in soil storage .

One of the best methods to quantify the water availability is the use of hydrologic models at spatial and temporal resolution with reliable data sets such as available observed hydro-meteorological data to estimate water availability. The water balance in Wadi-Naghamish catchment is modeled using the Soil and Water Assessment Tool (SWAT+) model. The SWAT+ modeling had been conducted for 41 years, from 1986 to 2000

#### 2.3.3.3.1 The Water balance equation

Water balance equation is a mathematical representation of change in volume of the moisture Storage resulting from the total inflow, minus the total outflow (actual or potential) in hydrosphere which may be at local, regional or global scale. Water balance for a given basin should be worked out for sufficiently long period so that the various items approach a steady state average condition as possible.

#### P=Q+AET+GW+DS

The main components of the water balance equation are precipitation (P) 171 mm, Runoff (Q) (5.83) mm, actual evapotranspiration AET (167.83) mm, GW is exchange with groundwater aquifer and DS is change in soil storage (Figure 2.3.4.3). The last two terms are usually small and could be ignored in long term analysis. The catchment receives about 171 mm of annual precipitation. Actual Evapotranspiration is the largest water balance component, which consumed about 167.83 mm representing 98%. Estimated actual evapotranspiration is the highest component within the study area. This is likely caused by the prevailing high temperatures and low relative humidity.

The average modelled runoff in Wadi-Nagamish was around 3.41% of total precipitation. The streamflow/precipitation is 0.03, which means that 3% of the precipitation became streamflow. Percolation and deep drainage are 0. Thus, no water percolation took place into the deeper layer. ET/precipitation was 0.98. Consequently, most of the precipitation was lost by ET. These results are in good agreement with arid and semi-arid conditions (high ET, low streamflow).

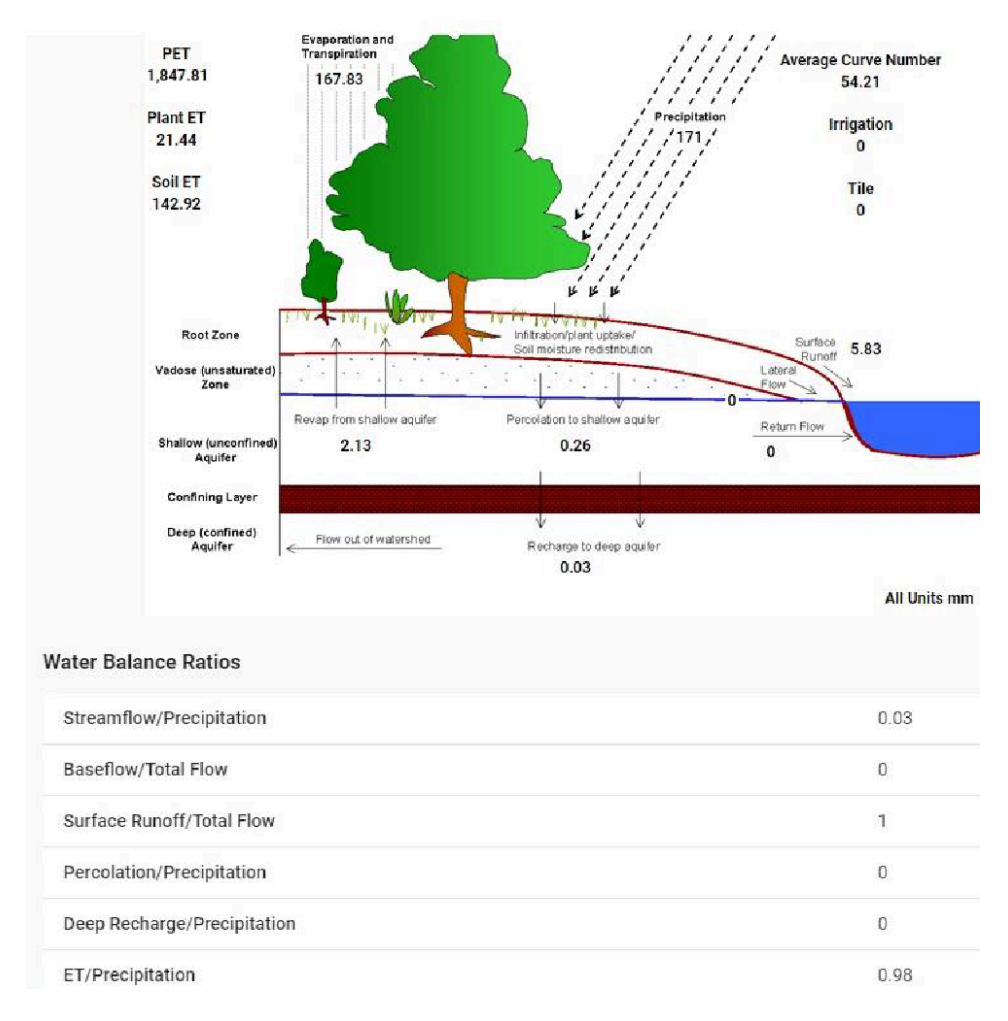


Figure 2.3.4.3: The water balance resulted from SWAT+ in wadi Nagamish.

# Land use distribution

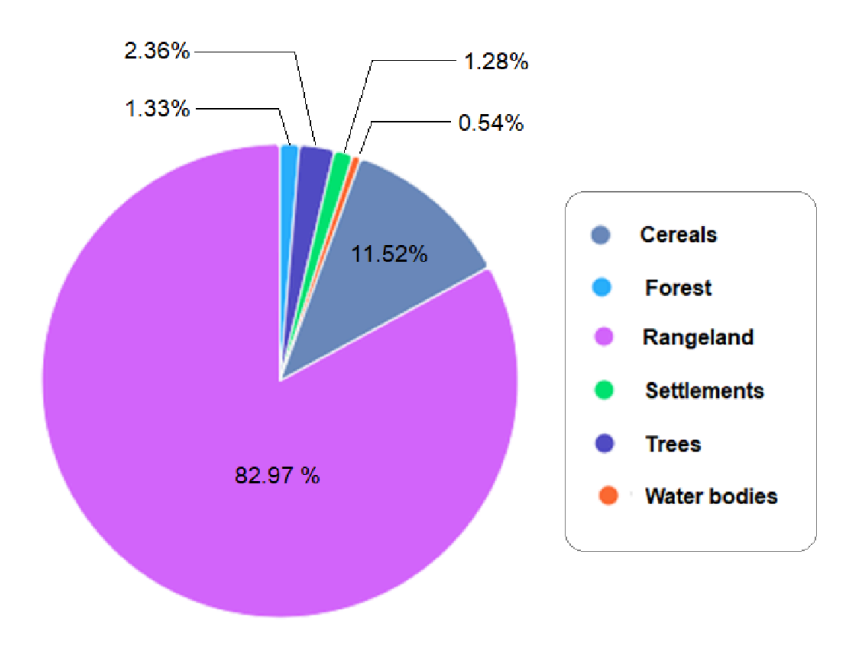




Figure 2.3.4.4: land use distribution in Wadi Nagamish (from SWAT+ modeling)

Data in figure 2.3.4.4 presents the distribution of different land use classes in Wadi Naghamish, which indicates that rangeland is the dominant land use in the watershed, occupying about 83% of the total watershed area (199 km2).

To validate SWAT plus runoff output, the results of a previous study conducted in 1994 were employed. In that study, five micro hydrologic cistern watersheds were conducted to address water runoff in Wadi Naghamish (Abd-Alla 1997), out of which three cisterns were selected for the validation task. The remaining two cisterns had insufficient data measurements. Each hydrologic watershed contains only one underground cistern. These cisterns had been built since 1970 with assistance of North-Western Coast Development Agency (NWCDA). The catchment topography was determined in the field using an electronic theodolite. Differences in elevations for each cistern watershed were determined using a 5-meter grid system. The micro hydrologic cistern watershed outlet was directed by artificial earth or stone ridges made by Bedouins. To measure the cistern watershed area, lengths and angles between borders were calculated using the electronic theodolite. A 5 X 5-meter grid system strategy was used for each cistern watershed, where head square points were employed to determine the elevation above the mean sea level by the electronic theodolite. The geometrical boundary of each cistern watershed is depicted in Figures (2.3.4.6, 2.3.4.7 and 2.3.4.8) (Abd-Alla 1997).

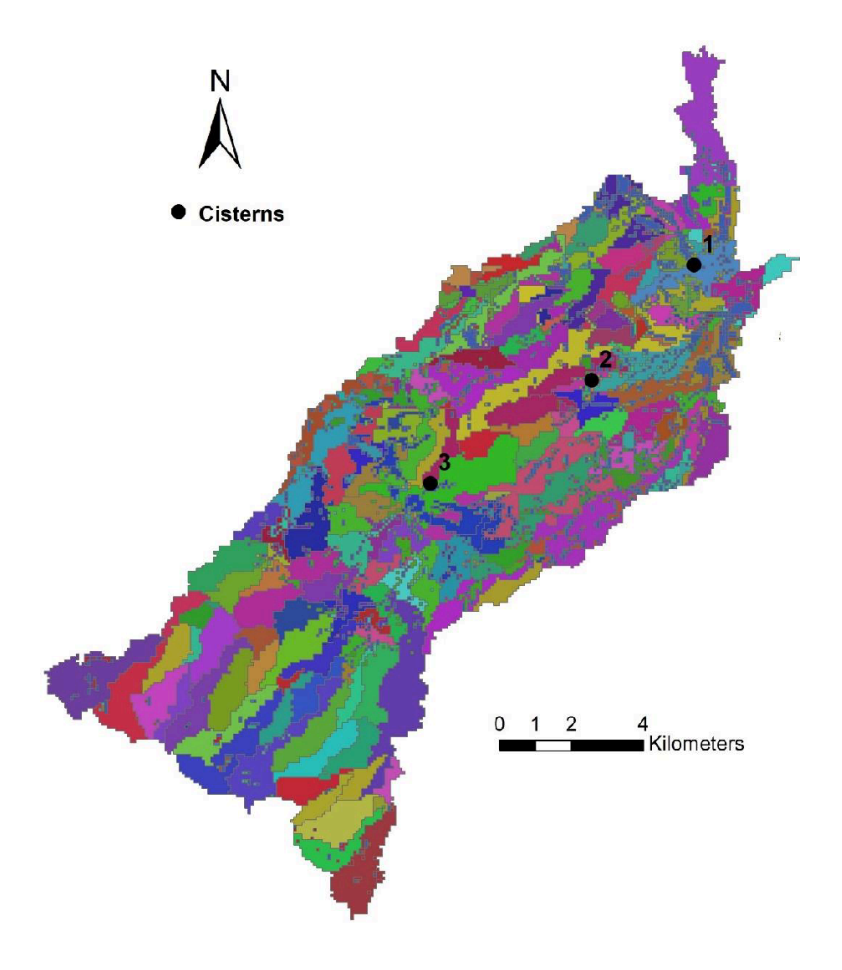


Figure 2.3.4.5: Locations of the three cisterns (1994) used for the SWAT+ runoff validation



Table (2.3.4.2) represents coordinates, watershed area and total volume of each cistern (Abd-Alla 1997). Table (2.3.4.3) shows the recorded rainfall in 1995, the measured annual water runoff for each cistern watershed, and the simulated average annual runoff from SWAT+. The results indicated that the runoff/rainfall ratios in 1995 were 6.20, 2.31 and 5.08 for cistern no. 1,2 and 3, respectively. On the other hand, the runoff/rainfall ratio that resulted from SWAT+ modelling was 3.41.

Table 2.3.4.2: Watershed area and volume of the selected cisterns for SWAT output validation

Cistern	East	North	Elevation	Watershed	Cistern
			(m)	area (m2)	volume (m3)
1	530697	3456276	70.45	13230	217.28
2	526211	3453399	68.07	4326	246.24
3	533207	3454588	34	8694	49.59

Table 2.3.4.3: Rainfall and runoff for each cistern in 1995, SWAT+ precipitation and runoff

Cistern	On-ground measurements (1995)			Modelling with	SWAT+	
	Rainfall (mm)	Runof f (mm)	Runoff/rainfall ratio	Precipitation (mm)	Runoff mm/y	Runoff/rainfall ratio
1	148	9.18	6.20	171	5.83	3.41
2	148	3.43	2.31	171	5.83	3.41
3	148	7.52	5.08	171	5.83	3.41

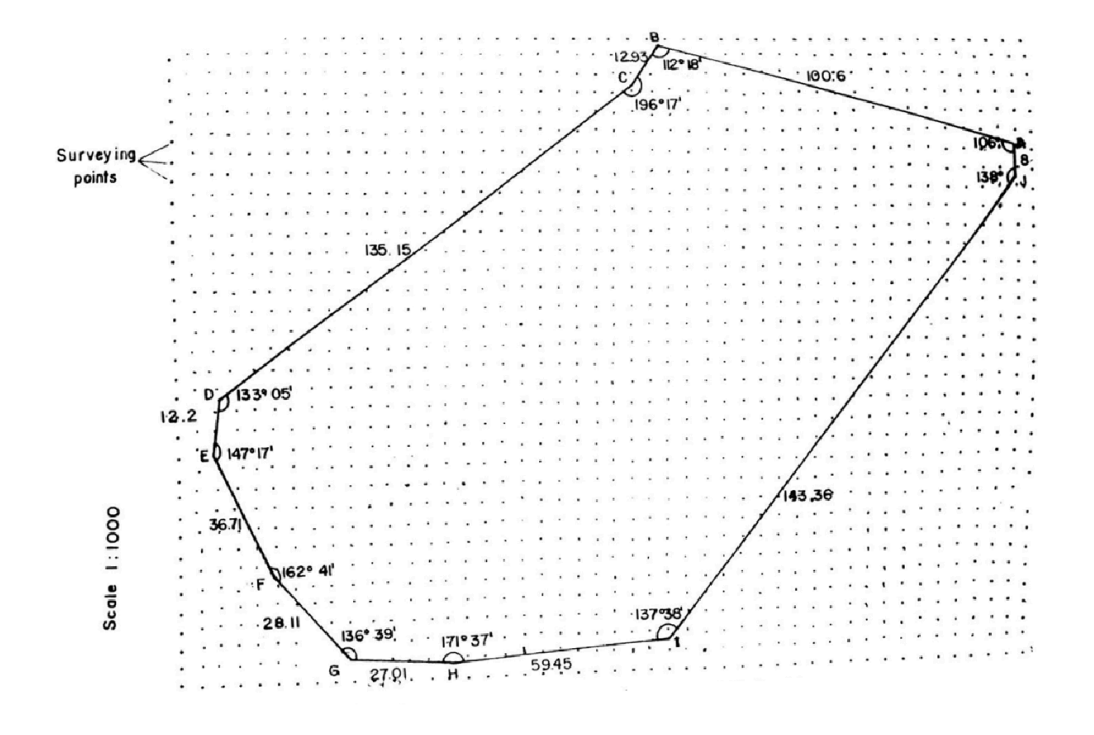


Figure 2.3.4.6: Schematic diagram of the cistern watershed No. 1 (After: Abd-Alla 1997)

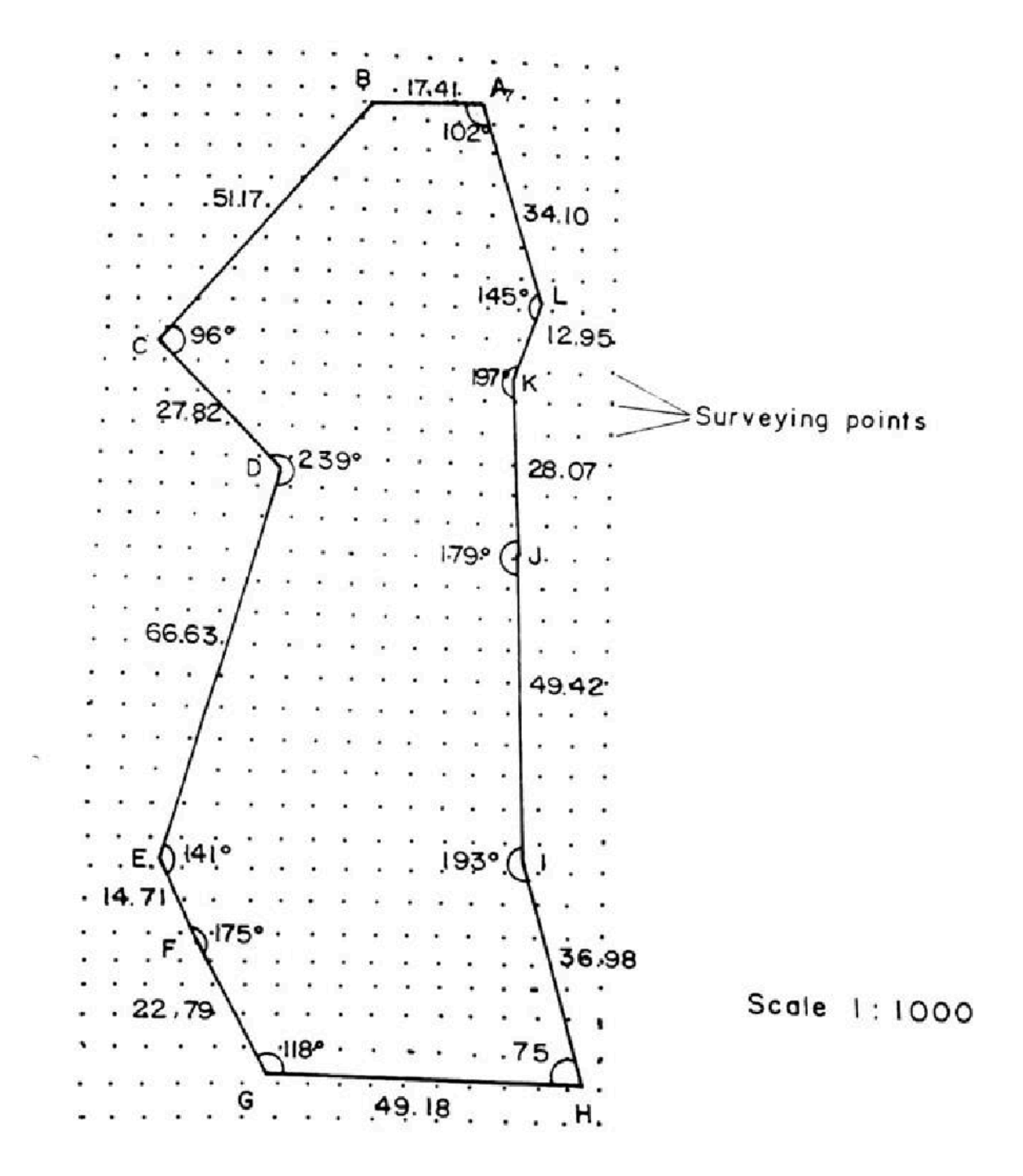


Figure 2.3.4.7: Schematic diagram of the cistern watershed No. 2 (After: Abd-Alla 1997)

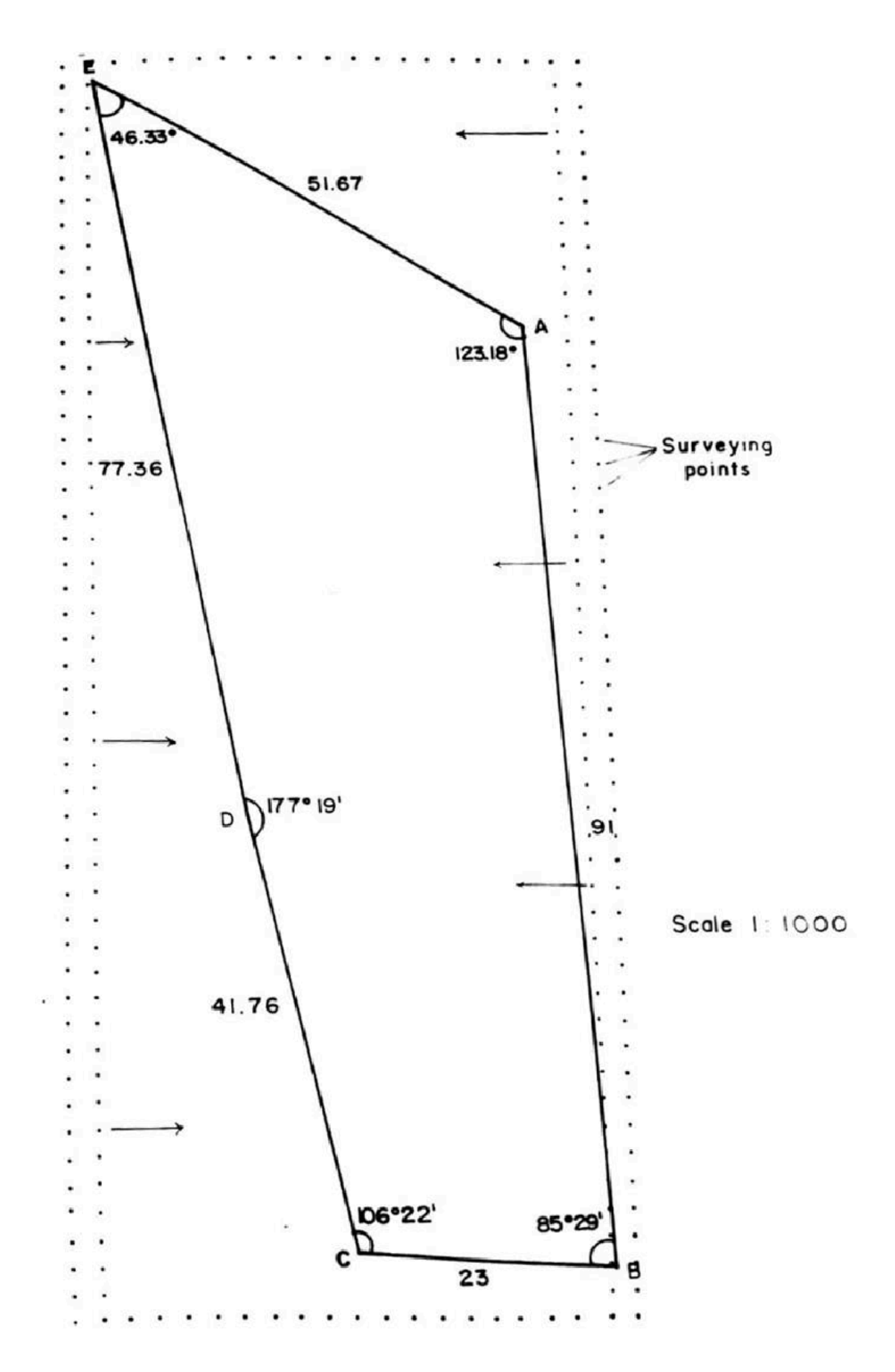


Figure 2.3.4.8: Schematic diagram of the cistern watershed No. 3 (After: Abd-Alla 1997)



## 2.3.4 ALGERIA / TUNISIA

In response to stakeholder requests, we incorporated the option of storing water in the ground for later use as a reservoir. To address this, the SWAT model was coupled with the MODFLOW model to simulate potential aquifer storage. While a single, calibrated and validated SWAT model (as detailed in Section 3.1.1) was used for the entire basin, MODFLOW was developed and implemented separately for the Algerian and Tunisian aquifers, treating them as distinct units rather than a single, unified system.

#### 2.3.4.1 State of the Art

The Lekbir basin or the Oued El Kebir transboundry basin (Figure 2.3.3.1) is a transboundary basin shared between Algeria (Tebessa) and Tunisia (Gafsa and Kasserine), covering an area of approximately 6,491 km². Of this total, 4,508 km² around 69.5% lies within southwestern Tunisia. The basin is encircled by a perimeter of about 813 km. Geographically, it extends between coordinates 451,193.469 E and 3,788,894.237 N (UTM Zone 32N). The catchment is characterized by a varied and dynamic topography, featuring wide wadis with sinuous channels that frequently intersect low-lying areas. These features contribute to a semi-endorheic system, significantly influencing surface water flow and hydrological connectivity.

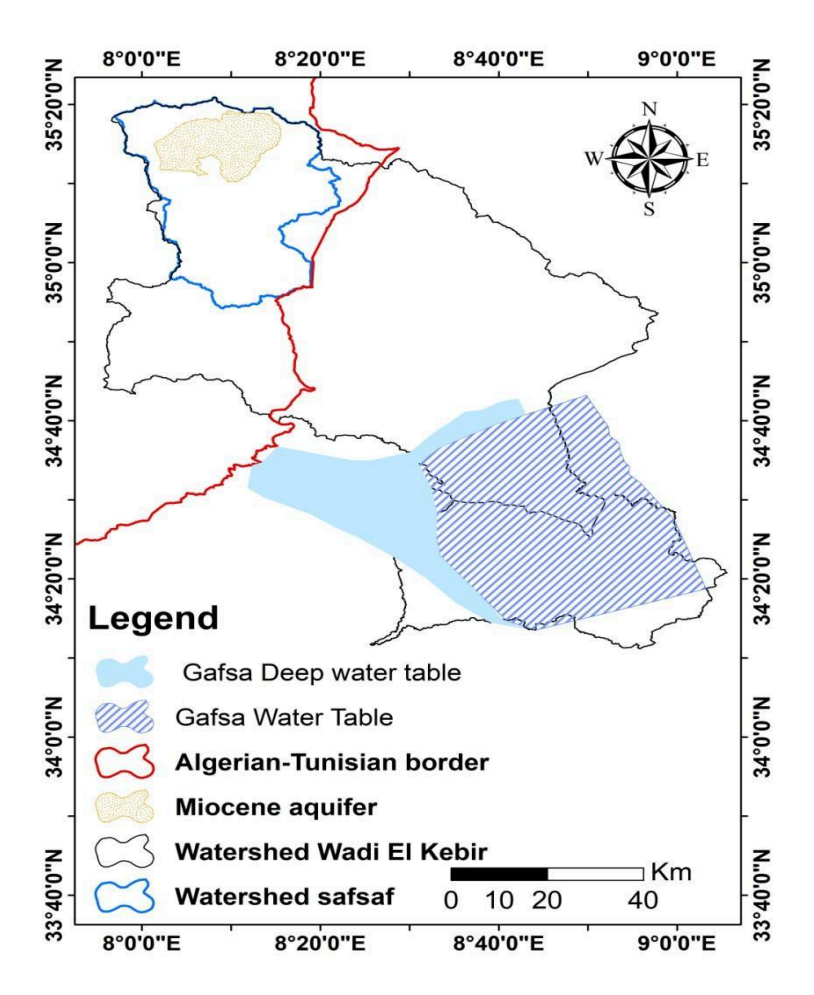




Figure 2.3.3.1: Location of the study area

Administratively, the catchment spans two governorates in Tunisia (Gafsa and Kasserine) and one in Algeria (Tebessa). It encompasses a diverse natural landscape, including deserts, oases, and mountainous regions, with elevations ranging from near sea level up to 1,711 meters. The climate is predominantly arid to semi-arid, with average annual rainfall rarely exceeding 400 mm. Human settlements are mainly concentrated in the plains and along the river and its tributaries.

# 2.3.4.2 Study Area of Algeria

The transboundary Oued El Kebir basin, located on the Algerian-Tunisian border, is characterised by a semi-arid climate. The region has experienced intense drought due to overexploitation of water reserves, particularly shallow aquifers which are the main source of drinking water, and climate change (lack of precipitation, rising temperatures and intense evapotranspiration). This has led to a significant lowering of the aquifer's piezometric level. The El Ma El Abiod plain, part of this study area, is situated at the Algerian-Tunisian frontier. Its northern boundary is defined by Dj. Doukkane, Dj. Anoual, and Dj. Bouroumane, representing a significant ridge line in the local geography, as it is part of the watershed division line between the Mellague in the north and Wadi El Ma El Abiod. The aquifer comprises Cretaceous outcrops and Miocene and Quaternary formations.

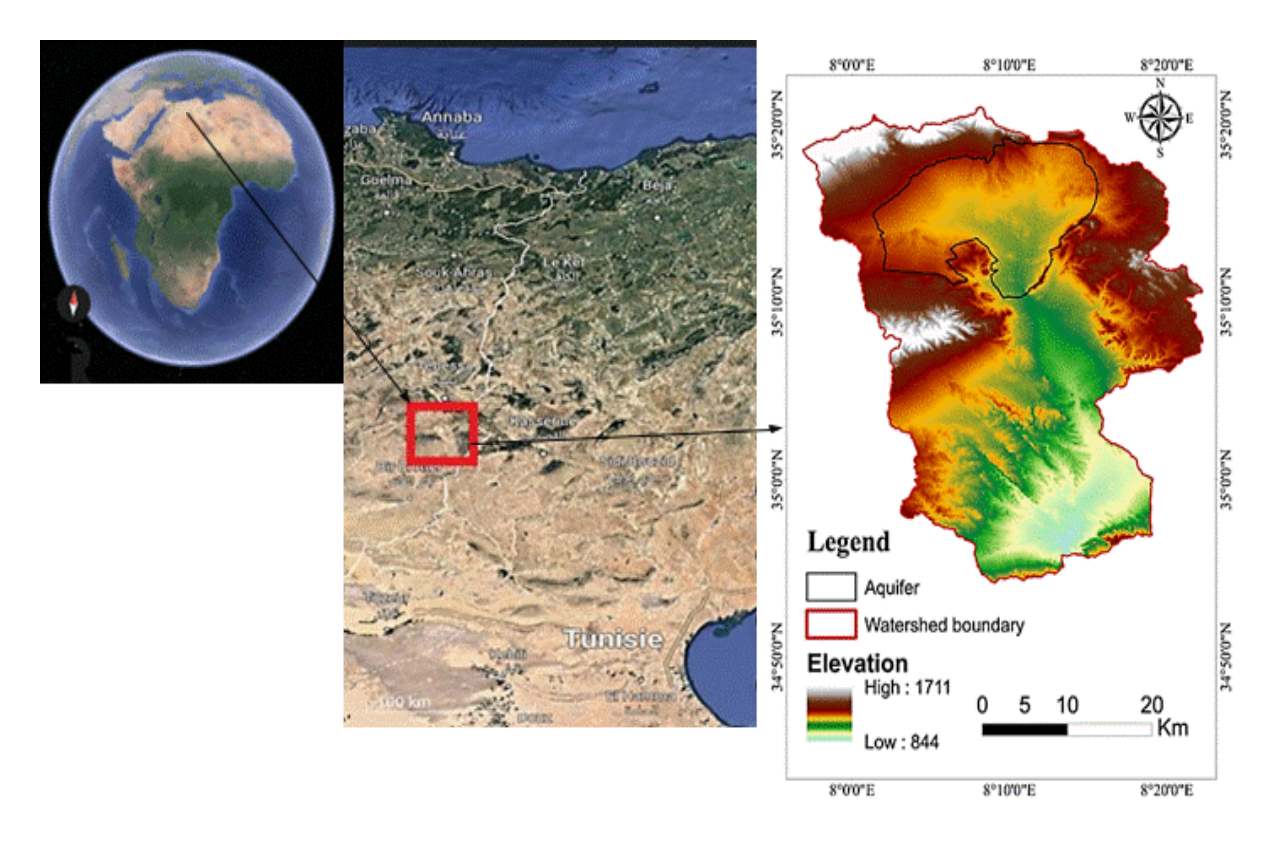


Figure 2.3.3.2: El Malabiod aquifer

# 2.3.4.3 Study Area of Tunisia

Located north of the city of Gafsa, horizons enclosed aquifer in the Miopliocene, or in the limestone of Zabbag Superior. Due to the lack of a watertight barrier between them, they behave as one single hydrogeological unit.



The Deep Gafsa North contains continental detrital deposits that are discordant with those of the Upper Cretaceous (Abiod, Aleg and Zebbag formations). It is limited by the relief of borders and by the fault of Gafsa to the south. In the North-West, it passes in hydraulic continuity with de Majen bel Abbés. The numerous boreholes in the area, several of which have penetrated the water table to its full capacity, have made it possible to establish hydrogeological cuttings over the entire basin.

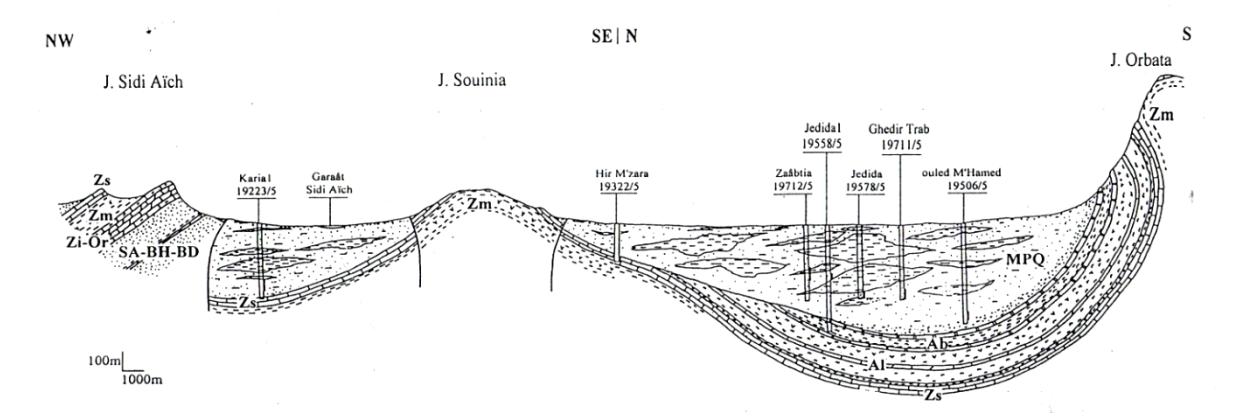


Figure 2.3.3.3: Hydrogeological section through the centre of the basin and between the anticlines of Souinia and Sidi Aïch (Moumni, 2010)

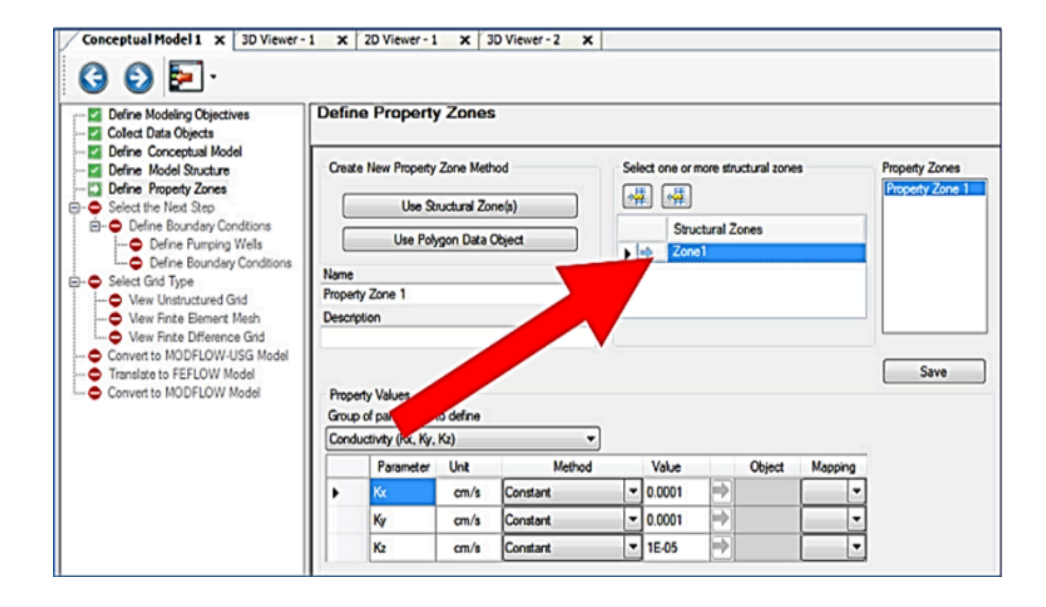
## 2.3.4.4 Conceptual Modelling stages

This section details the hydrological modelling efforts concerning aquifer recharge within the transboundary basin.

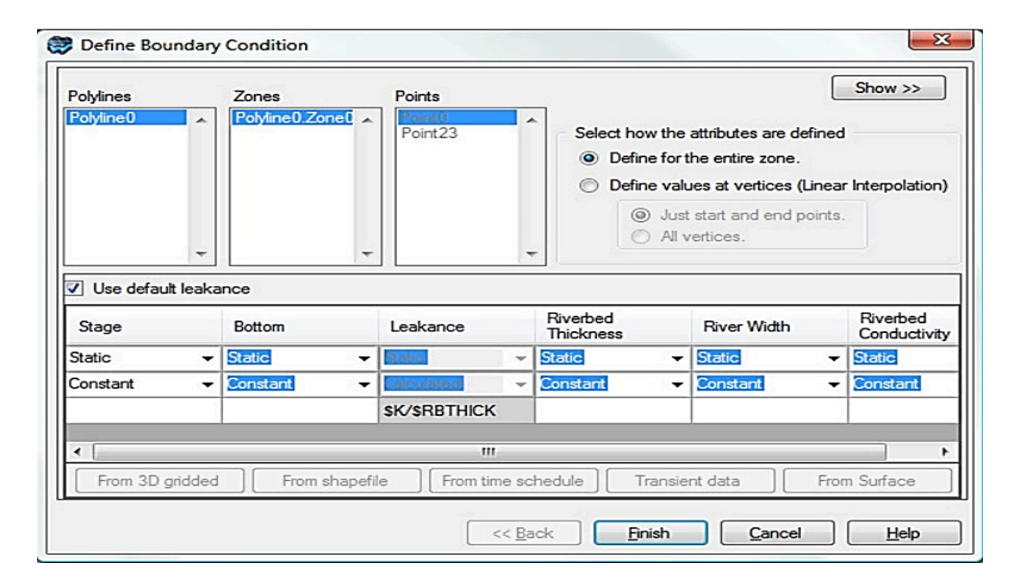
The hydrological model, developed using MODFLOW Flex V6, has been enhanced to incorporate non-conventional water sources (NCWS) and the storage of surface water in the aquifer through artificial recharge tools. The main objective is to reconstruct the water table piezometry and predict future flows under different scenarios.

**Property Zone:** For the purpose of building the appropriate zone layers, top and bottom levels are now added to the model. The initial head values, storage properties, and hydraulic conductivity (kx, ky, and kz) are added to each layer's specific layers.





**Boundary Conditions:** Some of the boundary conditions of the model that are most likely to exist include recharge, streams, reservoirs, evapotranspiration, pumping wells, etc.





#### 2.3.4.4.1 Conceptual model of the Miocene aquifer

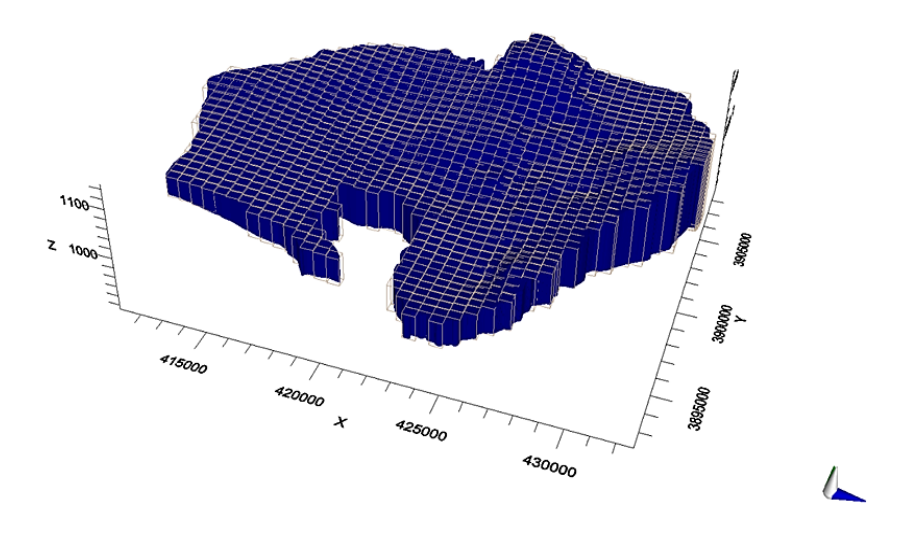


Figure 2.3. xxxx 3D Numerical grid created for Miocene groundwater model

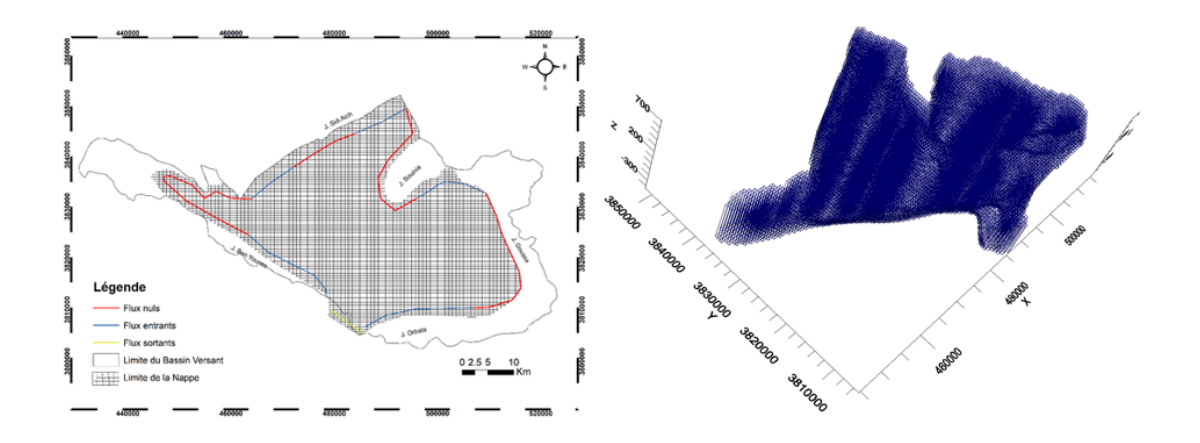


Figure 2.3.3.4: Discretization of the aquifer domain (mesh) by Modflow Flex 6 (finite difference method)

# 2.3.4.5 Aquifer Recharge (Algeria)

Piezometric maps of the Miocene aquifer between 2001 and 2024 reveal a significant drawdown, reaching 57 m in the central study region, primarily attributed to overexploitation for irrigation. Groundwater modelling methodology involved data input, calibration, and exploitation stages, including conceptual modelling, defining property zones, and establishing boundary conditions for the Miocene aquifer.

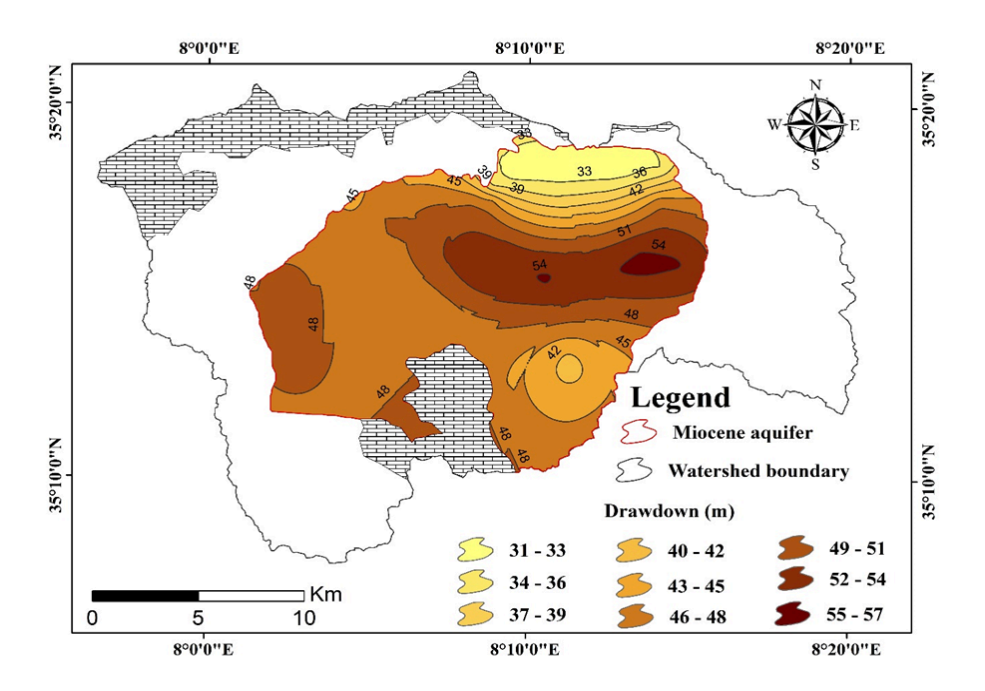
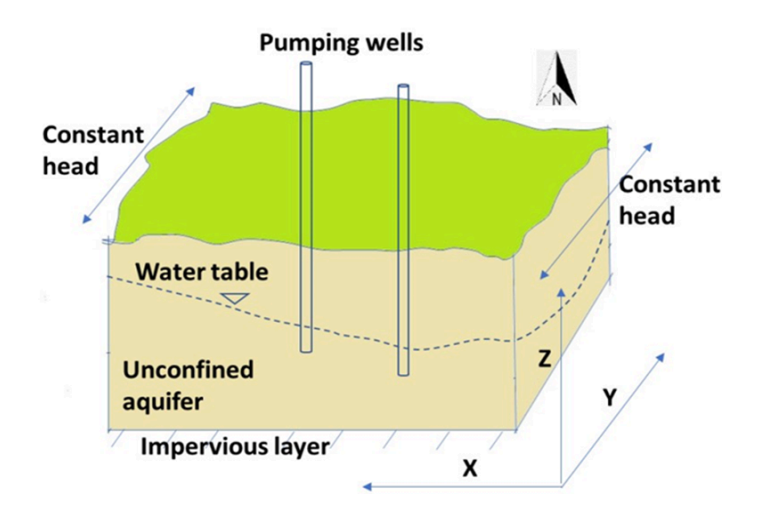


Figure 2.3.3.5: Groundwater level decline Map between 2001-2024

# 2.3.4.5.1 Methodology (groundwater Modelling)

Hydrological and hydrogeological modeling has become a recognized tool to support sustainable water resource management. The role of modeling is to simplify the representation of a hydrological or hydrogeological system and to measure the degree of understanding of its functioning and interactions with the external environment.



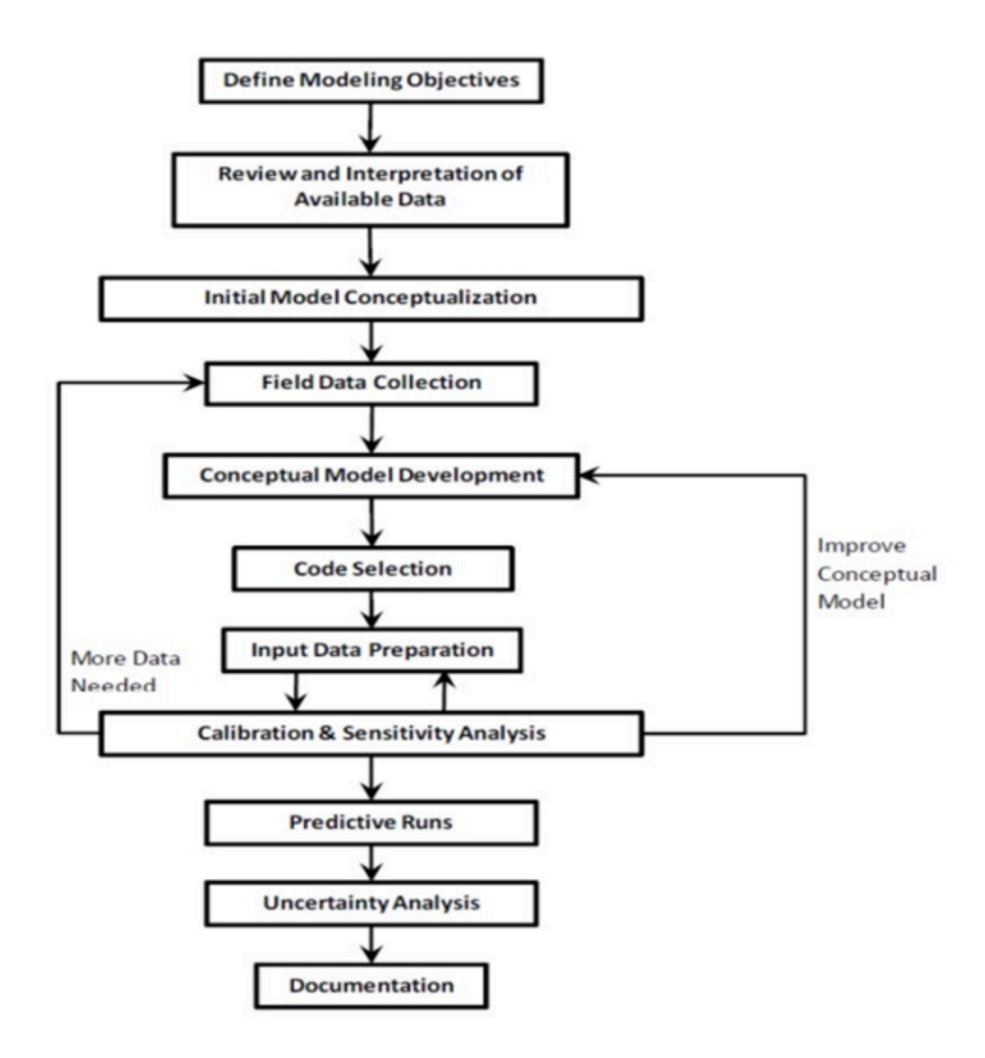
## 2.3.4.5.2 Model development stages

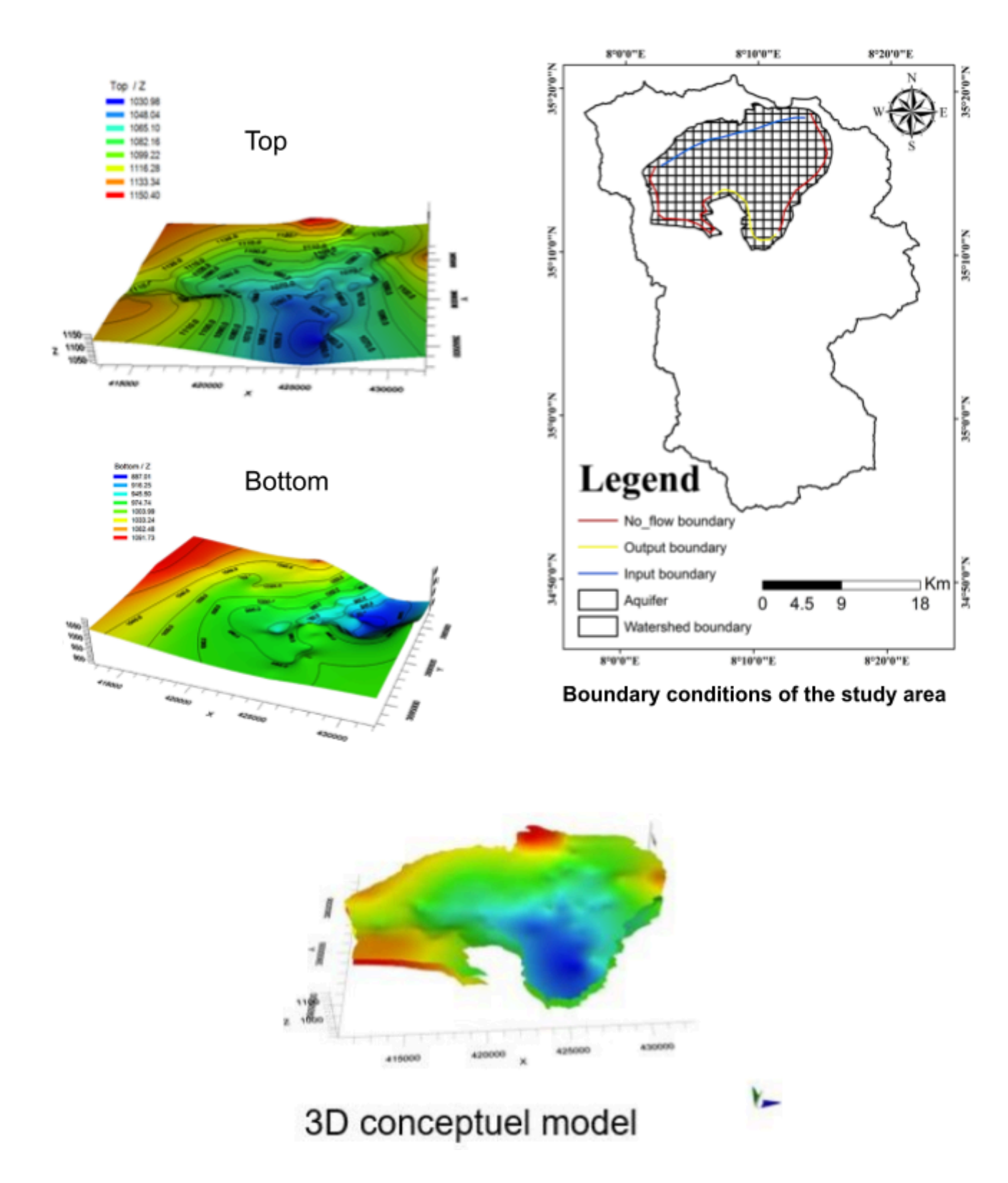
**Data input**: After defining the initial conditions and boundary conditions and discredited the domain to be modeled into a certain number of meshes, we introduce for each mesh the physical data of the system like the piezometric gradient of the reference map, aquifer geometry hydrodynamic parameters T, K, S., climatic parameters (effective recharge).



**Model calibration:** The aim of this phase is to minimize between model responses (calculated) and system responses (observed). This calibration is important, as it will enable us to carry out simulations on the field studied.

**Exploiting the model**: This is the final stage where the model reveals its usefulness. Its main purpose is to forecast the future hydrodynamic response of the aquifer system to possible development scenarios (exploitation, drought, recharge, etc.)





2.3.4.5.3 Model Results:



# 2.3.4.5.3.1 Steady State Calibration

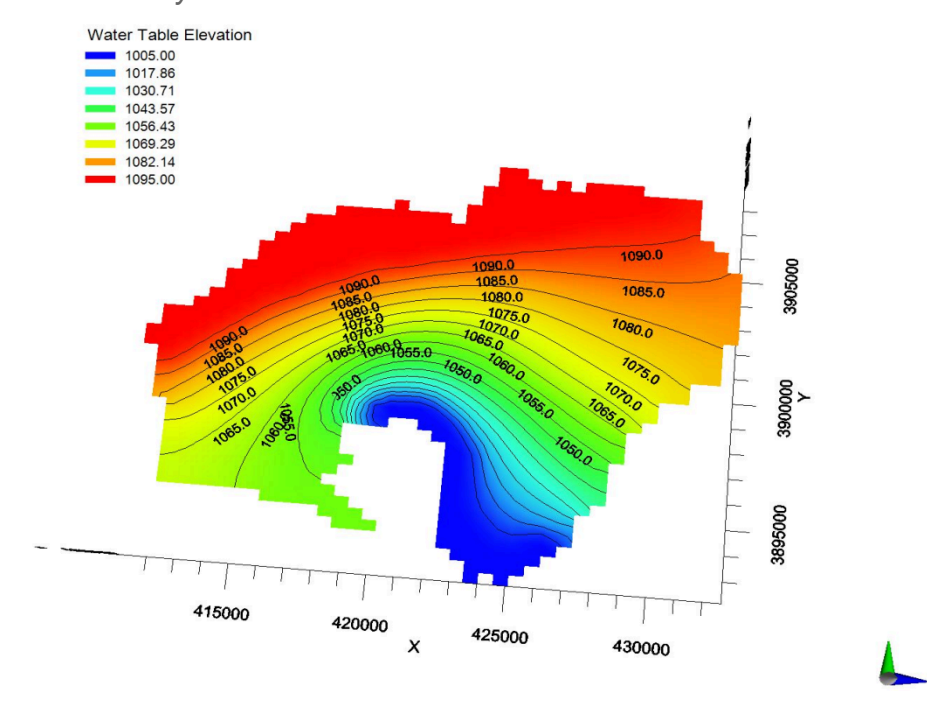


Figure 2.3.3.6: Reconstitution of the piezometric map in steady state, March 2001

In this model development, steady state calibration involved comparing hydraulic head simulations from MODFLOW to the measured aquifer heads. 96 observation wells that were observed during March 2001 were used for the calibration.

#### 2.3.4.5.3.2 Calibration in transient regime

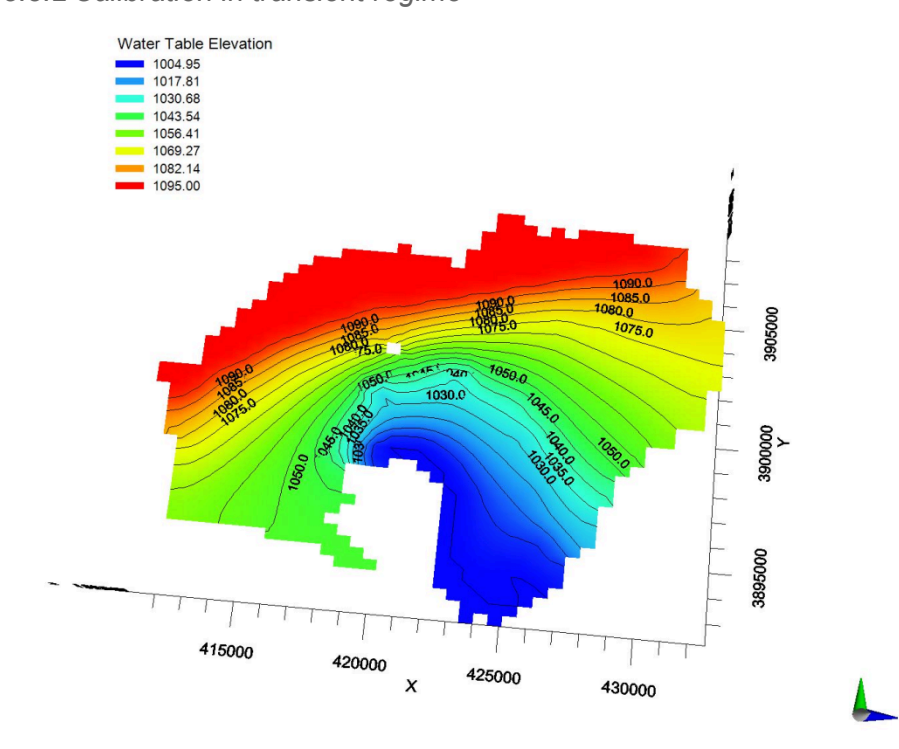


Figure 2.3.3.7: Reconstitution of the piezometric map in transient state, March 2004

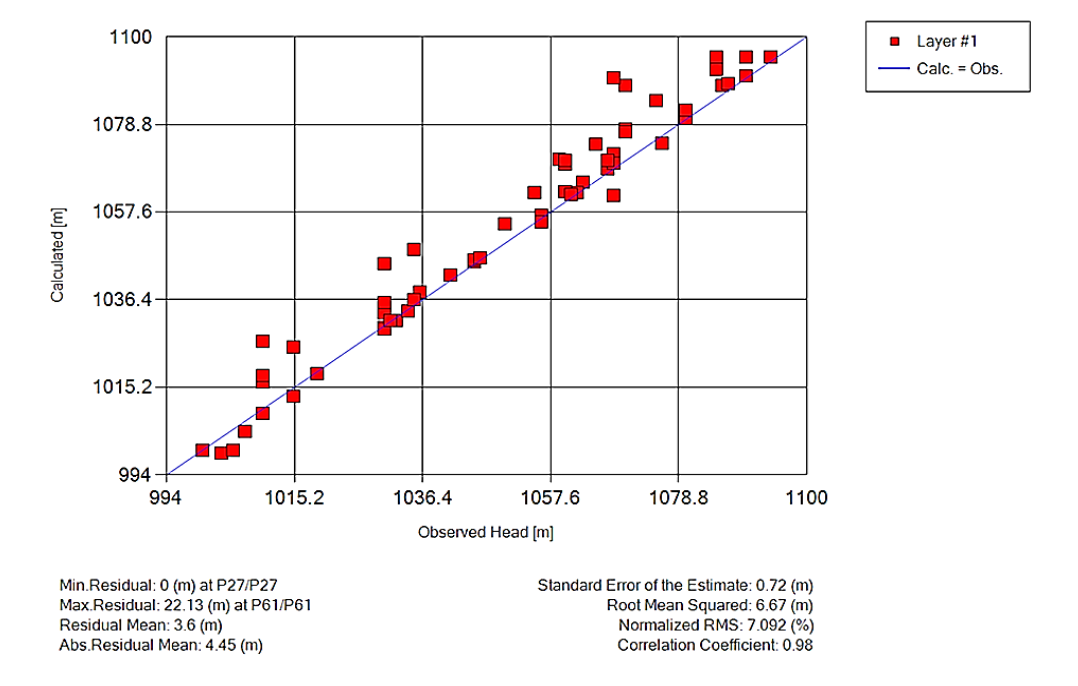


Figure 2.3.3.8: Model calibration

Despite some discordance between the calculated and measured piezometric levels in some areas, the model remains valid, probably due to measurement errors, and to specific hydrogeological conditions. The linear correlation between the observed and calculated hydraulic heads yields an acceptable RMSE error of the order of 20.52% with correlation coefficient of 19.47.

#### 2.3.4.5.4 Numerical simulations and scenarios

For the second stage of this study, a 3D transient numerical model based on the finite difference method will be used to simulate groundwater flow from 2023 to 2033 using the same software (Visual MODFLOW Flex). During the modeling process, three scenarios will be proposed:

- Maintaining the same well pumping rate without any recharge,
- Recharge of the entire study area through efficient infiltration, without pumping.
- Introduction of artificial recharge through surface water infiltration basins.

#### 2.3.4.5.4.1 1st Scenario

The first scenario is to maintain constant well pumping rates from 2001 to 2024 without any recharge.

 As a result, a decrease of 7 to 10 meters in the piezometric level of the aquifer is observed.

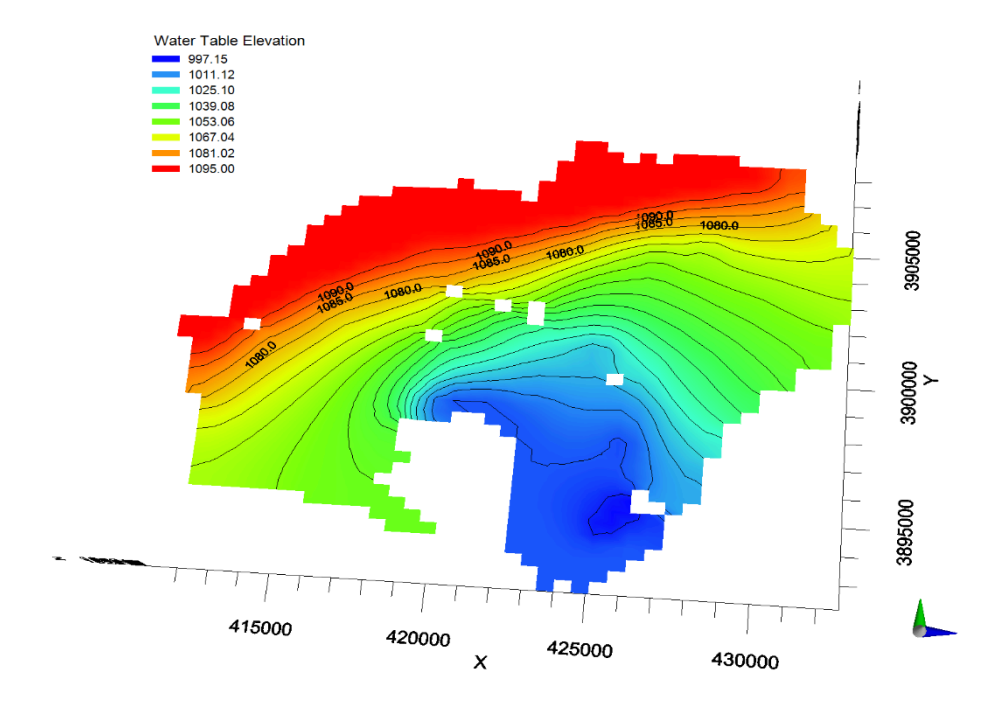


Figure 2.3.3.9: Reconstruction of the piezometric map in 2024, with the same pumping rates as in 2001, without any recharge.

#### 2.3.4.5.4.2 2nd Scenario

The second scenario highlights the impact of natural recharge over a ten-year period, leading to an increase in the piezometric level from 1.3 cm to 1.78 m in the northeastern part.

Nevertheless, it is evident that the groundwater response to natural recharge remains modest, with an increase ranging from 0.58 m to 1.6 m in the central and southern parts.

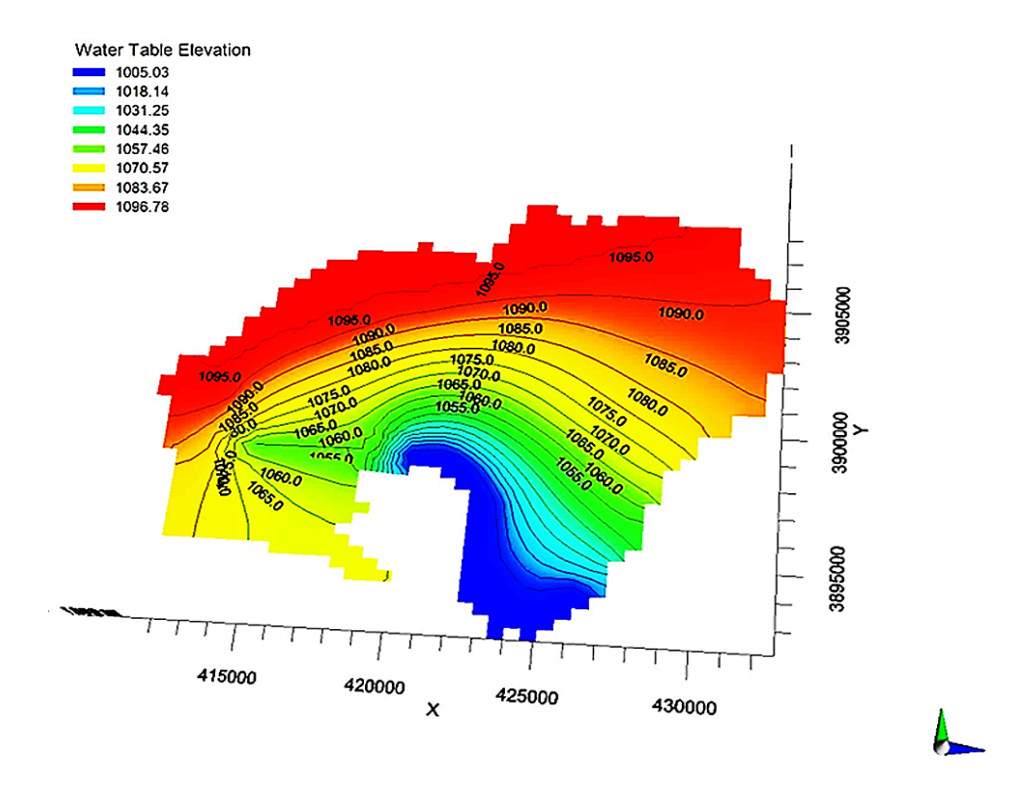


Figure 2.3.3.10: Simulation with natural recharge without pumping 2034

#### 2.3.4.5.4.3 3rd Scenario

The third scenario is introducing artificial recharge by surface water infiltration basins. The choice of recharge sites is based on several criteria:

- Hydrogeological criteria: porosity, transmissivity, depth of water table.
- Geomorphological criteria: slope, soil type, land use.
- Climatic and hydrological criteria: precipitation regime, availability of surface water.
- Socio-environmental and economic constraints: public acceptability, development costs, ecological impact.

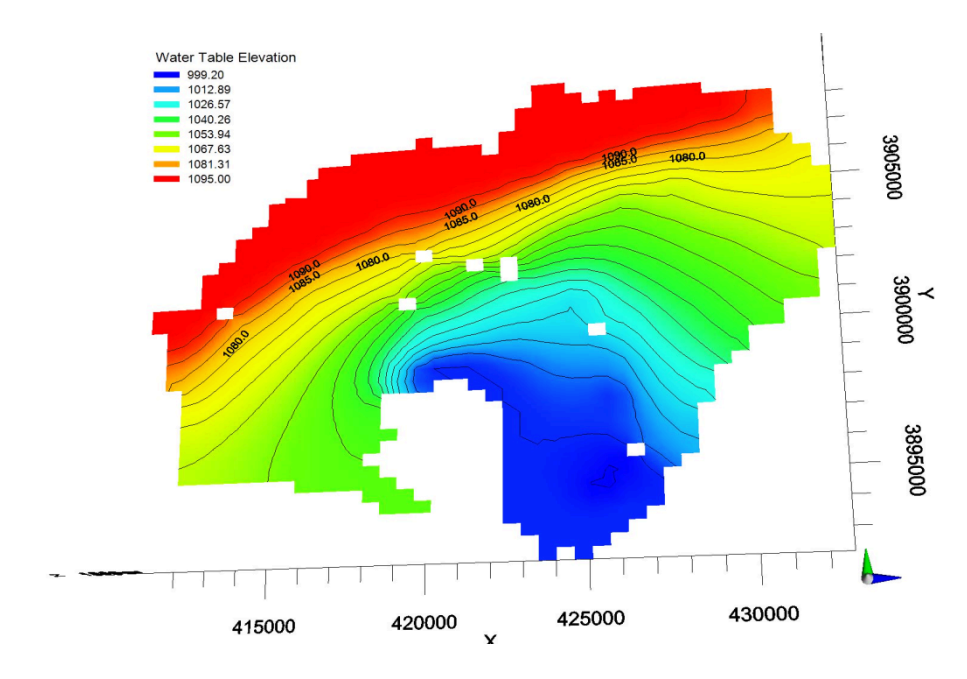


Figure 2.3.3.11: Artificial recharge results at the recommended recharge area

#### 2.3.4.5.4.4 4th Scenario

Quality impacts modeling (PhreeqC simulation), of the aquifer recharge using surface water. This simulation was carried out using different ratios; 0.2:0.8; 0.15:0.85 and 0.1:0.9.

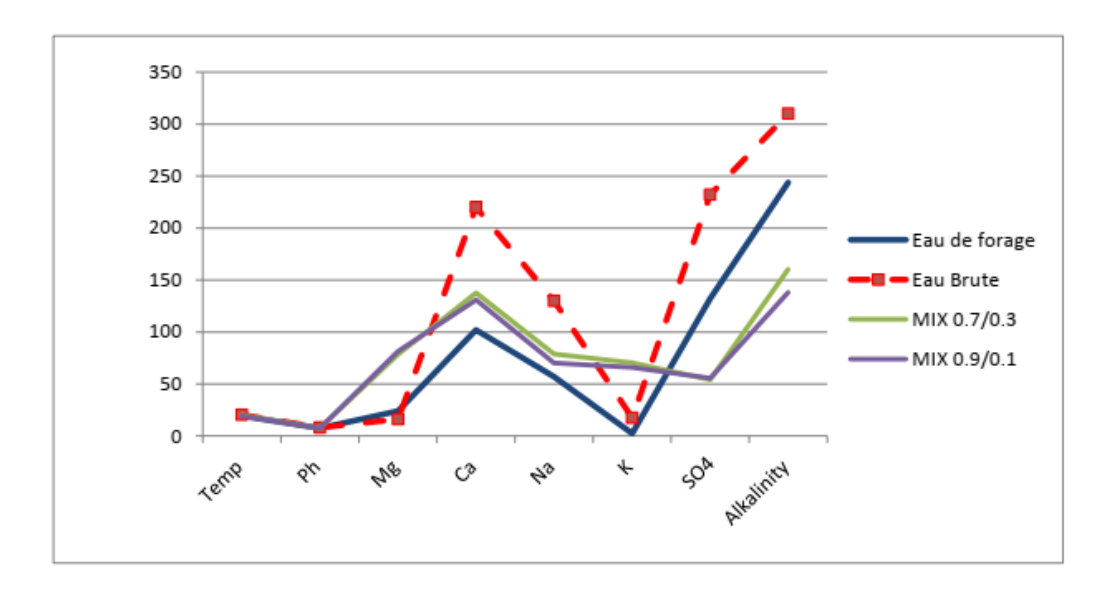


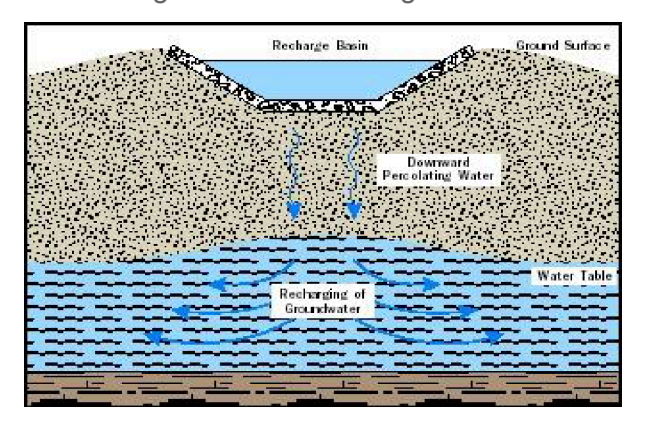
Figure 2.3.3.12: Comparison of groundwater qualities versus surface water and different Mixing solutions

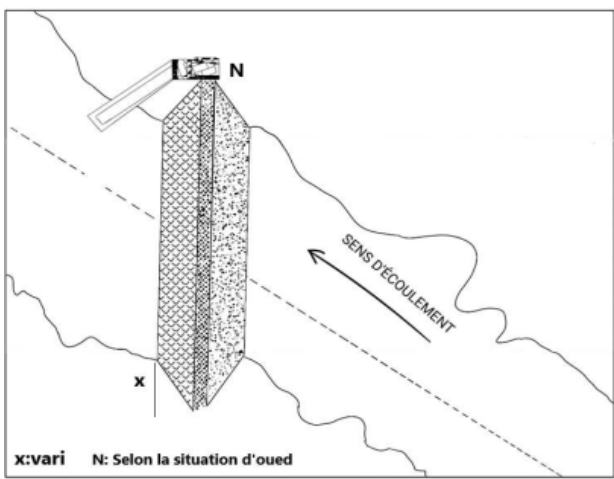
The mixture shows a significant increase in the concentrations of calcium (Ca), chloride (CI), sodium (Na), and sulfate (SO4). This suggests that the groundwater, which is richer in these elements than the surface water, influenced the composition of the final mixture, even with a ratio of 90% borehole water to 10% raw water.



In conclusion, the new mixture of the two waters, with a ratio of 70% groundwater to 30% surface water, resulted in significant changes in the chemical composition and physicochemical properties of the water. It is important to monitor these changes to avoid potential problems related to mineral precipitation or other adverse reactions

# 2.3.4.5.5 Proposal and sizing of artificial recharge sites





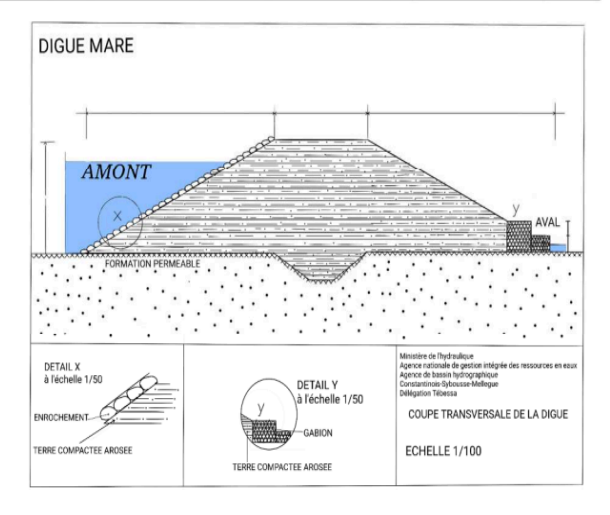


Figure 2.3.3.13: First calculations of the sizing of groundwater recharge dams



Figure 2.3.3.14: Examples of artificial groundwater recharge dams

#### 2.3.4.5.6 Stakeholder-Driven simulations:

Local surface water and groundwater potential and constraints were integrated, reflecting Living Lab-specific priorities (The groundwater level decline, due to overexploitation of the Miocene aquifer).

#### 2.3.4.5.7 Model Expansion:

New modules were proposed to well simulate NCW availability, as well as, quality impacts by hydrochemical speciation (PhreeqC simulation), and integration with conventional supplies (by combining SWAT model results with a groundwater model).

#### 2.3.4.6 Aguifer Recharge (Tunisia)

#### 2.3.4.6.1 Surface water resources

Average rainfall increases by 100 mm/year in the south and 180 mm/year in the north of the basin The hydrographic network is relatively dense, the most important wadis are those of Sidi Aich and Oued el Kébir that only flow during heavy rains. The inputs from Oued el Kébir (Figure, 3) are increased by runoff from the Ben Younes and Bou Ramli rivers.

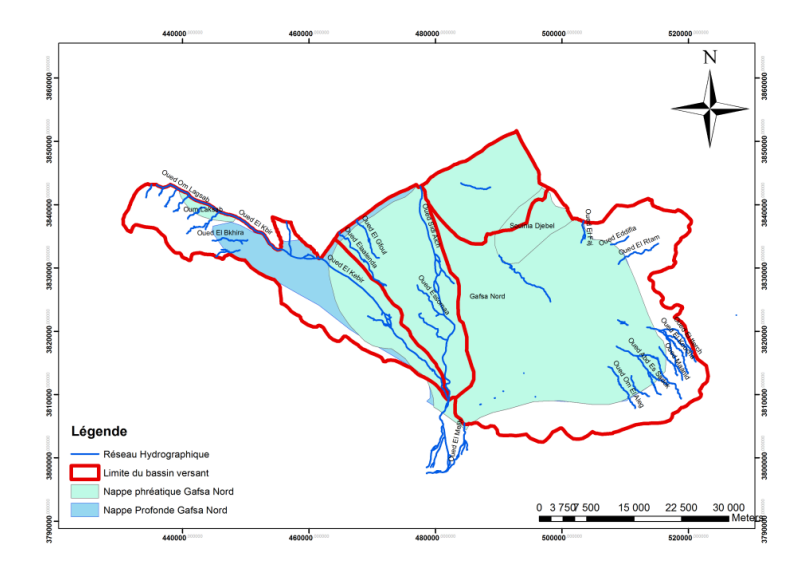


Figure 2.3.3.15: Hydrographic system/ Gafsa North basin water table



Table 2.3.3.1: Hydrological characteristics of the watersheds

	S (km²)	P (km)	H <sub>max</sub> (m)	<i>Н</i> <sub>тоу</sub> ( <b>m</b> )	Index of Compact ness $(K_G)$	I <sub>G</sub> (m/k m)	D <sub>d</sub> (km/k m²)	topogra phy (m)	specific elevatio $n [D_s]$
Sidi Aich	320,6	87,5	1312	447,5	1,38	4,8	1	$R_4$	86
Al Kabîr	335,4	138,7	1000	590	2,05	5,4	1,9	R <sub>5</sub>	114
G.Sidi Aich	207,9	58,8	900	557,5	1,15	10,5	0,7	R <sub>5</sub>	151
El Malah	1200,7	167,3	1150	542,5	1,44	5,8	0,9	R <sub>5</sub>	201

	B.V. Sidi Aich	Garât Sidi Aich	Al Kabîr	El Malah
<i>P</i> ( <b>mm</b> )	215	215	170	160
$L_r$ (mm)	8	11	10	10
runoff coefficient (%)	4	5	6	6
Shortage of supply (mm)	207	204	160	150
Average annual	2 471,994	2371,22	4452,2	12007
contribution		2		
(A) (10 <sup>3</sup> m³)				
V <sub>2ans</sub> (m <sup>3</sup> )	494 399	474222	890 440	2 401 400
V <sub>5ans</sub> (m <sup>3</sup> )	2 471 994	2371110	4 452 200	12 007 000
V <sub>10ans</sub> (m <sup>3</sup> )	6 674 383	6401996	12 020 940	32 418 900
V <sub>20ans</sub> (m <sup>3</sup> )	12 359 968	11855548	22 261 000	60 035 000
V <sub>50ans</sub> (m³)	30 899	2963887	55 652	150 087 500
	920	0	500	
V <sub>100ans</sub> (m <sup>3</sup> )	38 315	3675219	69 009	186 108 500
	901	9	100	
Module (m³/s)	0,078	0,075	0,141	0,380
specific discharge (I/s/km²)	0,244	0,361	0.317	0,317

# 2.3.4.6.2 Numerical modelling of the aquifer system

It is a set of programming modules that allows the modeling of groundwater flow and mass transport in solution in porous media.

It is a quasi-three-dimensional hydrodynamic model based on the finite difference method. It simulates the effect of wells, rivers, imposed flow limits, infiltration and evapotranspiration. This model also calculates the consolidation in the aquifer following the change of piezometric dimensions.



The software has a results extractor that allows you to display the results of each simulation, a calculator for the overall water balance of the aquifer and that of the zones specified by the user, a graph viewer that shows the evolution of calculated quantities such as the piezometrics, concentrations and time-based offsets; an output manager and a program that allows current lines to be drawn, the equipotential and velocity vector of the flow.

## 2.3.4.6.2.1 Data collection and input preparation

Before starting steady-state modelling operations, it is necessary that issues relating to the functioning of the aquifer system are clarified as input data

Input/Parameter	Description	Source
MODEL BOUNDARY		
Top of layer	DEM	Topographic investigation
Ground	Piezometric map	Etude hydrogéologique du bassin de Gafsa Nord, Moumni and Farhat
Bottom	Iso-depth map	Electrical prospecting, HDR Gousmia Moez
Well	Pumping and observation wells	Annuaire exploitation et piezometrie (CRDA)
PROPERTIES		
Conductivity (Kx, Ky, Kz)	Pumping tests	Well's description sheet
Initial head		
Storage		
BOUNDARY CONDITION	ONS	
Constant head	Alimentations area	Topographic map
Evapotranspiration	Evapotranspiration (mm/y), extraction depth (mm)	Meteorological data (ONM)
Specified flux	Recharge rate by fault area	Geological study
River	Stages, bed, depth, thickness and conductivity	Satellite and field investigation

A model is nothing more than a process that allows the expression of the physical phenomenon using mathematical equations expressing the conservation of matter, the modelling of a given physical phenomenon must follow the following steps and procedures:

 The first step in the modelling process is to formulate a conceptual model of the system which is nothing more than a set of assumptions simplifying reality allowing the transition to an acceptable version from the point of view of the planner's objectives



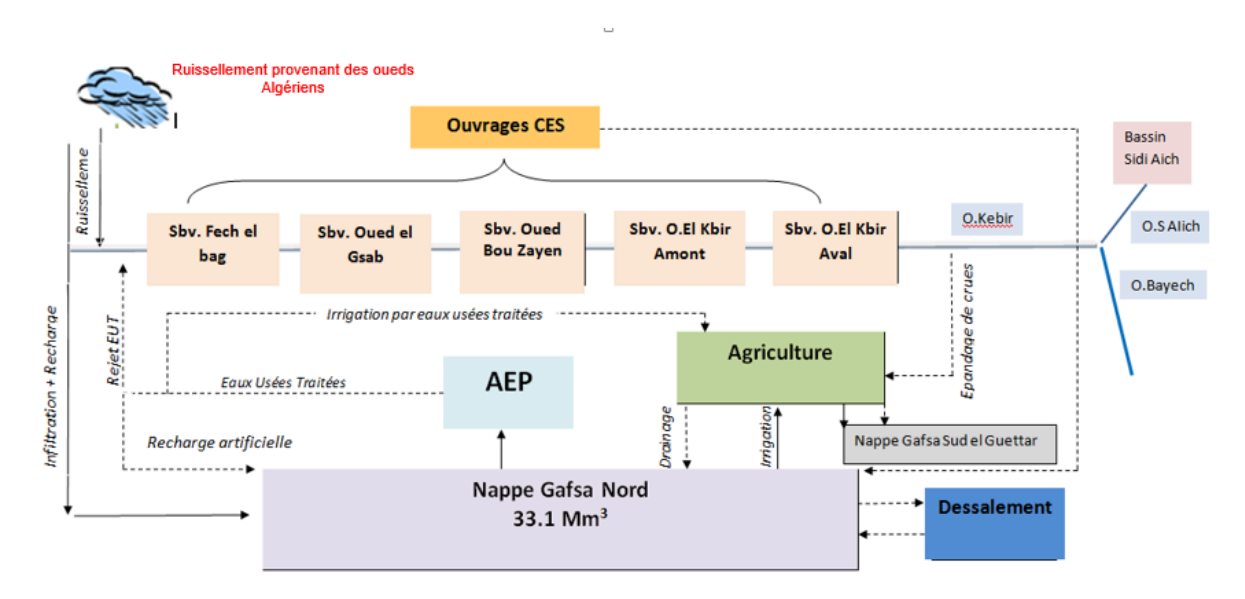


Figure 2.3.3.16: Theoretical conceptual model illustrating the inputs/outputs and links for the Gafsa North tablecloth

 The second step is to express the conceptual model in the form of mathematical equations describing all the physical processes involved. This step consists of defining the geometry of the domain and those limits that determine the interaction of the system with its environment

# **IDENTIFICATION DES PROPRIÉTÉS DE LA ZONE**

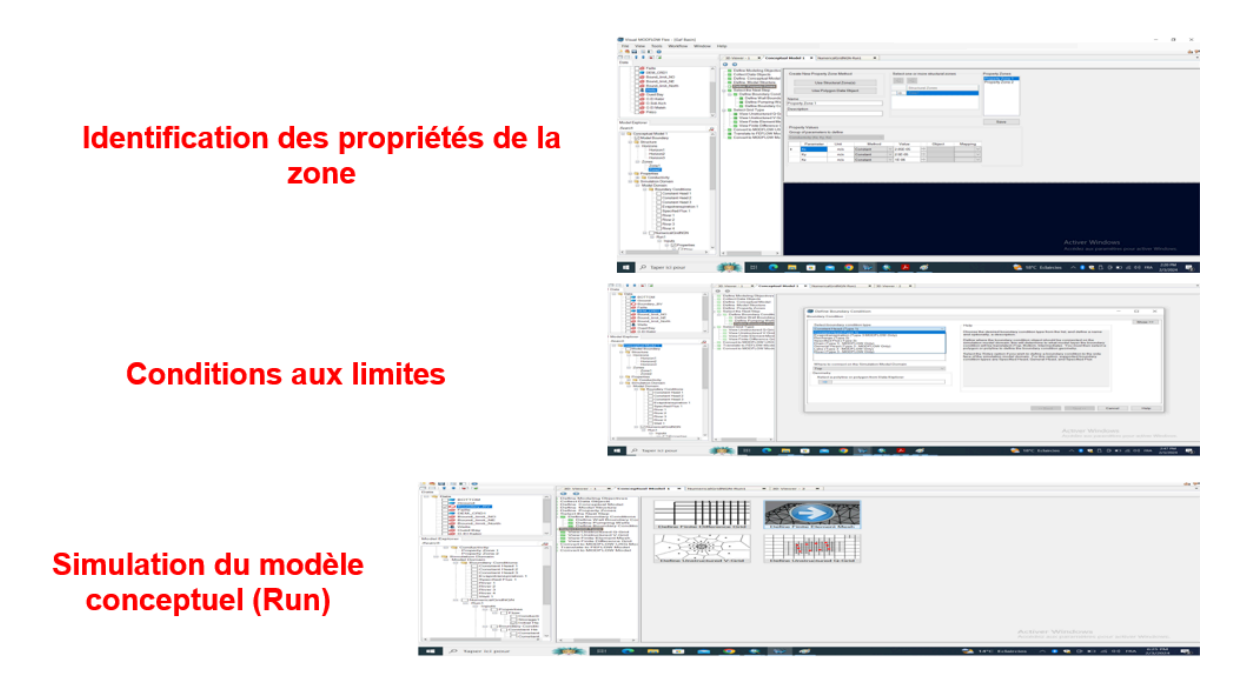


Figure 2.3.3.17: Conceptual model by ModflowFlex 6



# GÉOMÉTRIE DE L'AQUIFÈRE (MODEL BOUNDARY)

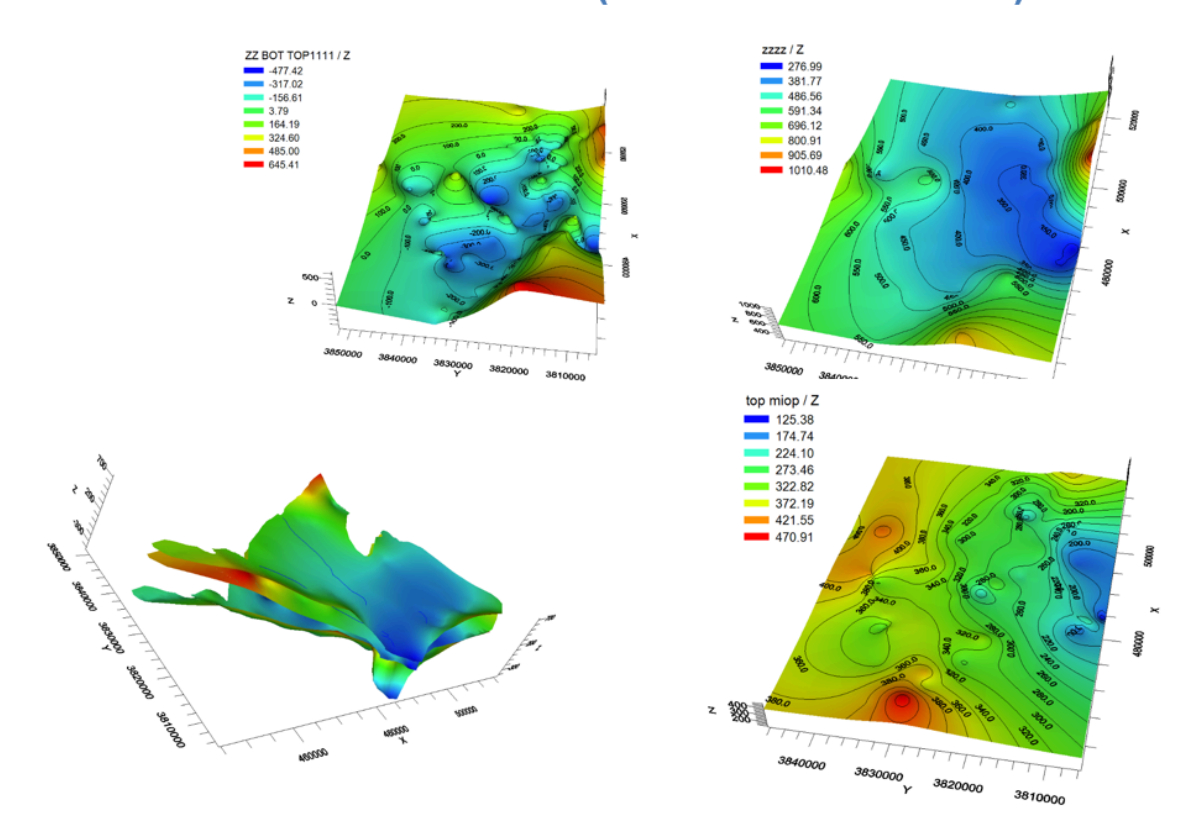


Figure 2.3.3.18: Geograph of the aquifer by Modflow Flex 6

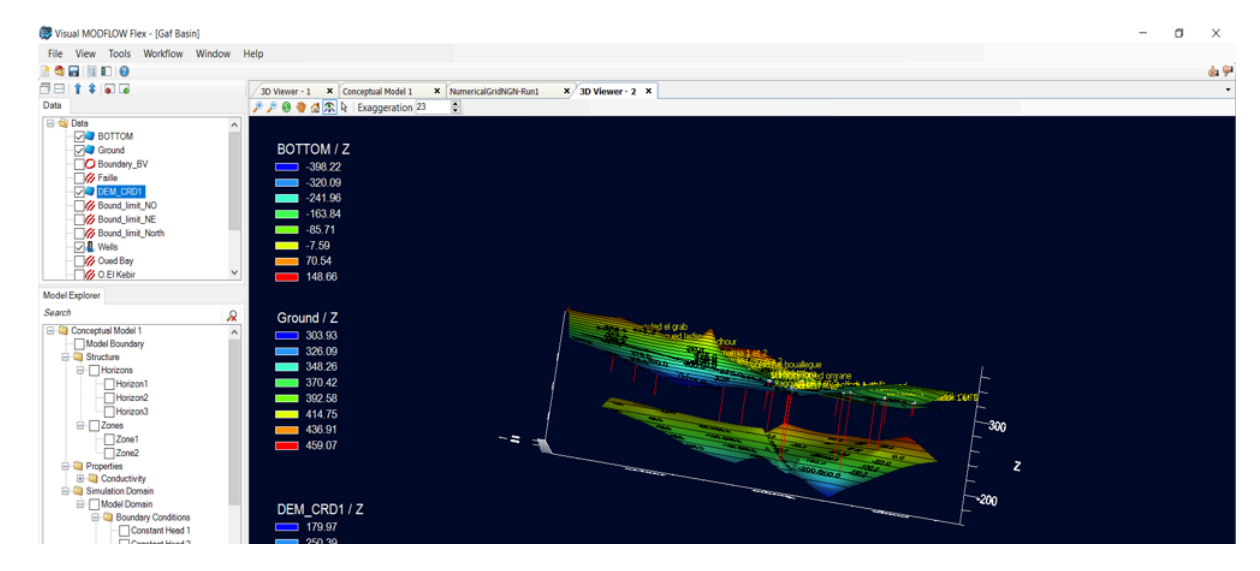
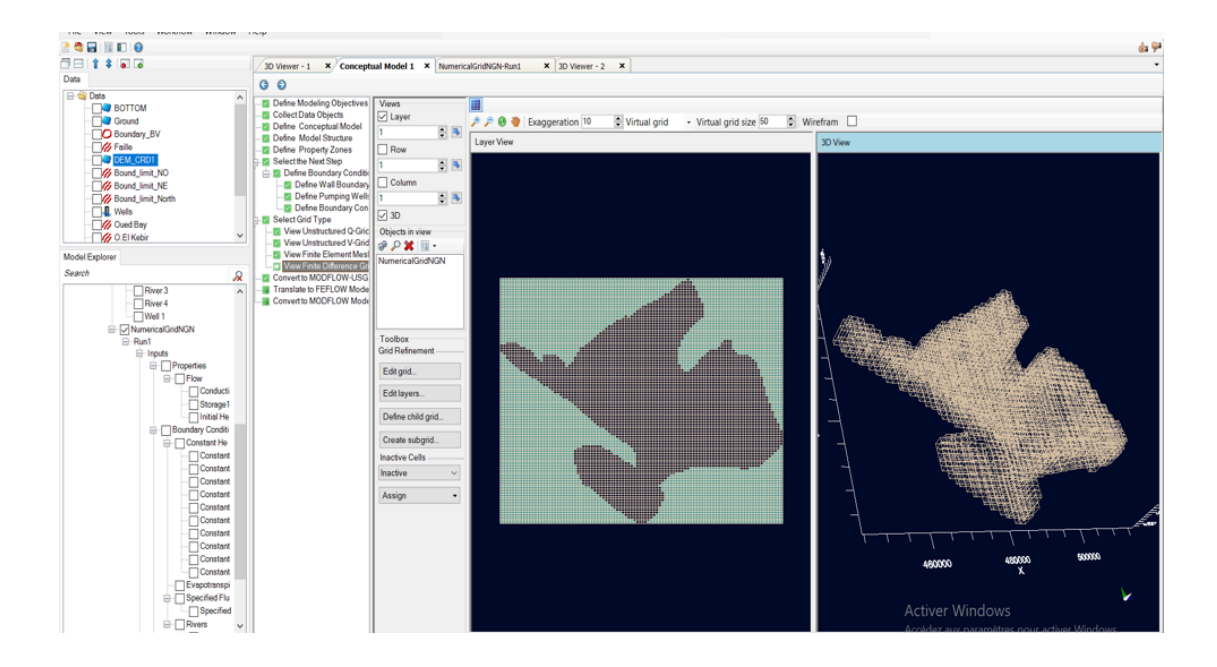


Figure 2.3.3.19: 3D Geograph of the aquifer by Modflow Flex 6 (drilling visualization)

The field of study is divided along the three directions of space into parallelepiped elements called meshes. Each mesh is characterized by its length  $\Delta$  x, its width  $\Delta$  y and its thickness  $\Delta$  z. The center of a mesh is called a node and is identified in terms of line: line (i), column (j) and layer (k).



# Définition du domaine par différences finies

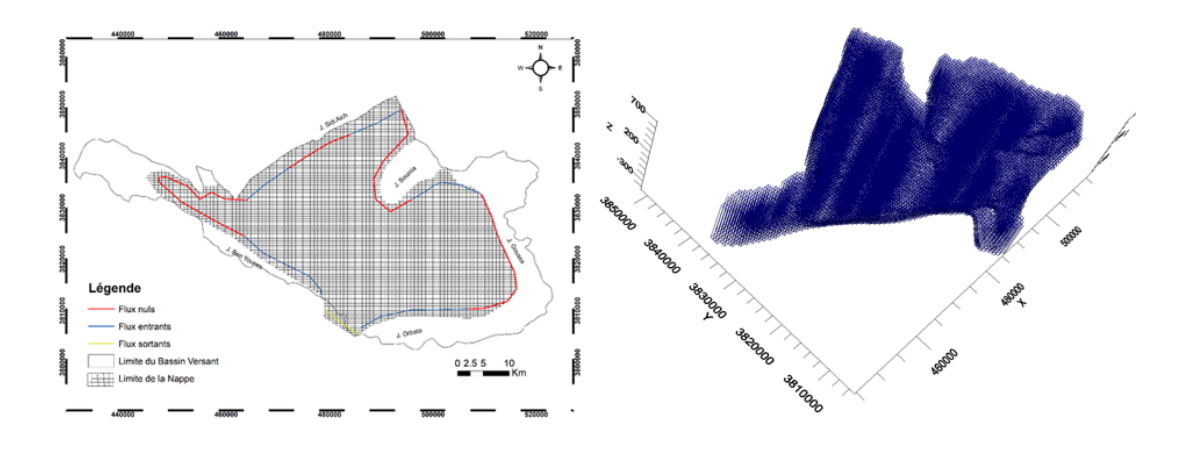


Figure 2.3.3.20: Discretization of the aquifer domain (mesh) by Modflow Flex 6 (finite difference method)

# 2.3.4.6.2.2 Evaluation of exploitation

Table 2.3.3.2 shows that there was a significant increase in the exploitation rate of the Gafsa North deep water from 1998 to 2012. This rate has risen from 79% in 1998 to 115% in 2012, which corresponds to an increase of 36% over 14 years, or an increase of about 2.5%/year. The number of wells and boreholes have increased considerably up until recent years (fig. 2.3.3.21 and fig. 2.3.3.22)



Year	nbr Breholes	harvestable resources (Mm³/an)	Exploitation (Mm³/an)	Ratio
1998	76	33.1	26.16	79
2000	94	33.1	28.92	87
2002	129	33.1	37.47	113
2004	136	33.1	31.34	94.5
2006	156	33.1	33.42	101
2008	173	33.1	33.3	100
2010	197	33.1	39	117
2012	225	33.1	38	115

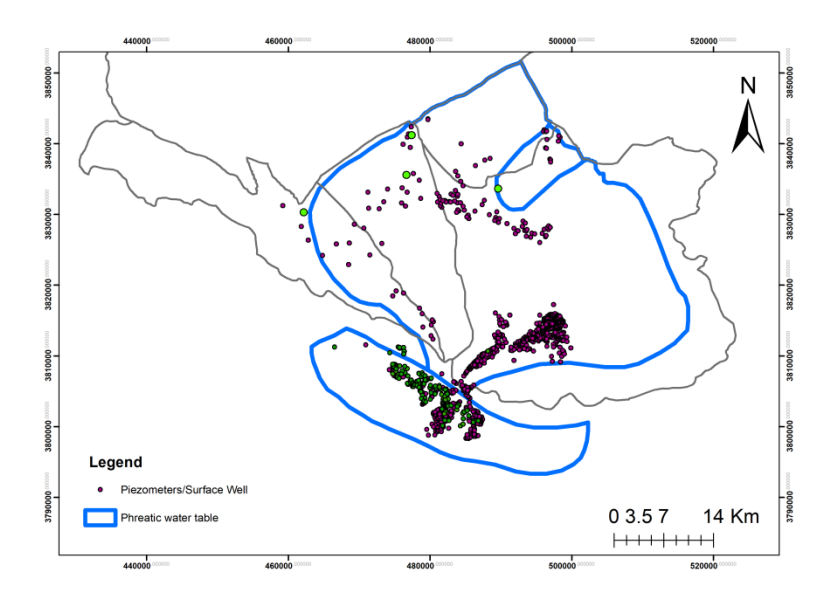


Figure 2.3.3.21: Boreholes in the Gafsa Nord Nappe

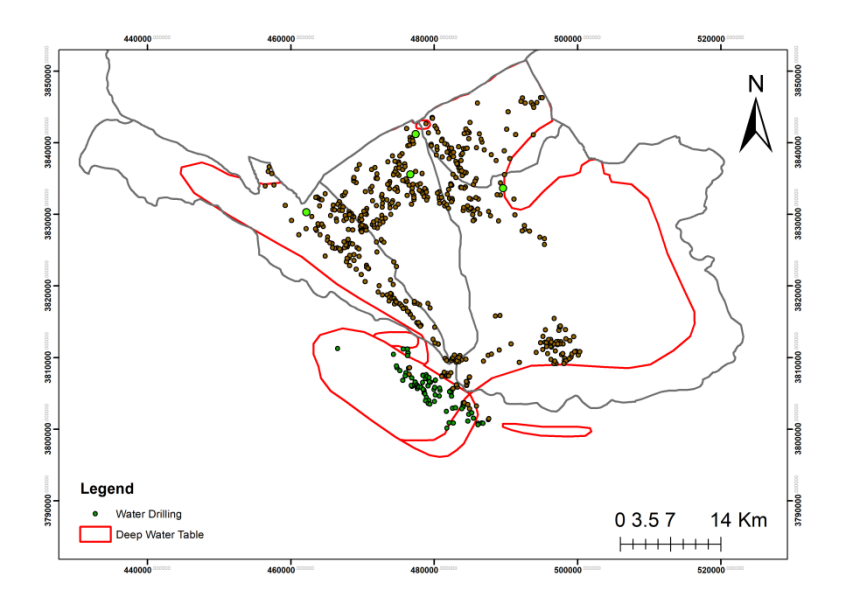


Figure 2.3.3.22: Boreholes in the Gafsa Nord Nappe

According to Choura (2012), the increase in the exploitation rate was mainly due to additional pumping on agricultural wells due to water shortages during the least rainy years. Indeed, the plain of Gafsa is the seat of an intense agricultural activity with enlargement of the irrigated perimeters both public and private.

#### 2.3.4.6.2.3 Piezometry

The piezometric map of the plio-quaternary aquifer system shows a general flow from North to South allowing the diverging waters of the Majel Bel Abbes basin in the Gafsa Nord basin (Fig. 9). The supply of this aquifer is ensured by the infiltration of flood waters from the hydrographic network descending from the Hoguef, Goure Souane and Toualet jebels throughdirect infiltration of rainwater.

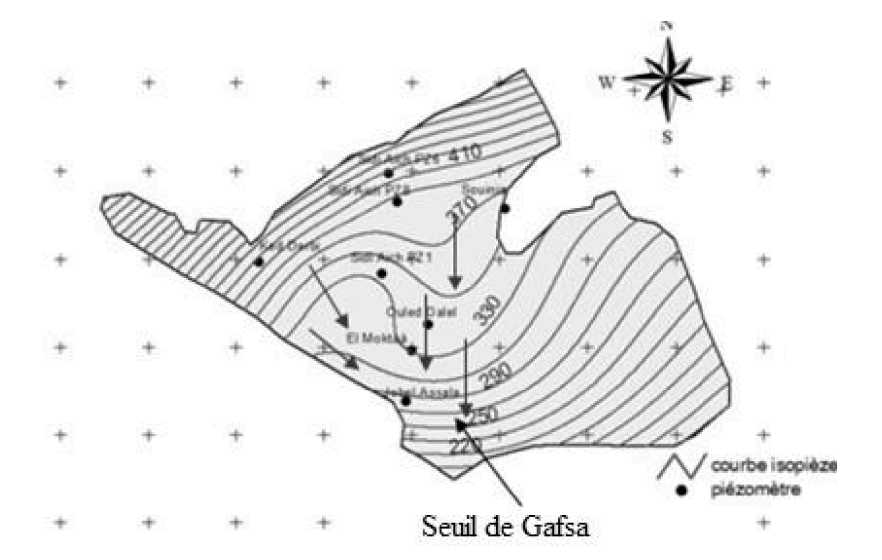




Figure 2.3.3.23: Piezometric map for the year 2012 (Majdoub et al, 2014)

The piezometric map of the Gafsa Nord (for the year 2012), shown in Figure 9, revealed that piezometric levels vary between 200 m downstream of the plain and 400 m NGT at the Sidi Aich (PZ8) piezometer located upstream. The flow direction is from North, Northwest to South.

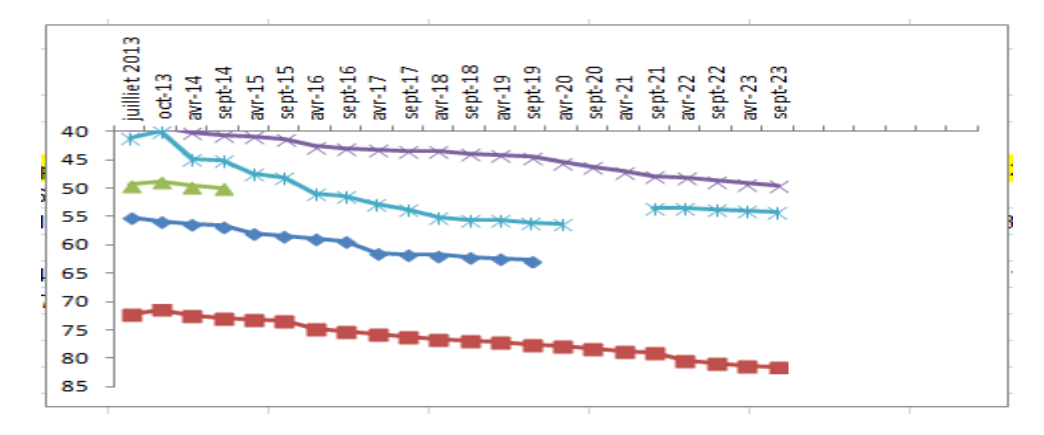


Figure 2.3.3.24: Evolution of the depth of the water table

### 2.3.4.6.3 Recharge scenarios

The operating rate rose from 79% in 1998 to 115% in 2012, which corresponds to an increase of 36% over 14 years, or an increase of about 2.5%/year.

For this reason, the reference year was chosen as 1998 to model the stationary state and to carry out the calibration by returning the values of the hydraulic loads and closing the balance sheet

The calibration procedure adopted consisted of simulating the behaviour of the model in steady state by adjusting mainly the horizontal and vertical transmissivity so that the velocity of the returned piezometric map corresponds to that observed and that the flows calculated are consistent with the balance sheet terms observed.

#### 2.3.4.6.3.1 Transient regime

The transient regime restores the rebates according to time, the imposed loads become imposed flows, and the storage is taken into account, next to the exploitation for each step of time, this retrieval of the history of the table is a starting point for future simulations.

The transient calibrated model can be used to simulate the impact of the change in balance sheet parameter(s) according to previously selected assumptions, these assumptions will be classified as follows:

 Increased use of treated wastewater for irrigation (this would result in modflow by reducing the production rate in the relevant boreholes in the 'well' file),

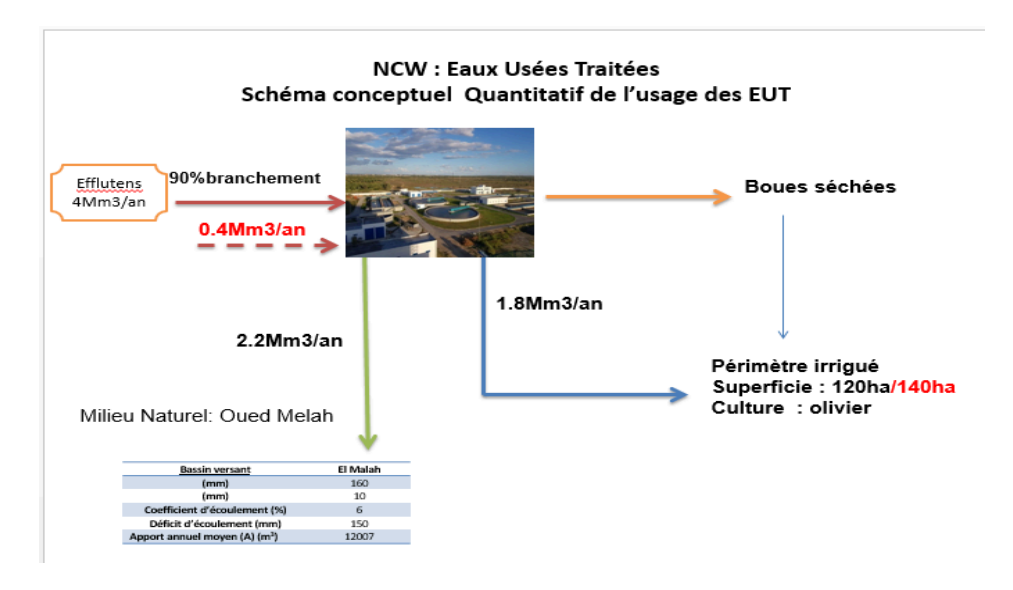


Figure 2.3.3.25: Treated wastewater reality and planning

• Increase artificial recharging by CES works (this would result in an increase in the volume of recharging in the 'Recharge' file

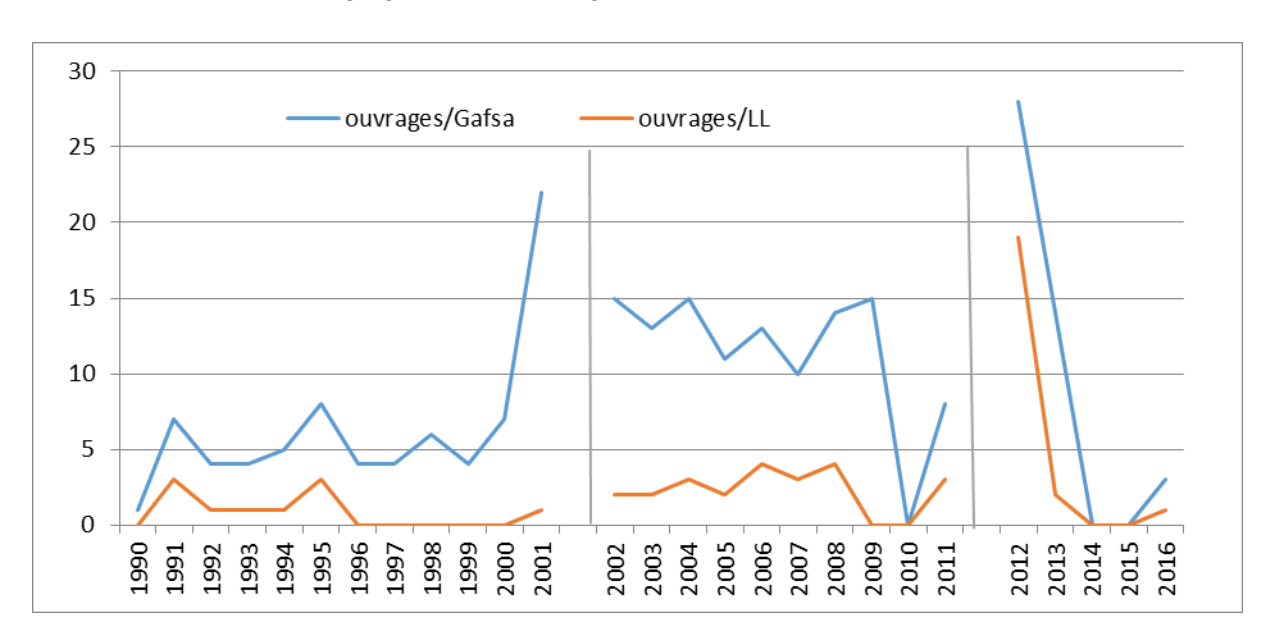


Figure 2.3.3.26: Evolution of the number of water and soil conservation works during development plans (CRDA, Arrondissement CES)

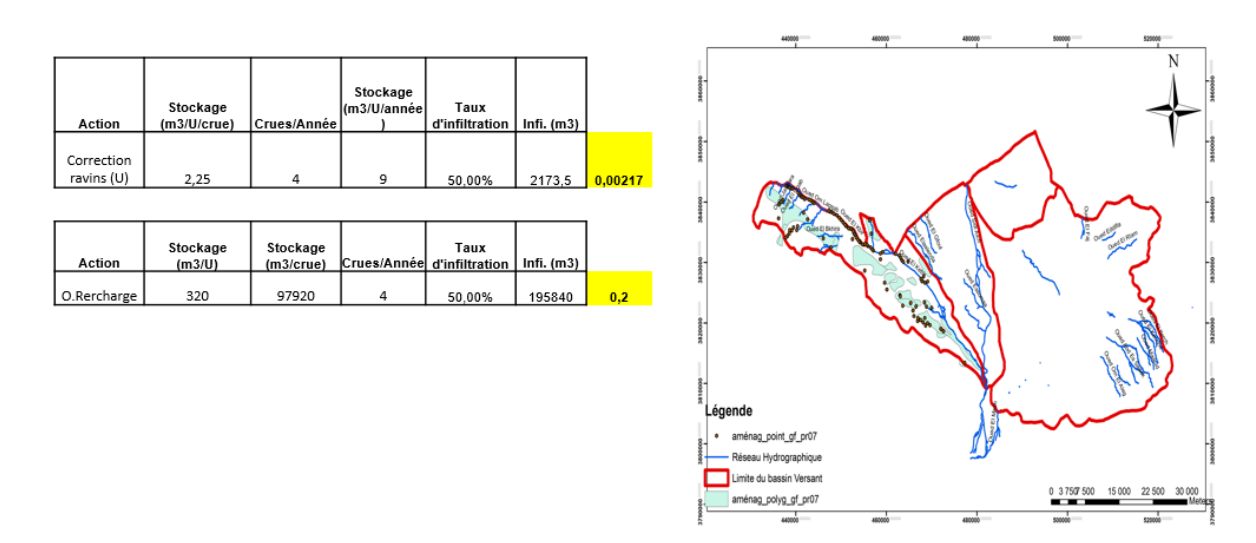


Figure 2.3.3.27: Supply of recharging works (CRDA, CES District)

- Optimization of the drainage system and reuse of excess water
- Better management of Dam releases

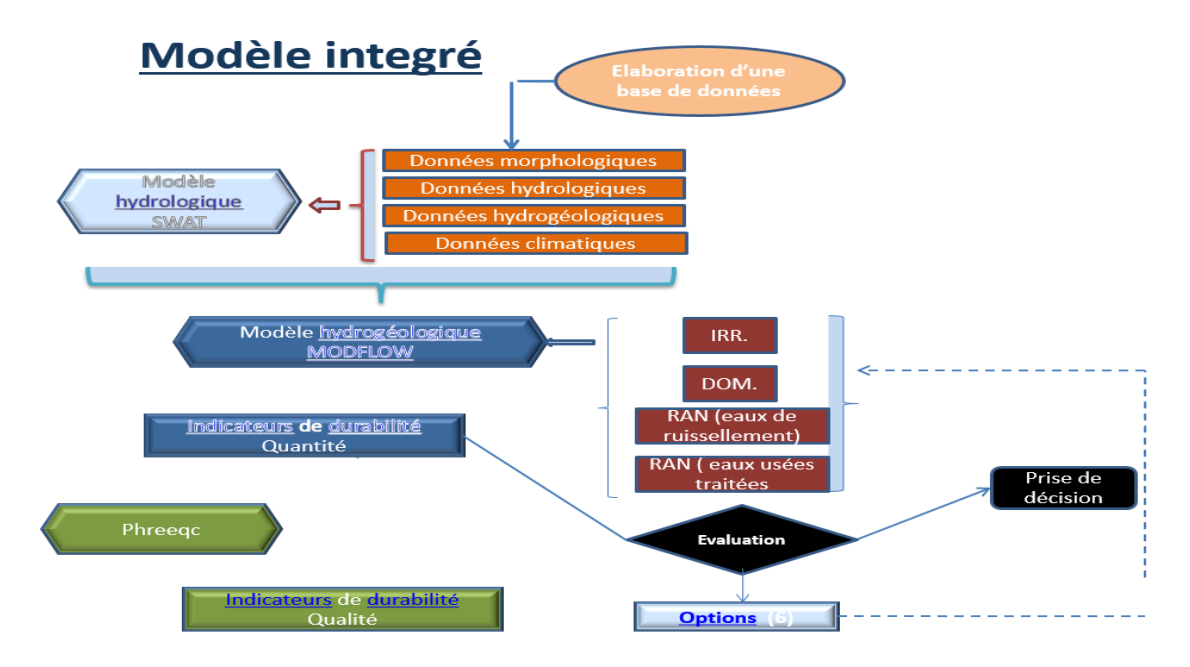


Figure 2.3.3.28: Flowchart of the decision support process for water resources management

# 2.3.4.6.3.2 Exploitation (pumping) scenarios

Given the evolution of water demand as a function of population growth, and the increase in irrigated agricultural areas, it could be assumed that the evolution continues at the past pace following the trend of historical

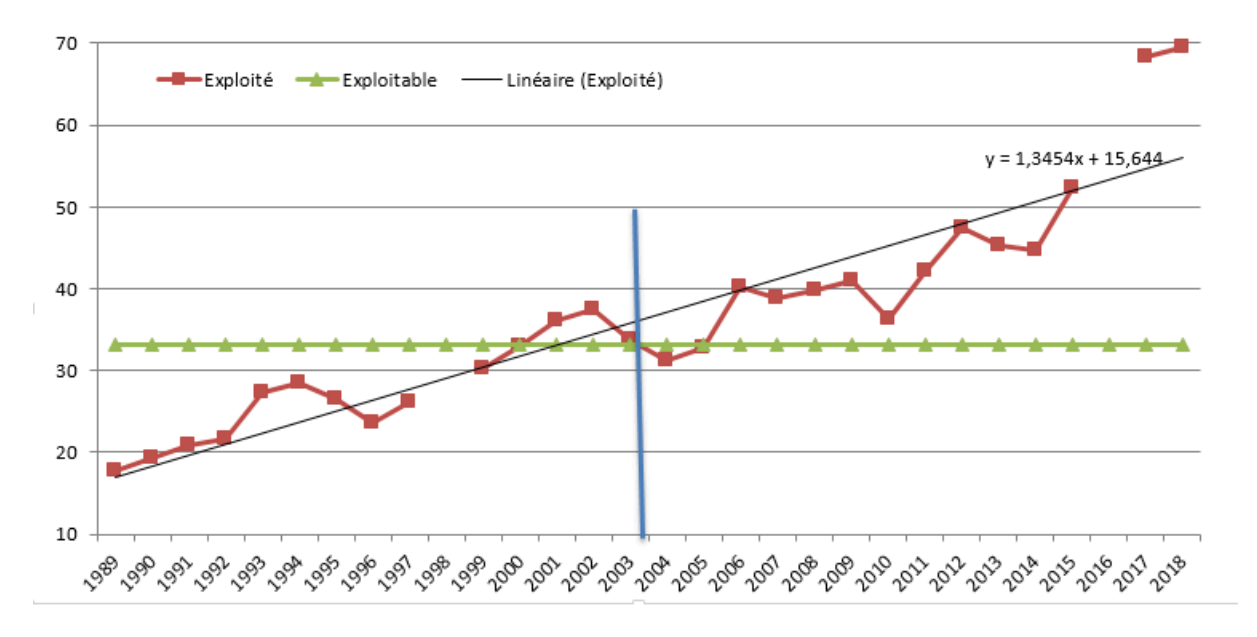


Figure 2.3.3.29: Operating trend = trend history

• Exploitation dwindles in favour of the use of non-conventional waters Exploitation dwindles in favour of the use of non-conventional waters

# 2.3.4.6.3.3 Introduction of the supply of refill structures in Modflow inputs

Artificial recharge is the increase in the amount of water benefiting groundwater reservoirs through artificial devices (Todd, 1959). It can be argued that artificial recharge of groundwater is a practice which aims to increase the volumes of groundwater available by promoting, through anthropogenic means and practices.

Several recharge methods and techniques are practiced such as:

- The release of water from flood dams into flat surfaces or depressions (spreading) and into the beds of the Oueds (recharge);
- Construction of the braking works and extension of the water flow speed in particular (the thresholds of gabions, diguettes, collinaires lake...);
- Infiltration of treated wastewater into developed basins;
- Direct injection of clean water into surface wells and drilling directly to the groundwater.

Regarding the study area, the artificial recharge of the Gafsa Nord tablecloth was practiced by two types of feeding, one by the construction of the recharge works and the other by the construction of the Sidi Aich recharge dam which feeds the water table through the waters of the rivers.

Indeed, the wadi Sidi Aich benefits from the loose. To estimate the recharge rate in this area we applied the same principle of the climatic method, so that the releases are considered as precipitation but with some differences, taking into account the role of the recharge works carried out in this area.



Integration of the PHREEQC code was done as a decision support tool for the location of artificial recharging facilities.

The equation adopted is therefore:  $V_{R2} = V_R + (L_{ch} *C_i) + (T_{r.o} *n)$ 

- $V_{R2}$ : Estimated recharging volume after artificial recharging (Mm3/year);
- $V_{p}$ : Estimated diffuse recharge volume (Mm3/year);
- $L_{ch}$ : Quantities of water following dam discharges (Mm3);
- $T_{r,o}$ : Estimated water rates due to infiltration by refill structures.
- n: Number of good charging facilities in the area.

#### 2.3.4.6.3.4 Non-conventional water for artificial recharge

Potential sources for artificial recharge of the water table are stormwater and treated wastewater from the Gafsa city sewage treatment plant (Table 2.3.3.4), both meet environmental discharge standards (Table 2.3.3.5);

Table 2.3.3.3: Environmental discharge standards (Ministry of Environment Tunisia)

	Domaine Public hydraulique
	(Oued)
Azote organique et	1
ammoniacal (mg/l)	·
Bioxyde de chlorure (mg/l)	0.05
Calcium (mg/l)	500
Chlore actif (mg/l)	0.05
Chlorures(mg/l)	600
Demande biologique en	30
oxygene DBO5 (mgO2 /l)	
Demande Chimique en	125
Oxygene DCO (mgO2/l)	120
Detergent Anioinique(mg/l)	0.5
Florures dissous F (mg/l)	3
Graines et huiles saponifiables	20
Magnesium Mg (mg/l)	200
Matières décantables (mg/l)	0.3
MES (mg/l)	30
Nitrates NO3 (mg/l)	50
Nitrites NO2 (mg/l)	0.5
PH	6.5 à 8.5
Phosphores (mg/l)	0.05
Potassium K (mg/l)	50
` • ′	
Sodium S (mg/l)	300
Sulfates (mg/l)	0.1



Tables 2.3.3.4 & 2.3.3.5: Concentrations in major elements non-conventional waters for RAN (April 2025)

Eaux pluviales	Résultat
	S
Sodium, Na (mg/l)	7.13
Potassium, K (mg/l)	4.68
Calcium, Ca (mg/l)	17.75
Magnésium, Mg (mg/l)	8.16
Chlorure, cl (mg/l)	17.75
Sulfate, SO <sup>2-</sup> <sub>4</sub> (mg/l)	14.85
Bicarbonates, HCO-3	183
(mg/l)	

Eaux Usées Traitées	Résultat s
Sodium, Na (m/l)	532.5
Potassium, K (mg/l)	23.9
Calcium, Ca (mg/l)	904.5
Magnésium, Mg (mg/l)	154.8
Chlorure, cl (mg/l)	212.7
Sulfate, SO <sup>2</sup> - <sub>4</sub> (mg/l)	1782.7
Bicarbonates, HCO <sub>3</sub> (mg/l)	350

A first sampling campaign has been carried out in the south of the basin, the boreholes are located in the area already irrigated by treated wastewater, in this region, it could be proposed to recharge with stormwater, therefore, the location of the structure will be influenced by:

- Feasibility (permeability, slope...)
- Land condition (Figure 2.3.3.30)
- The depth of the table
- The concentration in major elements
- The best mixing between groundwater and artificial recharge

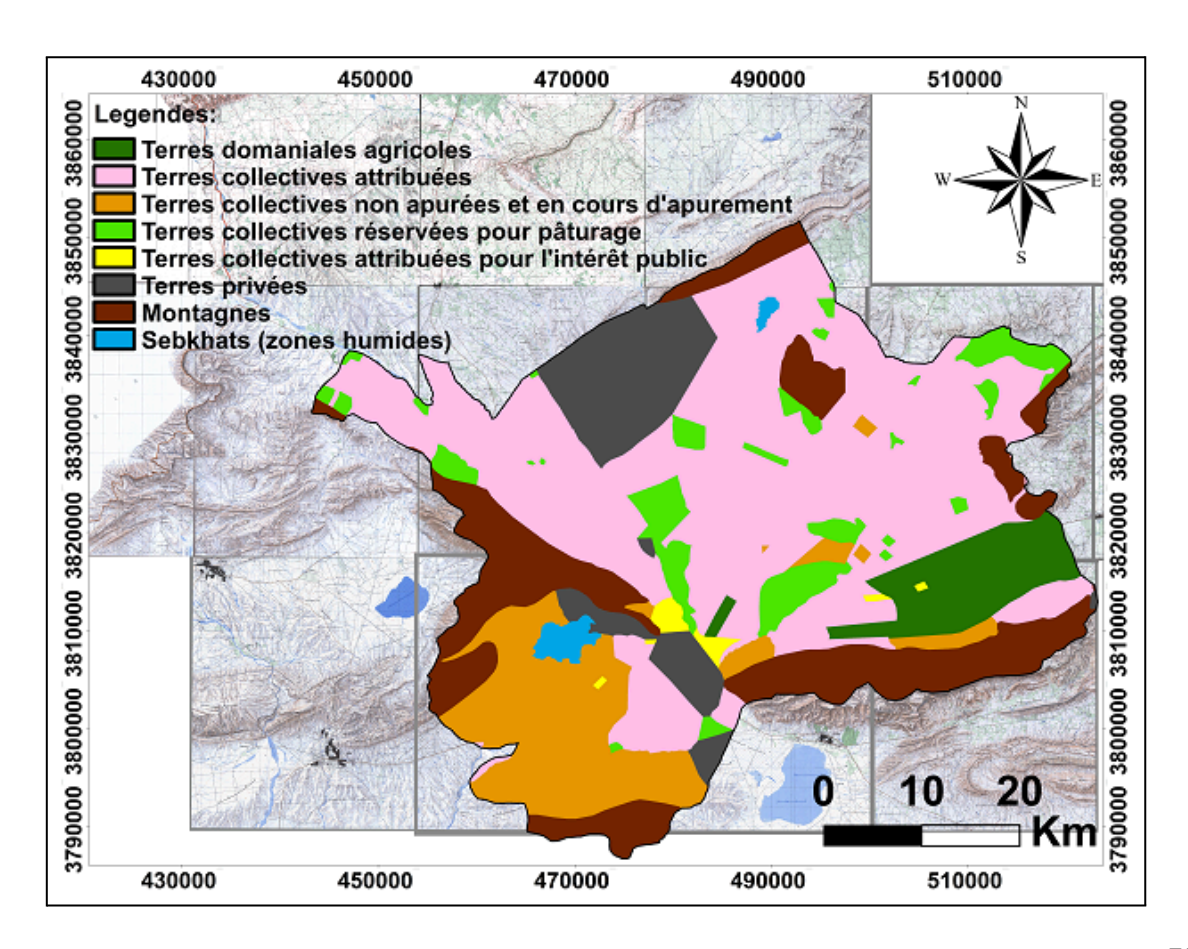




Figure 2.3.3.30: Legal status of land map (source: agricultural map, CRDA)

Table 2.3.3.6: Major drilling elements in areas irrigated by treated wastewater

Wells	(MF)	(AO)	(FB)	(SF)	(JD)	(MF)	(FG)	(NL)
Sodium, Na (mg/l)	716.3	607.5	460	1074.8	533 .8	716.3	785	342.6
Potassium, K (mg/l)	50.6	69.9	263.4	58.3	69.8	50.6	71.9	61.4
Calcium, Ca (mg/l)	910.7	843.4	944.3	1068.7	911.3	910.7	920.2	942.1
Magnésium, Mg (mg/l)	206.1	184	100.4	296.1	163.1	206.1	240.3	105
Chlorure, cl (mg/l)	496.3	496.3	425.4	780	496.3	496	567.2	283.6
Sulfate, SO <sup>2-</sup> <sub>4</sub> (mg/l)	9723.1	2017.7	1345.7	3012.1	1701	9723.1	2182.6	2420.9
Bicarbonates , HCO-3 (mg/l)	512.5	268.5	366.1	463.7	390.5	512.2	488.1	561.4

# 2.3.5 Summary table

# AG-WaMED Living Lab Summary Table

Living Lab (Country)	Main Challenge	Model Used	Main NCW Solution Tested	Main findings
Orcia (Italy)	Seasonal water scarcity for irrigation due to climate change and limited groundwater access	SWAT+ (calibrated with streamflow and ET data), WATNEEDS for irrigation demand	Small agricultural reservoirs (SmARs) integrated into SWAT+	Modelled 329 SmARs covering ~80% of total reservoir volume; demonstrated potential to meet peak irrigation demand under climate change scenarios.
Campo de Cartagena (Spain)	Decreased availability from Tagus-Segura transfer due to revised ecological flow requirements	SIMPA for water balance, Aquatool (SIMGES module) for reservoir and transfer simulation	Evaluation of Tagus-Segura Transfer under different flow rules and assess the role of desalination	Simulated impact of revised ecological flows; found 73 hm³/year reduction in transfer volume, highlighting need for desalination or water reuse.



Wadi Naghamish (Egypt)	Extremely low rainfall and negligible runoff in arid climate conditions	SWAT+ for watershed modeling and cistern runoff validation, WATNEEDS for irrigation demand	Modeling and integration of traditional rainwater harvesting cisterns	Validated traditional cistern systems using SWAT+; found 98% of precipitation lost to ET, reinforcing cisterns' role in water harvesting.
Al Kabir (Algeria/Tunis ia)	Aquifer depletion and salinity due to overextraction and limited surface water availability	SWAT+ for watershed balance, coupled with MODFLOW for groundwater and aquifer recharge modeling, PhreeqC for water quality	Artificial aquifer recharge using surface water and treated wastewater, with water quality assessment	Demonstrated feasibility of aquifer recharge; modeled water table recovery under artificial recharge scenarios using MODFLOW and assessed quality with PhreeqC

# 3. Discussion

The modeling results highlight, as expected, a common challenge across all Living Labs (LLs): limited water availability, with higher intensity in North African LLs. In each LL, the disparity between agricultural demand and the actual water availability becomes strikingly evident, in conjunction with some other challenges raised by stakeholders as water access, water quality (i.e. salinity registered in Algerian/Tunisian LL and Italian LL), and lack in policy and water. Results for the current status clearly emphasize the critical issue of current water scarcity, a concern that necessitates urgent and effective solutions, that are already being discussed among stakeholders in each LL (WP2) and that will be implemented in the next step of D3.1 to check the effectiveness of the solution proposed. The irrigation demand quantified with the WATNEEDS model often exceeds the local availability of water resources, especially in the Egypt and Algerian/Tunisian LL where the runoff is mostly negligible, and the groundwater is often characterized by increasing depth and low quality. The present scenario reflects the overarching problem of water scarcity in these regions, as well known by local stakeholders, with the need to identify potential strategies to overcome better water management, including non-conventional water solutions, as well as crop re-allocation as proposed within the WP5.2 of the AG-WaMED project. The modeling of alternatives demonstrates rooms for potential successful applications of alternate strategies wherever applicable. These results will help the definition of policies as By Wp4.



# 4. References

- Abd-Alla G. M.H. 1997. Assessment of rainfall-Runoff Dynamics at east Matrouh, Noart West Coast, Egypt. PhD thesis, Soil and Water department, faculty of Agriculture, Alexandria University.
- Álvarez, J., Sánchez, A., & Quintas, L. (2005). SIMPA, a GRASS based tool for hydrological studies. *International Journal of Geoinformatics*, 1(1).
- Arnold, J. G., Kiniry, J. R., Srinivasan, R., Williams, J. R., Haney, E. B., & Neitsch, S. L. (2012). *Soil & Water Assessment Tool. Version 2012*. 654. http://swat.tamu.edu/media/69296/SWAT-IO-Documentation-2012.pdf
- Chiarelli, D. D., D'Odorico, P., Müller, M. F., Mueller, N. D., Davis, K. F., Dell'Angelo, J., Penny, G., & Rulli, M. C. (2022). Competition for water induced by transnational land acquisitions for agriculture. *Nature Communications*, *13*(1), 1–9. <a href="https://doi.org/10.1038/s41467-022-28077-2">https://doi.org/10.1038/s41467-022-28077-2</a>
- Chiarelli, D. D., Passera, C., Rosa, L., Davis, K. F., D'Odorico, P., & Rulli, M. C. (2020). The green and blue crop water requirement WATNEEDS model and its global gridded outputs. *Scientific Data*, 7(1), 1–9. https://doi.org/10.1038/s41597-020-00612-0
- d'Andrimont, R., Verhegghen, A., Lemoine, G., Kempeneers, P., Meroni, M., & van der Velde, M. (2021). From parcel to continental scale A first European crop type map based on Sentinel-1 and LUCAS Copernicus in-situ observations. *Remote Sensing of Environment*, 266(October). <a href="https://doi.org/10.1016/j.rse.2021.112708">https://doi.org/10.1016/j.rse.2021.112708</a>
- European Environment Agency. (2021). CORINE Land Cover User Manual. In *Copernicus Land Monitoring Service: Vol. 1.0* (Issue European Union).

  <a href="https://land.copernicus.eu/pan-european/corine-land-cover/clc2018?tab=metadata%0Ahttps://land.copernicus.eu/pan-european/corine-land-cover/clc2018%0Ahttps://land.copernicus.eu/pan-european/corine-land-cover/clc2018%0Ahttps://land.copernicus.eu/pan-european/corine-land-cover/clc2018%0Ahttps://land.copernicus.eu/pan-european/corine-land-cover/clc2018%0Ahttps://land.copernicus.eu/pan-european/corine-land-cover/clc2018%0Ahttps://land.copernicus.eu/pan-european/corine-land-cover/clc2018%0Ahttps://land.copernicus.eu/pan-european/corine-land-cover/clc2018%0Ahttps://land.copernicus.eu/pan-european/corine-land-cover/clc2018%0Ahttps://land.copernicus.eu/pan-european/corine-land-cover/clc2018%0Ahttps://land.copernicus.eu/pan-european/corine-land-cover/clc2018%0Ahttps://land.copernicus.eu/pan-european/corine-land-cover/clc2018%0Ahttps://land.copernicus.eu/pan-european/corine-land-cover/clc2018%0Ahttps://land.copernicus.eu/pan-european/corine-land-cover/clc2018%0Ahttps://land.copernicus.eu/pan-european/corine-land-cover/clc2018%0Ahttps://land.copernicus.eu/pan-european/corine-land-cover/clc2018%0Ahttps://land.copernicus.eu/pan-european/corine-land-cover/clc2018%0Ahttps://land.copernicus.eu/pan-european/corine-land-cover/clc2018%0Ahttps://land.copernicus.eu/pan-european/corine-land-cover/clc2018%0Ahttps://land.copernicus.eu/pan-european/corine-land-cover/clc2018%0Ahttps://land.copernicus.eu/pan-european/corine-land-cover/clc2018%0Ahttps://land.copernicus.eu/pan-european/corine-land-cover/clc2018%0Ahttps://land.copernicus.eu/pan-european/corine-land-cover/clc2018%0Ahttps://land.copernicus.eu/pan-european/corine-land-cover/clc2018%0Ahttps://land.copernicus.eu/pan-european/corine-land-cover/clc2018%0Ahttps://land.copernicus.eu/pan-european/corine-land-cover/clc2018%0Ahttps://land.copernicus.eu/pan-european/corine-land-cover/clc2018%0Ahttps://land.copernicus.eu/pan-european/cor
- Forzini, E., Villani, L., Castelli, G., Bresci, E. (2025). Participatory Modeling of Small Agricultural Reservoirs in the Orcia Watershed, Italy. In: Sartori, L., Tarolli, P., Guerrini, L., Zuecco, G., Pezzuolo, A. (eds) Biosystems Engineering Promoting Resilience to Climate Change AIIA 2024 Mid-Term Conference. MID-TERM AIIA 2024. Lecture Notes in Civil Engineering, vol 586. Springer, Cham. <a href="https://doi.org/10.1007/978-3-031-84212-2">https://doi.org/10.1007/978-3-031-84212-2</a> 14
- Galli, N., Chiarelli, D. D., Ricciardi, L., & Rulli, M. C. (2023). A blue water scarcity-based method for hydrologically sustainable agricultural expansion design. *Water Resources Research*. <a href="https://doi.org/10.1029/2023wr034473">https://doi.org/10.1029/2023wr034473</a>
- Global Land Cover. (2003). *Global land cover 2000 database. European Commission, Joint Research Centre*. <a href="http://www.gvm.jrc.it/glc2000">http://www.gvm.jrc.it/glc2000</a>
- Govoni, C., Chiarelli, D. D., Luciano, A., Pinotti, L., & Rulli, M. C. (2022). Global assessment of land and water resource demand for pork supply. *Environmental Research Letters*, *17*(7). https://doi.org/10.1088/1748-9326/ac74d7
- Hoekstra, A. Y. (2003). Virtual water trade. Proceedings of the International expert meeting on Virtual Water Trade. Research Report Series No. 12 (Vol. 12). IHE DELFT, The Netherlands.
- Hoekstra, Arjen Y., & Mekonnen, M. M. (2012). The water footprint of humanity. *Proceedings of the National Academy of Sciences of the United States of America*, 109(9), 3232–3237. https://doi.org/10.1073/pnas.1109936109
- MedECC. (2020). Climate and Environmental Change in the Mediterranean Basin Current Situation and Risks for the Future. In *First Mediterranean Assessment Report*.
- MITECO. (2023). *Modelo SIMPA. Periodo de simulación: 1940/41 a 2017/18*. https://www.miteco.gob.es/es/agua/temas/evaluacion-de-los-recursos-hidricos/evaluacion-recursos-hidricos-regimen-natural.html
- Moriasi, D. N., Arnold, J. G., Van Liew, M. W., Bingner, R. L., Harmel, R. D., & Veith, T. L. (2007). Model



- evaluation guidelines for systematic quantification of accuracy in watershed simulations. *Transactions of the ASABE*, *50*(3), 885-900.
- Moriasi, D. N., Gitau, M. W., Pai, N., & Daggupati, P. (2015). Hydrologic and water quality models: Performance measures and evaluation criteria. *Transactions of the ASABE*, *58*(6), 1763-1785.
- Portmann, F. T., Siebert, S., & Döll, P. (2010). MIRCA2000-Global monthly irrigated and rainfed crop areas around the year 2000: A new high-resolution data set for agricultural and hydrological modeling. *Global Biogeochemical Cycles*, 24(1), n/a-n/a. <a href="https://doi.org/10.1029/2008gb003435">https://doi.org/10.1029/2008gb003435</a>
- Qadir, M., Sharma, B. R., Bruggeman, A., Choukr-Allah, R., & Karajeh, F. (2007). Non-conventional water resources and opportunities for water augmentation to achieve food security in water scarce countries. *Agricultural Water Management*, 87(1), 2–22. https://doi.org/10.1016/j.agwat.2006.03.018
- Ricciardi, L., Chiarelli, D. D., Karatas, S., & Rulli, M. C. (2021). Water resources constraints in achieving silk production self-sufficiency in India. *Advances in Water Resources*, *154*(December 2020), 103962. <a href="https://doi.org/10.1016/j.advwatres.2021.103962">https://doi.org/10.1016/j.advwatres.2021.103962</a>
- Ricciardi, L., D'Odorico, P., Galli, N., Chiarelli, D. D., & Rulli, M. C. (2022). Hydrological implications of large-scale afforestation in tropical biomes for climate change mitigation. *Philosophical Transactions of the Royal Society B: Biological Sciences*, *377*(1857), 1–9. <a href="https://doi.org/10.1098/rstb.2021.0391">https://doi.org/10.1098/rstb.2021.0391</a>
- Rost, S., Gerten, D., Bondeau, A., Lucht, W., Rohwer, J., & Schaphoff, S. (2008). Agricultural green and blue water consumption and its influence on the global water system. *Water Resources Research*, 44(9), 1–17. https://doi.org/10.1029/2007WR006331
- UN. (2020). UN Water Analytical Brief. Unconventional Water Resources (Issue June).
- Vermeulen, S. J., Campbell, B. M., & Ingram, J. S. I. (2012). Climate change and food systems. *Annual Review of Environment and Resources*, *37*, 195–222. https://doi.org/10.1146/annurev-environ-020411-130608
- Villani, L., Castelli, G., Yimer, E. A., Chawanda, C. J., Nkwasa, A., Van Schaeybroeck, B., ... & Bresci, E. (2024). Impacts of climate change and vegetation response on future aridity in a Mediterranean catchment. *Agricultural Water Management*, *299*, 108878.
- Yu, Q., You, L., Wood-sichra, U., Ru, Y., Joglekar, A. K. B., & Fritz, S. (2020). A cultivated planet in 2010 Part 2: The global gridded agricultural-production maps. *Earth System Science Data*, c12(4), 3545–3572.